FOAM CHARACTERIZATION: BUBBLE SIZE AND TEXTURE EFFECTS

A THESIS SUBMITTED TO
THE GRADUATE SCHOOL OF NATURAL AND APPLIED SCIENCES
OF
MIDDLE EAST TECHNICAL UNIVERSITY

BY

TUNA EREN

IN PARTIAL FULFILLMENT OF THE REQUIREMENTS
FOR
THE DEGREE OF MASTER OF SCIENCE
IN
PETROLEUM AND NATURAL GAS ENGINEERING

SEPTEMBER 2004

Approval of the Graduate School of Natural and Applied Science

_____

Prof. Dr. Canan Özgen

Director

I certify that this thesis satisfies all the requirements as a thesis for the degree of Master of Science.

_____

Prof. Dr. M. R. Birol Demiral

Head of Department

This is to certify that we have read this thesis and that in our opinion it is fully adequate, in scope and quality, as a thesis for the degree of Master of Science.

_____

Assist. Prof. Dr. Mehmet Evren Özbayoglu

Supervisor

Examining Committee Members:

Prof. Dr. M. Birol Demiral	(METU, PETE)	_____
Assist. Prof. Dr. M. Evren Özbayoglu	(METU, PETE)	_____
Prof. Dr. Mustafa Versan Kök	(METU, PETE)	_____
Assist. Prof. Dr Serhat Akin	(METU, PETE)	_____
Prof. Dr Nurkan Karahanoglu	(METU, GEOE)	_____

I hereby declare that all information in this document has been obtained and presented in accordance with academic rules and ethical conduct. I also declare that, as required by these rules and conduct, I have fully cited and referenced all material and results that are not original to this work.

Name, Last name:

Tuna Eren

Signature:

ABSTRACT

FOAM CHARACTERIZATION EFFECTS OF BUBBLE SIZE AND TEXTURE

Eren, Tuna

M.Sc., Petroleum and Natural Gas Engineering Department

Supervisor: Assist. Prof. Mehmet Evren Özbayoglu

September 2004, 103 Pages

Foam is one of the most frequently used multiphase fluids in underbalanced drilling operations because of its high carrying capacity of cuttings, compressibility property, formation fluid influx handling, etc. Foam rheology has been studied for many years. Researchers tried to explain foam behaviour by using conventional methods, i.e., determining rheological parameters of pre-defined rheological models like Power law, Bingham Plastic etc., as a function of gas ratio. However, it is known that bubble size and texture of the foam is also effective on foam behaviour. When foam is generated by using different foaming agents, even if the gas ratio is constant, different rheological parameters are observed. Therefore a more general foam characterization method that uses the bubble size and texture of foam is required. Improvements on image analysis, and computer technology allow monitoring the bubble size and texture of foam bubbles.

A more comprehensive model of foam rheology definition in which the bubble size, and texture effects of the foam body is developed. Three different analysis methodologies are introduced; i) Generalized volume equalized approach, ii) Generalized volume equalized approach and image processing data, and iii) Image processing data only. The necessary information including the rheological information and image data is acquired from the experimental set-up developed for this study. It has been observed that, the pressure losses could be predicted as a

function of bubble size, circularity and general rheological parameters, in ±20 % certainty limit. It is also observed that using only the image information is possible to characterize the foam in an accurate and fast manner.

Keywords: Foam Characterization, Pipe-Viscometer, Image analysis.

ÖZ

KÖPÜK KARAKTERIZASYONUNDA KABARCIK BOYUTU VE DESEN ETKILERI

Eren, Tuna

Yüksek Lisans, Petrol ve Dogal Gaz Mühendisligi Bölümü

Tez Yöneticisi: Yard. Doç. Dr. Mehmet Evren Özbayoglu

Eylül 2004, 103 Sayfa

Köpük, yüksek kesinti tasiyabilme, sikistirilabilme ve formasyon akiskanini kaldirabilme özelliklerinden dolayi en sik kullanilan düsük basinçli sondaj akiskanlarindan birisidir. Köpük reolojisi üzerine birçok çalisma yapilmistir. Arastiricilar, köpük davranisini Power Law ve Bingham Plastik gibi daha önceden tanimlanmis modelleri ele alarak, köpük içerisindeki gaz oraninin bir fonksiyonu olarak geleneksel yollardan incelemislerdir. Ancak, kabarcik boyutu ve kabarcik deseninin köpük davranisinda etkili oldugu da bilinmektedir. Köpük, degisik köpük yapici kimyasallar kullanildiginda, gaz miktarinin ayni oldugu hallerde bile degisik reolojik davranislar göstermektedir Bu nedenle kabarcik boyutunu ve desenini de dikkate alan daha kapsamli bir köpük karekterizasyon modeli gereklidir. Görüntü analizi ve bilgisayar teknolojisindeki gelismeler, kabarcik boyutu ve deseninin gözlemlenebilmesini mümkün kilmaktadir.

Bu çalismada, köpügün reolojik tanimininin kabarcik boyutu ve desen etkilerini de dikkate alan daha kapsamli bir model gelistirilmistir. Üç degisik analiz metodu tanimlanmistir; i) Genellestirilmis hacim esitleme yaklasimi ii) Genellestirilmis hacim esitleme yaklasimi ve görüntü analizi datasi iii) Sadece görüntü datasi. Analiz için ihtiyaç duyulan reolojik ve görüntü bilgileri, bu çalisma için kurulmus olan ve farkli çaptaki dairesel borulardan olusan bir düzenek yardimi ile elde edilmistir.

Basinç kayiplarinin, kabarcik boyutunun, daireselligin ve genel reolojik parametrelerin bir fonksiyonu olarak ±20 % hata payi ile hesaplanabildigi gözlemlenmistir. Sadece görüntü bilgisinin kullanilmasi ile köpük karakterizasyonunun dogru ve çabuk bir sekilde yapilabilineceginin mümkün oldugu gözlemlenmistir.

Anahtar Kelimeler: Köpük Karakterizasyonu, Boru viscometre, Görüntü analizi.

To the father of a whole nation,

Mustafa Kemal Atatürk

For giving the greatest of all presents

Freedom.

ACKNOWLEDGEMENTS

I would like to give my very sincere and kind respect to my advisor Assist. Prof. Dr. Evren Özbayoglu for his constant guidance and support throughout my studies. I am also grateful to my instructor Assoc. Prof. Dr. Serhat Akin.

Many thanks to my friends, Surku Saraç, and Res. Assist. Çigdem Ömürlü for their invaluable contributions in construction of the loop, and performing the experiments. I would also like to thank to the technicians of the Petroleum and Natural Gas Engineering Department, Naci Dogru, and Ömür Girgin, for their valuable contribution in constructing the experiment loop.

I really am grateful to my family members, especially to my father for constantly imposing the importance of science and for his support, and advice for not to get aside from honesty, throughout my life.

This study was supported by TÜBITAK (The Scientific and Technical Research Council of Turkey) Research No: MISAG-251.

TABLE OF CONTENTS

LIST OF TABLES

TABLE

LIST OF FIGURES

FIGURES

NOMENCLATURE

Roman

V_g	Gas volume, ml
V_l	Liquid volume, ml
K	Consistency index, [Pa.s^n]
N	Flow behaviour index
P_i	Pressure at the input of the free body, psi
P_{atm}	Atmospheric Pressure at the lab elevation, psi
P_o	Pressure at the output of the free body, psi
ΔL	Characteristic length of the free fluid body, m
V	Volume of the free body, ml
v	Velocity of the free body, ft/s
R, r	Pipe radius, m
f	Friction factor, dimensionless
N_{Re}	Reynolds number, dimensionless
D	Pipe diameter, m
n	The outward direction unit vector
A	Area, cm^2
d	Bubble diameter, in
$\dot{m}$	Mass flow rate, g/sec
Q	Flow rate, ft^3/sec
N_{Re}	Reynolds Number
R	Universal Gas Constant, 10.732psi.ft^3/(lbm.^{o}R)
C	Correction Factor
PV	Plastic Viscosity, cp
#	Mesh, The number of apertures per unit inch of a screen (sieve).
X_E	Length of the flow conduit, m

Greek

Γ	Foam quality, (%)
τ	Shear stress, [Pa]
γ	Shear rate, [s^{-1}]
τ_y	Yield stress, [lbf/100ft^2]
μ_p	Plastic viscosity, [Pa.s]
ρ_i	Density at the input of the free body, g/cc
μ	Viscosity, [Pa.s]
ρ_o	Density at the output of the free body, g/cc
e	Specific Expansion Ratio, dimensionless
β	Slip Coefficient, ft/Pa.s
β_c	Corrected Slip Coefficient, ft^2/Pa.s
ρ_{mix}	Density of the mixture(surfactant + water), g/cc
ρ_{air}	Density of air, g/cc
ϕ	Pipe Diameter, in.
μ_F	Foam viscosity, [cp]
μ_l	Base Liquid viscosity, [cp]

Subscripts

i	Input location on the free body
o	Output location on the free body

Abbreviations

GEVE	Generalized Volume Equalized Principle
ave	Average
FG	Foam Generator
Cir	Circularity
ECD	Equivalent Circulating Density, ppg
VEP	Volume Equalized Principle
M	Master

CHAPTER I

INTRODUCTION

Foam is composed of a continuous liquid phase that surrounds and traps the gaseous phase. Its main characteristics are a relatively low density and extremely high viscosity.

The high viscosity allows efficient cuttings transport with relatively low gas injection rates. The low density ensures that the underbalanced conditions are established in the most practical circumstances.

Many researchers have investigated foam behavior, and as of yet no comprehensive methodology could have been evolved in order to define the rheological behavior of foams. Researchers investigated the foam samples, based upon a single surfactant type, and a single foam generation technique. However this study revealed that, when foams generated through different means their rheological behavior would have totally been different.

Not, so many researchers did take into account the effect of foam bubble properties; the bubble size and texture have been found to change with increased gas ratio. One of the motivations that draw this study to be carried out, is to investigate the orientation of foam bubbles with each other, and to arrive to a conclusion whether to comprehensively define a rheological foam behavior prediction.

It is know that foam when generated is composed of two phases, gas and the liquid, the gas constituent is compressible in its nature, turning foam out to be compressible

as well. This effect of compressibility has to be taken into account when investigating foam behavior prediction. A volume-equalized technique has been used in order to discard the effects of quality dependency of foam rheology definition. This technique when coupled with the slip correction, that is known to occur along side the pipe walls, gave one of the best foam rheology definitions.

This research covers construction of an experimental set-up that is formed of horizontal pipes, through which foam let to flow. The derived equations are utilized in interpretation of the acquired data.

Two different foaming agents, and foam generation technique was used to carry out the experiments. The image data of the acquired foam photos, were gathered during the experiments, and analyzed in order to characterize foam rheology. The result of this study revealed that foams could have been characterized when their bubble size and texture were taken into consideration. The findings of this study if used in the field are prominent to give successful, foam frictional pressure loss predictions.

CHAPTER II

LITERATURE OVERVIEW

2.1 Foam:

Foam is composed of gas bubbles dispersed uniformly throughout a continuous liquid phase and can be treated as a homogeneous fluid with both variable density and viscosity [1]. When foam is considered to be such a homogeneous fluid, it is probably the only known compressible non-Newtonian fluid.

Foams are thermodynamically unstable systems because they always contain more than a minimal amount of gas solution interface. This interface represents surface free energy, the amount of which can be estimated from knowledge of the surface tension and the interfacial area of the foam. Wherever a foam membrane breaks and the liquid coalesces, there is a decrease in surface free energy. Thus the decomposition of foam into its constituent phase is a spontaneous phase. Since the solution phase is always denser than the gaseous phase, there is a strong tendency for the former to separate or drain from the main body of foam unless it is circulated or agitated in some way. This drainage leads to instability of variation in physical properties with height and time, which precedes breaking. The surfactant, which does play an important role in stabilizing the films, entrapping the gas bubbles; allowing the foam structure to be persistent is also included in the liquid phase.

Because of the density differences between the two phases of the foam, there is always a tendency that liquid, the denser phase, will drain from the main body, unless there is continuous agitation.

Foams can have quite high viscosity values, a value that is greater than both constituents, for a constant shear rate. Also, foam has a density lower than that of liquid phase. Their high viscosity allows efficient cuttings transport and low density allows underbalanced conditions to be established. Drilling with foam has shown increased productivity, increased drilling rate, and reduced operation troubles such as lost circulation, differential stuck pipe, and gives improved formation evaluation while drilling [2]. Although drilling with foam is very valuable due to its very low density coupled to its excellent cuttings carrying ability, characterization of foam properties under drilling conditions is still incomplete and this could be an obstacle to the use of this technique by operators [3].

Foams are generally characterized according to their quality, which is defined as follows, in Equation 2.1;

$$\Gamma = \frac{V_g}{V_g + V_l} \times 100 \quad \text{..... (2. 1)}$$

where: V_g is the gas volume, V_l is the liquid volume, and Γ is the foam quality, (%).

As to give an example, 80-quality foam contains 80 percent gas by volume. It is accepted that, foam has a foam quality ranging from 52 % to 96 %. Use of foam in petroleum industry is in an increasing trend, because of the desirable properties that it exhibits. The reduced density of the foam fluids, their high cuttings carrying capacity, and their performance on eliminating filtrate and circulation losses are among these desirable properties during drilling operations. The fracturing fluid application of foam prevents fluid loss to the formation, and provides excellent fluid recovery right after the treatment. Foams have also been used successfully in oil and gas fields in well stimulation, clean up, and fishing operations. They are also used as a material in fighting with fire. It has been proved that, using foam as a drilling fluid

provided a very good lubrication property, lubricity index being between that of water base muds and oil base muds [3,4].

A low quality foam (wet foam) contains more liquid than a high quality foam (dry foam). Texture describes the size and distribution of the bubbles. Fine foam has smaller and spherical bubbles, and coarse foam has large and polyhedric bubbles. Combining these terms, sphere foam tends to be low quality; fine foam and polyhedric foam tends to be a high quality, coarse foam [5]. Whenever the quality of the foam exceeds a threshold level, the continuous liquid phase turns into discontinuous situation and results in formation of mist. There is no decision on what the upper limit for stable foam is. It certainly is a function of shear rate. Okpobiri and Ikoku, 1986 [6] found that foam collapsed to mist at a quality of 94, for shear rates below 5000 s^{-1}, but would persist up to 96 quality, for shear rates above 5000 s^{-1}. Beyer et al, 1972 [7] had given that the foam became unstable at liquid volume fractions of 0.02 to 0.03, and that when the quality exceeds 98 the foam tends to flow as intermittent slugs of foam and gas.

Composition of the liquid phase with the gas phase is important for the foam stability. Russel, 1993 [8] in his study found that, foam with good bubble stability was generated only by surfactant solution at 99.1 quality without polymers, known to be “stable foam”. On the other hand with the addition polymers it was observed to have stable foams generated at 99.65 quality.

The interaction of the dispersed gas bubbles within the foam structure will be intact until the quality reaches to 55 % [9]. Quality, gas fraction increases there will be an increase in the viscosity. If the quality exceeds 75 % then there will be interaction between the adjacent bubbles. Rankin et al [10], 1989 defined the stable foams to be in the range of 75 to 96.5 % quality values.

2.1.1 Advantages of Foam Operations

Foams with high viscosity and low density can provide the following positive outcomes;

- With comparison to air (an annular velocity of 3000ft/min is normally required for air drilling, [11]) or mist drilling, foam is far more efficient in the removal of cuttings at much lower annular velocities. Internal phase injection rate for foam is lower than those required for air or mist drilling.
- Underbalanced conditions within the wellbore are definitely to be achieved because of the low density in the nature of the foam. Rate of penetration for foam drilling is considerably higher than that of conventional mud drilling.
- Potential mechanical wellbore instability could be reduced with higher annular pressures whilst foam drilling, whereas possible erosion of the borehole could be overcome with low annular velocities.

Most commonly used internal phase for foam drilling in underbalanced operations is air because of its availability. A surfactant solution is mixed with a gas flow and the mixture is injected into the drillstring. After having been generated in a foam generator, foam is going to be generated whilst flowing through the bit as well.

Foams as mentioned above are complex mixtures of gas, liquid and a surfactant whose rheological properties are strongly influenced by parameters like temperature, absolute pressure, foam quality, texture, foam-channel wall interactions, liquid phase properties, and type and concentration of surfactant [4]. Therefore, the rheology of foams is more complex than that of other simple drilling fluids. However as contrary to the complexity of the rheological specification of foams as underbalanced drilling fluid, the ability to lift large quantities of produced liquids is most probably the main reason for its use. Foams are also good at removing the solid particles (cuttings transport) and also used when working-over wells in depleted reservoirs because of its successfully medium insulating property what if loss circulation was a problem.

2.1.2 Foam Texture

The shapes of the bubbles are used as a means of foam classification [52]. Bubbles will tend to be spherical in shape, as a result of minimum energy principle. If the bubble concentration is high and small or the foam is freshly generated, this type of foam is called sphere foams. Apart from this foams with polyhedral bubbles are named to be polyhedral foams. As it is known from geometrical relations the amount of liquid volume is higher in sphere foams than polyhedral foams. This is because of the facing in the case of the polyhedral foams to be more in order than the case of spherical foams. The liquid phase in the case of spherical foams is thicker than the polyhedral foams. The ideal foam in oil extraction/ reservoir stimulation purposes is desired to be as ideally polyhedral as possible, the bubbles could have as much 12-sides.

2.1.3 Foam Stability

Low quality foams formed of spherical bubble distribution will break down slower than the high quality polyhedron foams. There are two main causes for the foam to be disrupted, thinning of the bubble walls, and growth of large bubbles at the expense of smaller ones.

Gravity is one of the reasons to cause the disruption by forcing the liquid content towards the bottom whereas pushing the gas constituent towards the top to let them free themselves. The disruption is known to happen until the spherical walls are not capable to handle the surface tension. Stirring sphere foam to redistribute the bubbles can prevent excessive thinning. Any agitation of high quality polyhedron foam will, however, promote rupture of the thinned bubble walls.

Surface tension of the liquid in a bubble wall tends to collapse the bubble; the gas pressure inside the bubble balances this. The gas pressure within a bubble is inversely proportional to the bubble size. When a large bubble contacts a smaller bubble, the higher gas pressure inside the smaller cell causes the gas inside it to diffuse through the liquid separating the two bubbles, until the smaller bubble is fully absorbed by the larger.

If the walls of the bubbles are strengthened more, foam would be more stable and the drainage of the liquid retented. Surfactants are known to have strengthening effect against the excessive thinning. Certain proteins, for instance, if added into the liquid phase of an air foam would react with oxygen at the air-liquid interface to form a skin. Increasing the bulk viscosity of the liquid phase slows drainage. Surfactant mixtures can increase the surface viscosity of the base fluid, and this can also slow drainage through bubble walls.

2.1.4 Foaming Agents,

In foam operations temperature in the operation zone is important as much as the chloride content of the brine. Foam stability may immensely be affected by brine or hydrocarbon contamination. When brine influx occurs, it will tend to mix with the foam attacking the ionic character of the surfactant and thus reducing the surface tension. The expected performance from a surfactant in the course of a drilling operation is; the absolute necessity to maintain very low surfactant adsorption and limited mobility control in order to use foam in the reservoir that must survive when the capillary pressure is high [12]. Surfactant must somehow propagate where water is not mobile. The desirable properties of a surfactant are rapid propagation, limited mobility control, and mixed wettability versus water wetness.

With an increase in temperature the foam tendency in terms of decay increases. As the depth increases all the way further below subsurface, there is a predictable temperature increase. It is necessary to increase the surfactant concentration as the downhole temperature rises.

Surfactants consist of molecules having a hydrophilic group attached to a long hydrophobic tail, which is usually a fatty hydrocarbon chain. They are classified according to the nature of hydrophilic group, which may be anionic, cationic, amphoteric or non-ionic. Whenever possible, surfactant molecules orient themselves so that the hydrophilic group in an aqueous environment, and hydrophobic tail is in a non-aqueous environment. They will, therefore, concentrate at the liquid-gas interfaces in foams. They may increase or decrease the surface tension of the liquid,

and may strengthen or weaken the bubble walls. Not all surfactants will act as foaming agents some will destabilize the foam structure and can be used instead as defoamers.

Ammonium salts of alcohol ether sulphates are probably the most widely used, and their anionic surfactants are highly soluble in most liquids. These surfactant generate thermally stable foam, and also suitable for use at low temperatures as well. One contrary is their high cost. Olefin sulphonates are also anionic surfactants with comparatively low cost, and perform appropriately in fresh water. They are also resistant to hydrocarbon contamination. They are however, not able to function in low temperatures and in brines.

It is common to see foams to be composed of anionic primary foaming agents as well as foam boosters. Ethylene or propylene glycol butyl ethers or amphoteric betaines are also in use, functioning as primary additive to enhance foam stability.

Anionic surfactants being the most widely preferred additives, cations are not that much of choice. Quaternary ammonium chlorides do not perform well in fresh water, give poor to mediocre foam stability and must be used at high concentrations. Nevertheless, cationic surfactants may be worth considering for drilling water sensitive shales, because of their ability to stabilize clays.

The terminology, for critical foaming agent concentration is important. The desirable foam is the one with longest half-life at the minimal surfactant concentration. Conveniently, foam-stability should be perceived in regards to its half-life time. Half-life is the time required for the foam volume to decrease to one-half of its original volume. Half-life experiments are given in Appendix-A.

2.1.5 Defoaming;

The longer the half-life of foam, the more it is desired until the foam arrives in the blooie line (blooie line can be considered equivalent of the flow line as in conventional drilling activities). Because the foam in the blooie line is just about to

deploy the cuttings it brought from downhole, the foam has got to diminish in a way. Defoamers, those of which are a type of surfactant that destroy the foam to decay it. There are specific defoamers to destroy the particular foam. For instance, iso-octanol, an oil-soluble alcohol, is effective at destroying foam produced with the commonly used anionic foaming agents.

Rheological characterization of foam is difficult, i.e., foam properties vary depending on the surfactant type used, and the way foam has been generated. Texture of the foam and their bubble size distribution have to be taken into consideration for a proper characterization, which is the main objective of this study.

2.2 Foam Definition

Foam is a fluid that almost everybody come across at least a couple of times in daily life. Foam is also very preferably used as circulation fluid during drilling operations, as well as in completion and production operations. Foams consist of two phases, the continuous phase, that is the liquid, forming a cellular structure in which the gas that is entrapped as the discontinuous phase.

Depending mainly on the gas content, foams could be ranked as wet owing to spherical bubbles or as dry owing to the existence of polyhedral bubbles with less water and higher contact of gas bubbles entrapped [13].

In the literature, rheological characterization of foam can be categorized under two major groups; quality based approach, and volume equalized approach. However, none of these approaches take the bubble size and texture of foam into consideration while characterizing the foams.

2.3 Literature Review of Previous Foam Investigators

Raza, and Marsden, 1966 [14], made a study by generating aqueous foam flowing in both open and closed packed Pyrex tubes. They used four Pyrex tubes of 30 cm long

with internal radii ranging from 0.25-to 1.50 mm. They worked with foam viscosity range from 15 cp to 255 poise. They concluded that the foam used in their work behaved like a pseudoplastic fluid. They mentioned that as Γ (quality) increases the foam tends to lessen mass of liquid membranes. They stated that velocity distribution perpendicular to flow direction at low flow rates is parabolic; at higher flow rates it indicated a type of plug-like flow, the degree of which depends on both tube radius, and foam quality. They also gave that apparent viscosity increased with both tube radius and foam quality. They derived an equation describing the streaming potential of Non-Newtonian fluids in circular pipes, where the streaming potential could be defined as the voltage difference between the ends of a capillary tube.

Amiel and Mardsen, 1969 [15], made a study in which they measured the bubble size and bubble size distribution under a microscope, and checked the change of bubble size with time through photomicrographs. The foam flowed through a capillary tube viscometer having four interchangeable glass tubes with different radii. In their study they theoretically considered the effects of foam slippage at the tube wall and the foam compressibility. They found that bubble size distribution and bubble size (diameter) were dependent on quality. They also found that apparent viscosity was independent of foam quality when corrected for both slippage and foam compressibility. They reported that the foam behaved like pseudoplastic (powerlaw) fluids with very low gel strengths, which increases slowly with quality.

Mitchell [16], studied on foam rheology. Different qualities of foams were flown through small diameter tubes. In his study it was found that foam behaved like Newtonian for quality levels up to 55. It can be deduced from this, that up to this quality viscosity does not depend on shear rate. The following relation by using statistical approach was given for the foams in this range,

$$m_F = m_L(1+3.6\Gamma) \quad \text{.....(2.1)}$$

where, μ_F is foam viscosity (cp), μ_L is base liquid viscosity (cp), Γ is foam quality, (fraction) . As given by Mitchell, it is apparent that quality levels above 55 percent behaved like Non-Newtonian actually approximately as Bingham plastic. He stated that foam viscosity depends on quality and shear rate.

Mitchell, describing the flow of drilling muds, also gave the following relation,

$$t = t_y + \frac{PVg}{479}, g \le 2\times10^4 s^{-1} \quad \text{..... (2.2)}$$

where τ is shear stress, [psi], τ_y is yield point, [lbf/100ft^2], PV is plastic viscosity, cp, γ is Shear Rate, (sec^{-1}).

He also observed that wall slippage effect did not exist at the instance of flowing foam, and also foam viscosity was increasing at constant shear rates with increasing quality.

Beyer et al, 1972 [17], performed laboratory and pilot-scale experiments aiming incorporation of the results into a mathematical model. They reached to a conclusion that foam quality was principally effective in its flow behavior; such as there was tendency in higher viscosity generation and better particle transportation with higher quality levels. The given equations accounted for slippage at the pipe wall and the fluidity component. As given by Beyer et al. the finite difference model made explicit allowance for foam slippage for possible eccentricity of the drillstring. The proposed model worked with an accuracy of approximately 10%, with fixed 5-psi pressure steps.

Blauer et al, 1974 [18], proposed a model in which iteration was not necessary. They arrived at a method predicting friction losses in laminar, transitional, and turbulent flow regimes for flowing foam. They proposed that effective foam viscosity, actual foam density, average velocity and the pipe diameter were functions of Reynold's Number and Fanning friction factor, by conducting experiments in capillary tubes,

and also oil field tubings. They concluded that foam behaved as a single phase Bingham Plastic fluid and that if Reynold's number was used together with friction factor, friction losses for foam could be determined.

Lord, 1979 [1], mathematically developed an equation of state in which he described volume of the compressible fluid as a function of pressure and temperature. This relation was extended to the formulation of foam density in terms of pressure, temperature, liquid density, and the gas mass fraction, presuming real gas behavior. He developed a mechanical energy balance for both static and dynamic conditions for the foam circulation in which foam quality, density, and pressure could be calculated at any position within the column of the borehole. Frictional pressure loss was estimated by a mean value of the inlet and outlet friction factor, which was considered as a constant. The developed model for the prediction of injection pressures is based on the solution of the differential form of the mechanical energy balance, which required numerical solution, i.e., the flowing pressures had to be predicted, and the friction factor had to be carefully determined. The model accurately predicted downhole pressures when proppant-laden foam was pumped down a well.

Sanghani and Ikoku, 1983 [19], conducted an experimental study on foam rheology with a concentric annular viscometer that closely simulated actual hole conditions. They reached to a conclusion that flowing foam is a powerlaw (pseudoplastic) fluid for wall shear rates below 1000 sec^{-1}, and effective viscosity decreased with increasing shear rate. Their study also revealed that most foam drilling operations could be carried out in laminar flow region because of low density and high viscosity of foam, if bottomhole quality was not less than 55 percent. They developed tables that showed the quality dependence on model parameters. They also stated that, a Bingham plastic model and a yield pseudoplastic model without large errors could represent their data.

Okpobiri and Ikoku, 1986 [20], presented a model that predicted pressure drop across bit nozzles. The accounted for the compressibility of foam assuming negligible

pressure losses resulting from friction and elevation change. The model they developed for predicting minimum volumetric requirements for foam accounted for frictional losses caused by the solid phase, pressure drop across bit nozzles and particle-settling velocity. Their results indicated that volumetric requirements increased with increasing hole size, depth, and particle size. They presented charts for the determination of flow requirements for various backpressures, penetration rates and pipe specifications.

Reidenbach et al, 1986 [21], conducted an experimental study, backed up with mathematical modeling for the calculation of laminar and turbulent rheology of foams formed of N_2 and CO_2. Laminar flow data were collected in a recirculating flow pipe loop, and the turbulent flow data in a single-pass pipe system. Their study described that laminar flow was a Herschel-Bulkley yield pseudoplastic type as a function of quality, external-phase fluid type and texture. Turbulent flow was described by a modified scale-up relation for the flow of compressible foam. Their work revealed a good correlation with the pressured actual field treatment.

Harris and Reidenbach, 1987 [22], studied rheology of N_2 foam under high temperature and pressure, for well stimulation applications. They developed empirical equations to describe N_2-foam rheology behavior from 75-300^{o}F, 0-80 quality. Their study revealed that high-quality foams maintain their viscosity better at high temperatures than base-gel fluids at high temperatures.

Harris, 1989 [23], developed on an empirical approach to determine the effect of bubble-size distributions on the rheological properties of foam. In his study he observed the effect of quality, liquid-phase properties, surfactant type/concentration, gelling agent shear history of foam, pressure on foam rheology. His study revealed that foams were shear-history dependent fluids, which meant the bubble size and dispersion will adjust to an equilibrium state in time at a given shear rate. He mentioned that viscosity was substantially affected by quality and continuous-phase properties and that viscosity was less affected by texture. In his study, higher shear

rate, surfactant concentrations and pressure produced finer texture foams. He concluded that continuous phase chemical type was highly effective in foam texture.

Calvert and Nezhati, 1986 [24], studied rheology of liquid-gas foam by conducting experiments on cone and plane rheometers, and also pipe flow. Their study revealed that foam could be modeled by a modified Bingham Plastic system, with a liquid rich slip layer at solid surfaces. The consistency index and flow behavior index in their study were found not to be dependent on flow rate and expansion ratio, whereas the yield stress strongly was, and attributed to the differences in bubble size distribution. The slip layer thickness was found to depend on expansion ratio and flow rate, and on flow conditions as well.

Cawiezel and Niles, 1987 [25], carried out laboratory work with simple Nitrogen foams and gelled foams in order to find the rheological properties of foams by observing quality, pressure, temperature, and shear rate effect. Their work indicated that simple foams exhibit a yield stress, and fit the Herschel-Bulkley model, having a dependence on quality, being a function of foam structure. Their study revealed that apparent viscosity increased with increasing quality and become more pseudoplastic, increasing exponentially. Pressure significantly increased the viscosity of foams more in low-shear rate range, but less in higher shear. With an increase in temperature the apparent viscosity, decreased up to a critical temperature after which little change occurred. They observed no effect on foam rheological properties by exposing them to shear.

Khan et al, 1988 [26], experimentally studied the steady and time-dependent shear flow properties of high gas fraction liquid foams. In their study they mixed a stream of gas and liquid solution in porous structure in order to have gas volume fractions of up to 98% and observed liquid surface tension, the average bubble diameter, and the gas volume fraction. All of their rheological measurements were done by using a parallel plate mode of a rheometrics Mechanical Spectrometer, at room temperature. They set sand paper on the circular disks to eliminate the effect of the liquid film formation considering slippage at the wall in order to gather accurate rheological

measurement. The linear viscoelastic properties of foam were studied by using small amplitude oscillatory shear experiments. Their study revealed that steady-shear foam flow behaved like a Bingham Plastic (Shear thinning) with a viscosity being a function of shear rate even at very low shear rates, where as for low-shear rates, they concluded having observed a shear thinning viscosity inversely proportional to shear rate, indicating the yield stress to be the prominent contributor to viscosity, which was increasing function of quality. Their study also revealed that yield stress increased with increasing gas fraction. Oscillatory dynamic experiments revealed that foam behaved like an elastic solid for small deformations. In their study stress-strain behavior of foam was found to be independent of shear rate.

Rankin et al, 1989 [10], conducted laboratory work on the use of compressible fluid as a circulation fluid. They concluded that less formation damage, less lost circulation, and better hole cleaning would occur by the use of lightened rather than conventional fluids. Their study revealed the pumping rates, for dry air and aerated fluids in order to have a turbulent region to avoid flux momentum in the inclined portion of a borehole. Their study also gave that stable foams provided better hole cleaning than gases, mists or aerated muds.

Valko and Economides, 1992 [27], worked on foamed polymer solutions. They developed constitutive equations, by using large-scale vertical tubes and introducing the specific volume expansion ratio to characterize the gas content of the foam. The behavior of the foam was given as volume equalized power and volume equalized Bingham Plastic model those of which were developed by making use of the volume expansion ratio, the ratio of the sum of gas and liquid volumes to the liquid volume only. The graphical representation of the volume equalized principle revealed to serve as replacement top the flow curves of incompressible flow if the plot of “wall stress divided by the specific volume expansion ratio” was drawn against “shear rate divided by the specific volume expansion ratio” would collapse in a unique curve. One of the two advantages of the model proposed is assuming a constant friction factor easing the computation of the frictional losses in isothermal pipe flow. The second advantage is having less number of parameters, which made the estimation of

the parameters much easier than other models. The basic idea of Valko and Economides' model was to define constitutive equations for Non-Newtonian compressible fluids by using the invariance property of Reynold's number (constant friction factor) that was valid for incompressible Newtonian, compressible Newtonian, and incompressible Non-Newtonian fluids. The principle stated that all volume equalized shear-stress volume equalized shear rate points obtained in different qualities and different geometries collapsed on one curve in isothermal conditions.

Sporker et al, 1991 [28], investigated the rheology of multiphase fluids and constructed a flow loop to allow realistic downhole measurements under field-like conditions. The interactions between gravitational, frictional and other factors have been investigated. As in Lord's [1], work the system was assumed to have isothermally flowed, have a constant friction factor, have no phase hold- up and no change in solubility, also in this study the same assumption were the case for an improved version pressure drop equation after Lord. Although Lord used "engineering gas law" i.e. a constant compressibility factor, it was the gas behavior utilized in this study differing from Lord's by the pressure usage where as being the specific volume in original case. The proposed solution was not comprised of complicated pressure drop equation and in an incompressible flow case reduced to well known Fanning Pressure drop equation which was not the case for Lord's.

Valko and Economides, 1992 [29], performed large-scaled experiments to measure downhole rheology of various quality foams of CO_2, N_2 and mixture of their aqueous phases with polymers. A two-step methodology was suggested, first friction factors were obtained by solving the two-phase flow-equation, and then parameterized rheological models to describe quality dependence of rheology were investigated. They proposed a correlation to represent foam rheology, namely Volume Equalized Power-Law Model. A procedure was also suggested to calculate bottomhole pressure from known wellhead conditions during fracturing.

Winkler et al, 1993 [30], performed large-scale horizontal flow experiments. Applying volume-equalized power-law for polymer foams, they found that model was capable to describe isothermal horizontal compressible non-Newtonian flowing systems independent of pipe geometry. In their experiments increase of the foam temperature had no significant influence on the foam flow behavior, but on viscosity. Foam flow behavior in drag-reducing flowing regimes was also experimented.

Enzendorfer et al, 1994 [31], used five different small diameter pipes to characterize rheology of foam. The results depicted a relative dependence on the pipe diameter. Apparent slip concept was given to define this dependence. It was proposed that Jastrzebski method after being developed was capable for apparent slip correction rather than classical Mooney's slip correction. It was shown that the Mooney's approach to slip correction was not applicable for foams. The specific volume expansion ratio was introduced, it was shown that the flow curves of foams with different qualities and pressures are collapsed into one master curve, which showed power-law behavior with no indication of yield stress. It was obvious that viscosity increased with increasing quality. The phenomenon of curves to collapse into one master curve was a testimony of the application of volume-equalized principle giving the dependence of the rheology of foam to its gas and liquid constituents.

Gardiner et al, 1998 [32], worked on rheological investigation of compressed air foams, and also gave the velocity of foams flowing through horizontal tubes. They utilized Poiseuille-flow rheometers with three different diameter pipes with foam generation by means of compressed air. They showed that a master equation could have been drawn from the experimental data to account for a range of expansion ratios, and pressures encountered for polyhedral-in-structure foams. The data were corrected by the method of Oldroyd- Jastrzebski to account for slip correction that eliminated geometry dependence of foam. Volume equalization method was used resulting in collapse of data points in two different master lines depending on foam texture being either polyhedral or bubbly in its nature.

Kuru et al, 1999 [5], conducted a review study of foam and aerated drilling fluid technology. They found that there was no general agreement on which rheological model should be adapted. The effect of temperature on the behavior was yet to be investigated, and they also outlined the future needs of the research area.

Saintpere et al, 1999 [33], used blend of anionic surfactants commercially in use on drilling site in their experiments. They have worked on the formulation in order to enhance the stability of the foam, by changing the surfactant, salt and certain concentrations of water-soluble polymers. Having conducted all of their experiments under ambient conditions, they concluded that paying no attention to transitory regimes or not controlling slip at the wall in steady shear flow measurements would result in a wrong viscosity evaluation. They also concluded that bubble size had a tendency to decrease in size when pumped downhole.

Alvarez et al, 1999 [34], conducted a study correlating the effects of parameters like permeability and surfactant formulation on foam behavior in the two flow regimes (high-quality "dry", and low-quality "wet" regime) and on the transition between the two regimes. Hassler-type coreholder with 4 internal pressure taps was used. They used a video camera to record qualitative bubble texture through the visual cell at the outlet of the core, conducting the experiments at room temperature. Surfactant type and concentration, permeability, core layering and flow rates were varied whilst the experiments. They observed higher bubble sized foam in high-quality regime, as contrary smaller bubbles in low-quality regime. They correlated the shift in predominance between flow regimes as permeability; foam formulation and flow rates vary. After this study a guide to select foam formulation and foam quality for field applications in gas injection IOR and foam acid diversion have gained insight.

Rommetveit et al, 1999 [35], performed an experimental study in a vertical, instrumented test well, to plan an operation in order to better evaluate dynamic pressure and flow effects. The results of their study predicted gas injection rates fairly good, and the pressure curves of simulated and experimental curves matched well.

Silva et al, 2000 [36], developed an integrated analysis method incorporating multiphase flow calculations, gas and liquid injection rate optimization, hydrostatic gradient and frictional pressure loss calculations, cuttings transport, reservoir fluid influx (gas, oil, water).

Fernando et al, 2000 [37], experimented the rheology of foams by using aqueous and gelled foam types employing a pipe type viscometer. The loop they constructed consisted of pertinent equipment in order to determine rheological properties of foamed fluids under flow conditions. They concluded that apparent viscosity was a function of foam quality. Rheological behavior of foam was defined to be Herschel-Bulkley type. Higher quality foams produced higher shear stresses, and viscosities. At high qualities apparent viscosity increased exponentially with foam quality. The effect of temperature on foam stability was found to be adverse. More viscous liquid phase foams produced foams of higher viscosity at the same quality, shear rate, and temperature.

Herzhaft et al, 2000 [3], conducted a research to investigate properties of aqueous foams and their interaction with solids when in contact. They found that when swelling clays were added to the system very good stability properties without requiring any polymeric additives were achieved. When they investigated the interaction of foam with solids they found that settling velocity of particles were reduced with increased foam quality levels.

Martins et al, 2000 [38], conducted and experimental work on foaming agent selection, rheological foam characterization, carrying capacity of foam in high angle wells. Their study revealed the importance of the additive requirements in the case of fluid influxes, e.g. the foam should have been stable in the presence oil, and salt. Their study also resulted in the higher carrying capacity of high quality foams. The methodology proposed the prediction of bed heights as a function of foam qualities and liquid flow rates.

Ozbayoglu et al, 2000 [2], conducted foam flow experiments through 2", 3", and 4" diameter pipes and 8" by 4.5" annular section. They recorded gas/liquid flow rates, pressures, and temperatures. They investigated the degree of fit by Bingham Plastic, Power Law, and Yield Power Law, to the Generalized Foam Flow Curve. They concluded that wall slip effect may not be neglected and should be considered in establishing the flow curve representing the true flow behavior of foam in pipes. They proposed a foam rheology definition based of foam quality level, e.g. foam was depicted as Power Law model in the range of 70-80% quality, and Bingham Plastic model for 90%. Eventually they mentioned that there was yet no best model for the pressure loss prediction during foam flow in pipes.

Rojas et al, 2001 [39], evaluated the stability and rheological behavior of aqueous foams. A capillary tube viscometer was used to perform rheological foam flow investigation. Results they have found indicated that the sensitivity of foam to contamination with oil and salts highly depended on the chemistry of the foaming agent system, and crude oil used. The rheological evaluations revealed that flow behavior is highly related on the foam quality for a given pressure, the chemistry of polymer, and the tube diameter.

Sani et al, 2001 [40], employed an experimental work on xanthan gel and xanthan foam rheology on a pipe flow viscometer at 1000 psi, using a ½" pipe. They found that as the foam viscosity increased, there was an increase in foam quality. When the temperature was increased the viscosity was adversely affected. They developed correlations between liquid phase properties and foam qualities to predict apparent foam viscosity. They concluded that foam behaved like Herschel-Bulkley model.

Martins et al, 2001 [41], conducted experiments to develop a model in order to predict bore hole pressures while drilling underbalanced with foams. The results of their study revealed reliable rheometric data at different foam qualities and derived data to be utilized in designing effective hydraulic cuttings transport design.

Alvarez et al, 1999 [42], conducted experiments by Hassler-type coreholders with and without internal pressure taps were used. Foam bubbles were observed upstream and downstream of the core with two variable-aperture visual cells, and a video camera recorded the bubble texture at the outlet of the core. They found two different foam-flow regimes as high and low quality. It was understood that a single model could characterize foam behavior. This model correlates the shift in predominance between flow regimes as permeability, foam formulation, and flow rates vary.

Sudhakar and Subhash, 2002 [43], worked on friction pressure loss correlation development for guar based foam fluids through coiled tubing. They run their experiments on foam flow loop investigating the rheology of gelled foams. The loop was capable of characterizing the rheological behavior of foam fluids of different chemical compositions at different qualities under various experimental conditions. Their study revealed that significant pressure drop in coiled tubing is observed as compared to that of a straight pipe. The pressure drop along coiled tubing was determined to be a function of Reynolds number. They proposed the pressure loss correlation to be used for different dimensions of coiled tubing.

Sudhakar and Subhash, 2002 [44], investigated rheological behavior of guar gel and guar foam fluids using a ½" pipe viscometer at 1000 psi and temperature ranges of 100 to 200^{o}F. In their study they developed a prediction methodology of consistency index and flow behavior index determination of guar foams. They concluded that for the shear rate of investigation foam fluid rheological behavior followed a power law model. They also mentioned that higher quality foams produced higher shear stresses and viscosities, and at high foam qualities the apparent viscosity of foam increased exponentially with foam quality.

Guo et al, 2003 [45], developed a model coupling frictional and hydrostatic pressure components in vertical and inclined boreholes. The model is accurate enough for

planning foam drilling. Gas to liquid ratio is an important factor affecting depth limit and ECD in stable foam drilling.

CHAPTER III

STATEMENT OF THE PROBLEM

The motivation behind conducting this research is to arrive to a foam characterization methodology that is going to take into account the influence of gas bubble size and the texture of foam. The result of this study is envisioned to be utilized in frictional pressure loss calculations, in order to have an improved rheological definition of the foam whilst carrying out underbalanced drilling operations. As of yet it is known that, in the literature; foam has been characterized focusing on a single surfactant and foam generation method. Therefore, if any parameter, such as the surfactant properties or the generation technique is changed, the rheological properties of the foam significantly change. Thus, there is a need for developing a more general rheological characterization of foam, which should not vary with different surfactant types and foam generation methods. This is possible if bubble size and texture of foam is taken into consideration when conducting a rheological analysis.

In this study, the rheological characterization of foam is aimed to be generalized independent of surfactant type and foam generation method by including the bubble size and texture information into rheological calculations.

The following methodology is used in this study:

- Extensive literature review
- Derivation of a generalized foam characterization methodology modifying the existing Volume Equalized Principle

- Conducting foam flow experiments through circular pipes, and during experiments, establishing the images of foam for analyzing the bubble size and texture
- Analysis of the pressure loss information as well as bubble size and texture information obtained from the experiments
- Developing a mathematical correction factor as a function of bubble size and texture which enhances the frictional pressure loss calculations

Verification of the developed model with the experimental data

CHAPTER IV

THEORY

4.1 Foam Flow

It is very difficult to characterize the rheological behavior of foams. Due to the decrease in the pressure in the flow direction, the gas phase in the foam tends to expand. Thus, the friction factor along the pipe is no more constant, as in incompressible fluids. Because of not having a constant friction factor along the flow direction, difficulties are raised in pressure loss predictions, and rheological characterization of the foam flow. So far, in the literature, the foam rheology could only be defined in relation to foam quality [21,24].

Fig 4.1 illustrates when a compressible fluid flows from a point of high pressure (1), to a low pressure (2), along a circular pipe.

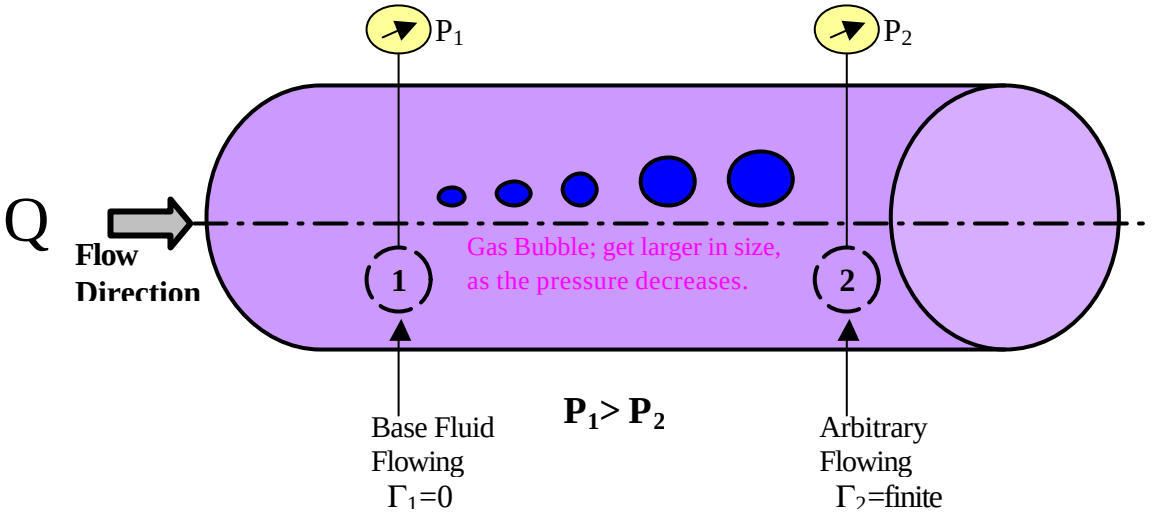

Figure 4. 1: Compressible Fluid Flow, after Winkler, 1992 [47].

Because of the frictional pressure losses, pressure at the second point along the flow direction is less than the first point. This would exert less pressure on gas bubbles, and would mean greater bubble sizes [15]. As the bubbles get larger in size, the quality will increase, causing the viscosity of the foam to rise. Having such a varying property along the flow path would mean that; the rheograms, i.e., shear stress vs. shear rate plots, cannot be developed as easily as for incompressible fluids.

Based on the continuity equation, the following relation can be written for a steady state flow condition;

$$\int_C \int_V (\vec{n})\, \rho v dA = 0 \quad \text{..... (4. 1)}$$

If the mass is conserved, and there is no accumulation Mass rate at point-1 and point-2 can be expressed as

$$\dot{m}_1 = \rho_1 v_1 \pi r^2 \quad \text{..... (4. 2)}$$

and

$$\dot{m}_2 = -\rho_2 v_2 \pi r^2 \quad \text{..... (4. 3)}$$

respectively. Since $\dot{m}_1 = \dot{m}_2$,

$$\rho_1 v_1 = \rho_2 v_2 \quad \text{..... (4. 4)}$$

Equation 4.4 means that, the product of velocity and density is constant at any point throughout the pipe with constant cross-sectional area. For all incompressible fluids

flowing in pipe of constant cross-section at a fixed temperature, the Reynolds number throughout the flow will be constant at a given mass flow rate and so the friction factor, since the density and viscosity of an incompressible fluid is not changing along the flow direction.

Foams, however when flowing through a pipe, will not exhibit a constant friction factor because of the compressibility in their nature, and the change in their viscosity.

It can be depicted from Fig 4.1 that, pressure at point 1 is greater than point 2. This means that, the gas bubbles would be under less pressure in point 2, and are greater in size than the ones at point-1. This would result in a higher quality level for point-2 when compared with point-1. Thus, there will be a variation in the wall shear stress in the flow direction.

4.2 Flow of a Compressible Fluid Through a Circular Pipe

A compressible fluid element flowing through a circular pipe can be represented as presented in Fig 4.2.

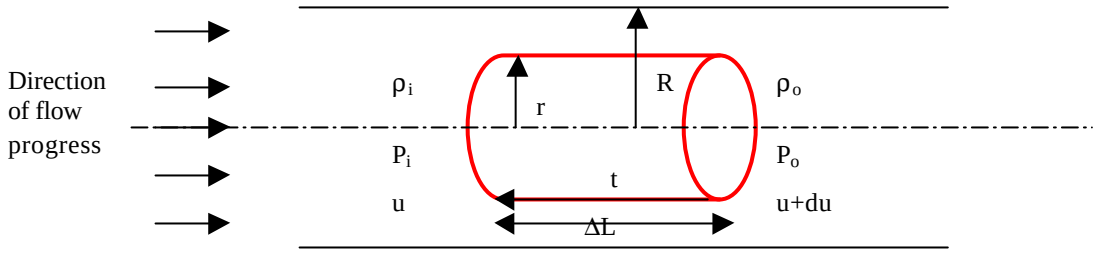

Figure 4.2: Free body diagram of a flowing medium inside a pipe.

Developing a force balance for this fluid element, and making necessary simplifications, shear stress at the wall can be derived as

$$t = \frac{\Delta P}{\Delta L}\frac{D}{4} - \frac{r_l}{e} rv \frac{dv}{\Delta L} \quad \text{..... (4. 5)}$$

where expansion factor, ε, is expressed as

$$e = \frac{r_1}{r_2} \quad \text{..... (4. 6)}$$

For a circular pipe, flow rate of a fluid can be derived as

$$Q = p\,\frac{R^3}{t_w^3}\int_0^{t_w} t^{\,2} f(t)\,dt \quad \text{..... (4. 7)}$$

after making necessary variable changes. Thus, solving equation 4.7 for the shear rate, $f(t)$, yields

$$f(t_w) = \frac{8v}{D}\left[\frac{3N+1}{4N}\right] \quad \text{..... (4. 8)}$$

where

$$N = \frac{\partial \ln t_w}{\partial \ln \frac{8v}{D}} \quad \text{..... (4. 9)}$$

Detailed derivation of Rabinowitsch-Mooney's Equation for compressible fluids, is presented in Appendix-B.

4.3 Slip Correction

Jastrzebski [49], observed the presence of slip at the wall of a conduit in which a fluid flows through. The effect of slip should obviously be considered in every rheology measurement.

Using the flow rate equation given in equation (B.7), as $Q = 2p\int_0^R vrdr$, it can be expanded as $Q = 2p\left[v\frac{r^2}{2} - \int\frac{r^2}{2}dv\right]_0^R$. The first term in the brackets on the left hand side of this equality would be dropped because of the assumption that, there was no slip at the pipe wall. However a slip is readily occurring there between the pipe wall and the flowing fluid. The slip coefficient introduced by Jastrzebski [49], is the ratio of slip velocity to the wall shear stress as given below,

$$b = \frac{v_s}{t_w} \quad \text{..... (4. 10)}$$

However, experimental analysis of the data indicated that, the slip coefficient has had to be modified as it was not only a function of shear stress, but also inversely proportional with the radius of the pipe, such as

$$b = \frac{b_c}{R} \quad \text{..... (4. 11)}$$

Modifying the flow equation, B.17, yields,

$$\frac{Q}{pR^3 t_w} = \frac{b_c}{R^2} + \frac{1}{t_w^4}\int_0^{t_w} t^2 f(t)dt \quad \text{..... (4. 12)}$$

Expanding the equation 4.12 gives,

$$\frac{\frac{p}{4}D^2 v}{p\left(\frac{D}{2}\right)^3 t_w} = \frac{b_c}{\left(\frac{D}{2}\right)^2} + \frac{1}{t_w^4}\int_0^{t_w} t^2 f(t)dt \quad \text{..... (4. 13)}$$

After necessary simplifications, equation 4.13 can be expressed as

$$\frac{8v}{D} = \frac{16 b_c t_w}{D^2} + \frac{1}{t_w^3} \int_0^{t_w} t^2 f(t) dt \quad \text{..... (4. 14)}$$

If a plot of $\frac{8v}{D}$ vs. $\frac{1}{D^2}$ is drawn, the slope would be $16 b_c t_w$. Since the value of t_w is known, the correction coefficient could be determined.

The relation between the observed flow rate and actual (true) flow rate including the effect of slip can be expressed as;

$$Q_{Observed} = Q_{True} + Q_{Slip} \text{..... (4. 15)}$$

From equation (4.15) it can be stated that,

$$\left(\frac{8v_{avg}}{D} \right)_{Observed} = \left(\frac{8v_{avg}}{D} \right)_{True} + \left(\frac{8v_{Slip}}{D} \right) \text{..... (4. 16)}$$

Expanding the slip term in equation 4.16 yields,

$$\left(\frac{8v_{avg}}{D} \right)_{Observed} = \left(\frac{8v_{avg}}{D} \right)_{True} + 16 b_c t_w \frac{1}{D^2} \text{..... (4. 17)}$$

After determining the slip term, as presented in equation (4.12), the slip correction could be carried out by means of the following equation,

$$\left(\frac{8v_{avg}}{D} \right)_{True} = \left(\frac{8v_{avg}}{D} \right)_{Observed} - \left(\frac{16 t_w}{D^2} \right) b_c \text{..... (4. 18)}$$

4.4 Generalized Volume Equalized Principle

An incompressible fluid would flow through a pipe with a constant Reynolds number, and friction factor, provided that the fluid velocity, density, viscosity, and the cross-sectional area of the pipe are constant. However, the Reynolds Number is not constant for a compressible fluid flow case, as considered in Fig 4.1. "*Volume Equalized Principle* (VEP)" assumes that, the friction factor along the flow path, for a constant diameter pipe and isothermal conditions, would be assumed as constant. It is known that, friction factor is a function of Reynolds number, i.e.,

$$f_f = f(N_{\mathrm{Re}}) \quad \text{..... (4. 19)}$$

According to the VEP, for any two arbitrary points taken in the flow direction, the friction factors for these points will be equal to each other. In other words, the Reynolds numbers for these points are assumed to be equal. Mathematically;

$$f_{f_1} = f_{f_2} \Rightarrow N_{\mathrm{Re}1} = N_{\mathrm{Re}2} \quad \text{..... (4. 20)}$$

If the Reynolds Number, in a basic form, is given as follows,

$$N_{\mathrm{Re}} = \frac{\rho v D}{\mu} \quad \text{..... (4. 21)}$$

and since the pipe has a constant cross-sectional area, the Reynolds Number at two different points is equalized as

$$\frac{\rho_1 v_1 D}{\mu_1} = \frac{\rho_2 v_2 D}{\mu_2} \Rightarrow \frac{\mu_2}{\mu_1} = \frac{\rho_2 v_2}{\rho_1 v_1} \quad \text{..... (4. 22)}$$

The ratio of the viscosities is equal to the ratio of the mass flow rates, at two different locations. In general, viscosity is expressed as

$$m = \frac{t_w}{g} \quad \text{..... (4. 23)}$$

Shear rate is the ratio of the velocity of the fluid to the pipe diameter,

$$g = \frac{8v}{D} \quad \text{..... (4. 24)}$$

Substituting Equation (4.24) into equation (4.23), one would determine the viscosity as

$$g = \frac{8v}{D} \Rightarrow m = \frac{t_w}{\frac{8v}{D}} \quad \text{..... (4. 25)}$$

It is proven that the equation of continuity will yield the following relation,

$$\int_C \int_V (\vec{n})\, rvdA = 0 \quad \text{..... (4. 26)}$$

Mass flow rate at one location is known to be the same,

$$\dot{m}_1 + \dot{m}_2 = 0$$

where

$$\dot{m}_1 = r_1 v_1 p r^2 \quad \text{..... (4. 27)}$$

and

$$\dot{m}_2 = -r_2 v_2 p r^2 \quad \text{..... (4. 28)}$$

Thus, from equations (4.27) and (4.28) it can be found that

$$r_1 v_1 = r_2 v_2 \quad \text{..... (4. 29)}$$

Using this equality, equation 4.19 becomes

$$\frac{m_2}{m_1} = \frac{r_2 v_2}{r_1 v_1} = 1 \quad \text{..... (4. 30)}$$

Using equation (4.25), a relation in between shear stresses and superficial velocities is given as follows,

$$\frac{\frac{t_{w_2}}{8v_2}}{\frac{t_{w_1}}{8v_1}} = \frac{r_2 v_2}{r_1 v_1} = 1 \Rightarrow \frac{t_{w_2}}{t_{w_1}} = \frac{v_2}{v_1} \quad \text{..... (4. 31)}$$

What equation (4.31), gives is the direct relation of the ratio of the shear stresses with the ratio of the velocities. Also, from equation (4.30), the following relation can be derived,

$$\frac{v_2}{v_1} = \frac{r_1}{r_2} \quad \text{..... (4. 32)}$$

Equation (4.31) depicts that, the wall shear stress at the first point (as in Fig. 4.1) can be acquired if the ratio of the velocity at the second point to the first is divided by the

shear stress of the second point. Valko and Economides [27] called this ratio, as e, ***specific volume expansion ratio.*** The ratio can be given as follows,

$$e = \frac{r_1}{r_2} = \frac{v_2}{v_1} = \frac{t_{w_2}}{t_{w_1}} \Rightarrow t_{w_1} = \frac{t_{w_2}}{e} \quad \text{..... (4. 33)}$$

The same relation of normalization is achieved by using the relation in equation (4.33);

$$v_1 = \frac{v_2}{e},\ g = \frac{8v}{D} \text{ and so } g_1 = \frac{g_2}{e} \quad \text{..... (4. 34)}$$

Plotting $\frac{t_w}{e}$ vs. $\frac{g}{e}$ will result in normalizing the foam rheograms for different foam qualities on to a single master curve, so that, instead of representing the foam with different rheological parameters for different qualities, foam rheological characterization can be determined using general master parameters for all foam qualities.

It has been shown in Appendix-B that, Rabinowitsch-Mooney characterized the fluid using two "general" parameters. Their approach, when used for plotting flow curves will result in having different K_M' and N_N' values for different foam quality values. General form of this approach is presented as

$$t_w = K'_{GEVE}\left(\frac{8v_{slipcorrected}}{D}\right)^{N'_{GEVE}} \quad \text{..... (4. 35)}$$

After plotting the flow curves based on this definition, one would end up with different K'_M and N_N' values corresponding to different foam qualities, making the foam characterization rather more complex to deal with. In this study, Rabinowitsch-Mooney's generalized model is combined with VEP, and a very general foam

characterization method is developed, in which for all foam qualities, the foam can be expressed using only two master rheology parameters, namely, $K_M^{'}$ and $N_N^{'}$. Simply, left hand side and right hand side of equation 4.35 is divided by specific volume expansion ratio, i.e.,

$$\frac{t_w}{e} = K_{GEVE}^{'}\left(\frac{\left(\frac{8v_{slipcorreated}}{D}\right)}{e}\right)^{N_{GEVE}^{'}} \quad \text{..... (4. 36)}$$

Expanding equation (4.36) yields,

$$t_w = K_{GEVE}^{'} e^{1-N_{GEVE}^{'}}\left(\left(\frac{8v_{slipcorreated}}{D}\right)\right)^{N_{GEVE}^{'}-1}\left(\frac{8v_{slipcorreated}}{D}\right) \text{..... (4. 37)}$$

The Generalized Reynolds Number is expressed as,

$$N_{RE} = \frac{8^{1-N_{GEVE}^{'}} rv^{2-N_{GEVE}^{'}} D^{N_{GEVE}^{'}}}{K_{GEVE}^{'}} = \frac{8rv^2}{t_w} \text{..... (4. 38)}$$

Inserting equation 4.37 into equation 4.21, Generalized Volume Equalized Reynolds number, including the specific expansion factor, can be derived as

$$N_{RE} = \frac{8^{1-N_{GEVE}^{'}} rv^{2-N_{GEVE}^{'}} D^{N_{GEVE}^{'}} e^{N_{GEVE}^{'}-1}}{K_{GEVE}^{'}} \text{..... (4. 39)}$$

The friction factor for laminar flow region would be given as;

$$f_{GENVE} = \frac{16}{N_{\mathrm{Re}_{GENVE}}} \text{..... (4. 40)}$$

In this study, apart from K'_{GEVE} and N'_{GEVE} values, the texture and bubble size of foams are also going to be scrutinized in the characterization methodology.

CHAPTER V

EXPERIMENTAL SET-UP

An experimental set-up is constructed to conduct experiments of this study. The set up is mainly composed of four parts, *horizontal pipe flow measurement* section, *pumping equipment*, *fluid quantity measurement/adjustment*, and *recording* devices, as shown in Fig. 5.1.

5.1 Horizontal Pipe Flow Measurement Section:

Horizontal pipe flow measurement section is connected to the foam flow line. The flow loop consists of four different diameter stainless steel, horizontally aligned smooth pipes, each with a length of 5 m. Fluid is let to flow through one of the four pipes at a time. The inner pipe diameters are 0.50 in, 0.75 in, 1.00 in, and 1.50 in (1.27 cm, 1.91 cm, 2.54 cm, and 3.81 cm).

Three pressure transducers are used to measure the pressure along the pipes while fluid is flowing. Pressure taps, through which pressure is measured, are formed by small holes carefully drilled through the pipe walls and rounded slightly on the inside by means of a fine file to remove burs. Aligned transducers had a capacity of 0-30 psig each. Transducers on each pipe are located 2 m away from each other and 0.5 m from the pipe ends, as given in the Fig. 6.1. The positions of the transducers are selected considering the end effects, as described by Govier and Aziz [51]. The distance required achieving fully developed flow profile if given as follows, in equation 5.1;

$$\frac{X_E}{D} \geq 50 \quad \text{..... (5.1)}$$

where X_E is the length of the flow conduit, and D is its diameter. Second and Third transducers are taken into consideration for pressure loss information.

There are visual cells backed up with the pressure transducers in the middle of each individual horizontal pipe. The digital photographs of each foam sample generated during a test have been taken in order to be analyzed using digital image processing methods for developing a relation related with the bubble size and texture of foams.

Liquid and gas flow rates can be adjusted for generating the desired foam quality and flow rate.

Two different foam generators are used during this study, which are constructed using metal screens with different mesh sizes; the screens were rolled and inserted into foam generator. One of the foam generators was 8.38 # (mesh), and the other 17 #. *Mesh* is defined as the number of apertures per unit area of a screen (sieve).

In the course of experiments, two different surfactants have been used. *Half-life* tests were performed to investigate the critical surfactant concentration of the surfactants and water, as described in Appendix-A.

Appendix-F gives the ranges of the data gathered. Liquid/Gas flow rates, quality, average bubble diameter, circularity , and pressure loss parameters are given.

5.2 Pumping Equipment:

A centrifugal liquid pump and a piston-type compressor are used to inject liquid and air, respectively. The 0.75-HP liquid pump has a capacity of pumping 40 gpm of liquid at 15 psi pressure, and the gas compressor has a capacity of 200 scfm of air at

70 psi. A magnetic liquid flowmeter and a turbine gas flowmeter are used for flow rate measurements. Based on the flowmeter readings, necessary adjustments are made for establishing the desired flow velocities and qualities.

5.3 Measurement (Recording) Devices:

The system was capable of observing and recording all of the necessary parameters on real-time basis.

Data acquisition system comprised of inputs from transducers, and flowmeters connected to a data logger, which ends up in the computer in order to archive the data. Data Recorder could record data up to 16 channels on the basis of 4-20 mA signal range, and get the average of 1 minute reading of data with 1-second sampling rate.

5.4 Image Analysis:

Image photography was taken from each pipe at the mid point. A plexiglas of 12 cm nominal ID was used for the housing to the foam samples and a circular glass of 8 cm in diameter was placed into the plexiglas with a clearance of 2 mm in between. Fig. 6-2 gives the drawing of the view cells.

Foam is collected into the visual cell. A microscope is used in order to magnify, so that foam structure can be viewed better and in more detailed way. A digital photo is taken through the vision port of the microscope by using an aparatus that magnifies the image 40 times. “ImageJ”, image analysis program, then, analyzes the images.

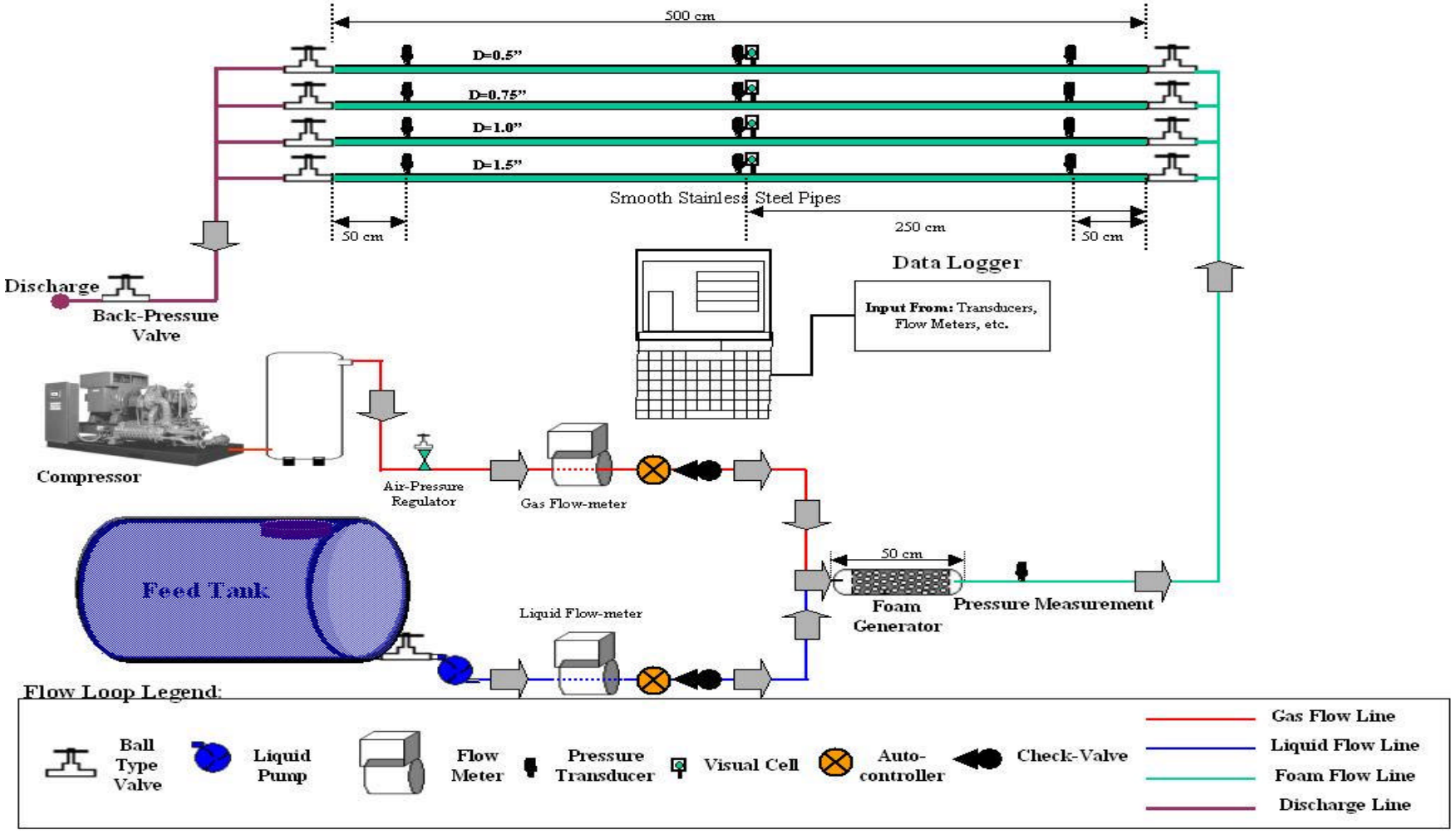

Figure 5. 1: Experimental Set up Flow Loop.

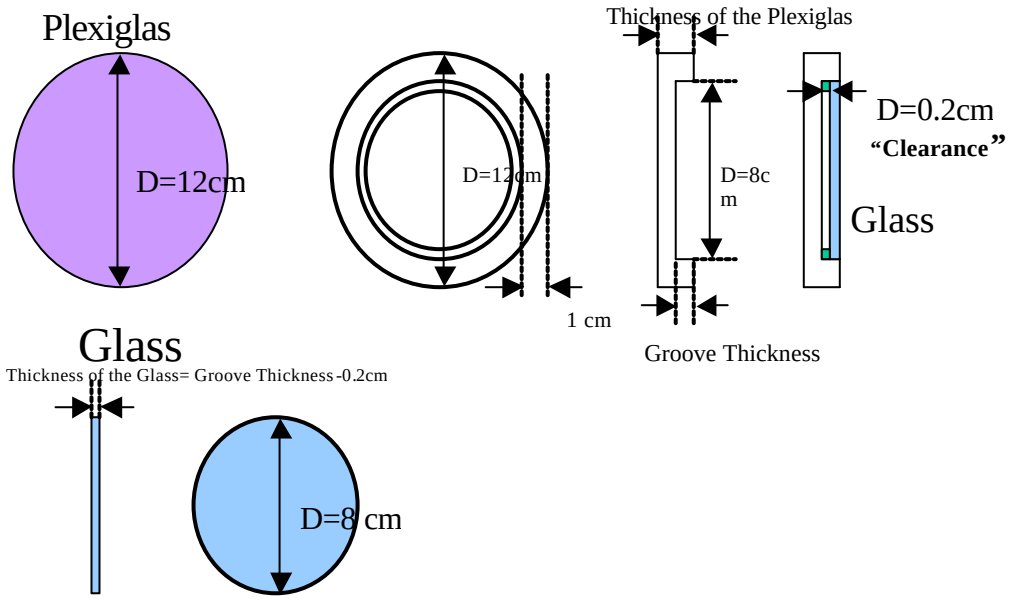

Figure 5. 2: Visual Cell Specifications.

5.5 Experimental Procedure for Foam Flow:

Experiments were conducted in room temperature, at an altitude of 3215ft (980m), an elevation read by GPS (Global Positioning System) instrument. The normal atmospheric pressure at the altitude of laboratory was calculated to be 12.975 psia. And so air density was calculated to be 1.0384 g/l.

The predetermined percent volume of surfactant is mixed with tap water in the tank. Desired flow rate of liquid is let to flow through liquid line in order to be mixed with gas that is also adjusted to the desired flow rate, so as to have a predetermined quality of foam at a certain point along the pipe, e.g. at the point where the middle pressure transducer is located. A pressure transducer placed at the junction point where gas and liquid phases meet, just before the foam generator, gives the gas pressure, in order to be included in calculations, to have the accurate flow rate of gas at the other locations of the loop by using *real gas law*. The generated foam is flowed through only one pipe at a time. Along the smooth pipes there are two points from which pressure readings are acquired. The data logger is connected to the computer, so that real time values are easily monitored, as both liquid / gas flow-rates, pressure readings are all consistent the average of the last 60 seconds are

recorded, simultaneously with capturing of the image. Every test is recorded with its reference code (e.g. its date, and respective time), liquid/gas flow-rates, and gauge pressure readings.

The laboratory scale experiments were carried out on an experimental set-up that was mainly composed of pipe viscometers of four different pipe diameters. Experimental data was acquired on real time basis, and recorded for each individual liquid and gas flow rate, values. For each reading six different parameters, i.e., three pressure transducer readings, gas pressure reading at the gas flow meter, liquid and gas flow rates, were recorded, those of which were used in rheogram building of foam flown through the experimental set-up.

The two different foam surfactants and their respective foam generator are termed as Birka Old, Birka New, Henkel New, and Henkel Old. Birka Old meaning that Birka Surfactant analyzed by 8.38 Mesh foam generator, and Birka New, meaning that Birka Surfactant analyzed by 17 Mesh foam generator, and so fort.

CHAPTER VI

RESULSTS and DISCUSSION

In this chapter, rheology of foam is characterized using the experimental data acquired from the constructed set-up. Three different processing applications were adopted to analyze the experimental results including pressure loss data, and digital images of investigated foams. These are;

- Rheological Prediction (**Calculated**)
- Image Based Prediction (**Image**)
- Image and Rheology Based Prediction (**Image Calculated**)

Rheological Prediction is the shear rate estimation methodology adopted after having determined the generalized parameters of the non-ionic surfactant and its respective foam generator experimented. Image Based Prediction is the methodology in which the generalized parameters are calculated as a function of circularity, and average bubble diameter, and substituted into a rheology equation of which will determine the shear stress as a function of shear rate. Image and Rheology Based Prediction is the methodology that includes the correction coefficients, which are a function of circularity, and average bubble radius, and will be multiplied by the calculated shear rate values.

The laboratory scale experimental pipe viscometer loop provided accurate definition of foam rheology by using *Generalized Volume Equalized Principle*, discarding the slip effect along the pipe wall, and quality dependency of foam rheology definition. The experimental matrix for this study is given in Appendix-F. The bubble size and

texture of the foam is measured in high accuracy and processed by image analysis methods. It is observed that no interaction of bubbles with each other took place up to 85% quality level. When bubbles come into contact with their neighbors, they distorted their boundaries and formed polyhedral like cells. The films shared between the bubble boundaries restricts the motion of the neighboring cells, yielding to formation of an apparent yield stress, causing the foam to move as a rigid plug. In accordance to these findings, there was a gradual expansion in bubble size after 85% quality for Henkel, and 90% quality for Birka.

6.1 Rheological Analysis

Rheological analysis of the acquired data is conducted by extensive amount of calculation. At the end of an individual experiment, in-situ liquid and gas flow-rates are the main parameters from which necessary parameters are derive. Appendix-E gives an example calculation for the determination of corrected shear stress-shear rate values.

The procedure for rheology analysis is given as follows,

1. Draw Generalized Volume Equalized shear stress vs. shear stress graph, ($\frac{t_w}{e}$ vs. $\frac{g_{Corrected}}{e}$)
2. Discard the slip effect, follow Appendix-C
3. Draw Slip corrected, Generalized Volume Equalized rheogram, determine N_{GEVE}' and K_{GEVE}'.

Volume Equalizing the shear stress and shear rate, e.g. dividing each term by specific expansion ratio, ε, draws the Generalized Volume Equalized rheogram curve. The slip effect when discarded gives the true values to be utilized in rheogram drawing of the acquired data; Appendix-C is a good reference for slip discarding procedure.

Once the slip corrected rheogram is drawn the reading of Generalized Volume Equalized Parameters are easily observed.

Fig. 6.1 gives the general rheology curve for the surfactants, and the foam generator types used. *Generalized Volume Equalized Principle* approach adopted to have single medium phase to define better rheology behavior and undesirable wall slip effects adversely affecting rheological behavior are discarded. The detailed slip analysis of each foam sample is given in Appendix-C. The graph below does include two different surfactant types used in the experiments, however it is observed that four different rheological behaviors are presented, this is because of using different foam generators.

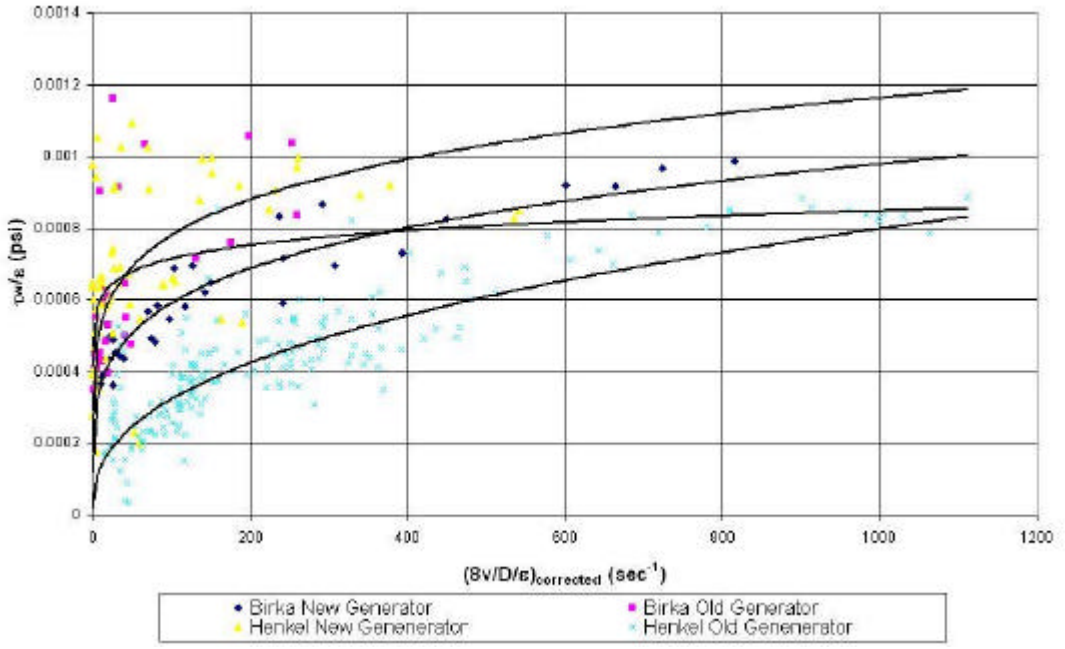

Figure 6.1: Generalized Volume Equalized Rheology Curve for two different Surfactants and Foam Generation methods.

Table 6.1 gives the results of generalized parameters found as a result of the study, for two surfactants and their respective foam generators used.

Table 6 1: Generalized parameters found as a result of the study.

Surfactant and foam generator used	K'_{GEVE} (psi. sec^N)	N'_{GEVE}
Birka-old Foam Generator	0.000223	0.2285
Birka-new Foam Generator	0.000183	0.2142
Henkel-old Foam Generator	0.000053	0.3975
Henkel-new Foam Generator	0.000344	0.1202

6.2 Image Analysis

Appendix D gives the scale calibration of the acquired images. Captured photos are first opened up in the "ImageJ" window, and then converted into 8-bit format, as in Fig. 6.2. The 8-bit data consists of data, amplitudes of which are a function of the light intensity; colour information in this gray-scale data has been discarded. Every sample has an amplitude, and a number varying from 0 to 255, corresponding to black, and white respectively.

The region of interest is selected and the program will allow passage of signals, corresponding to desired binary data setting a threshold value. The allowed signals can be observed in Fig. 6.3. In threshold image, binary coded image has two values; each pixel corresponds either to 1 or 0 being black or white respectively.

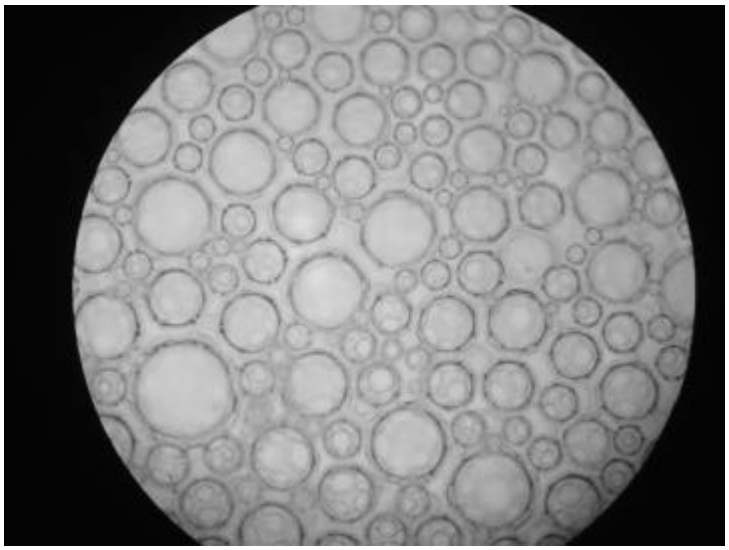

Figure 6. 2: 8-bit image.

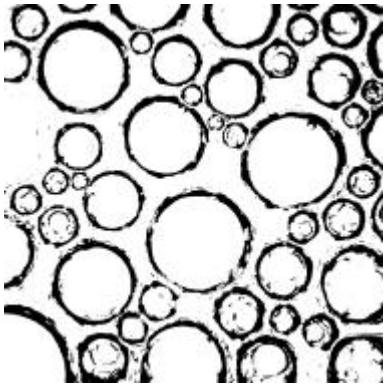

Figure 6. 3: Threshold image, of selected section.

Fig.6.4 shows the image of analysed image, each and every pixel in this image is accounted in the analysis. If the pixels do form a closure, their perimeter, size, circularity, and location is determined by the programme. The individual pixels those, which will disorder the accurate determination of foam bubbles, are discarded in the evaluation of the foam bubble characteristics determination.

Each and every pixel in analysed image is given a number, so that necessary application can be carried out. The encircled figures are recorded to be foam bubbles, together with their average radius, and circularity. In the calibration process of the image analysis program it was noticed that the program could not tag

the circularity of even perfect circles as 1. There was approximately 10% underestimation. So all of the results of the image processing is slightly biased.

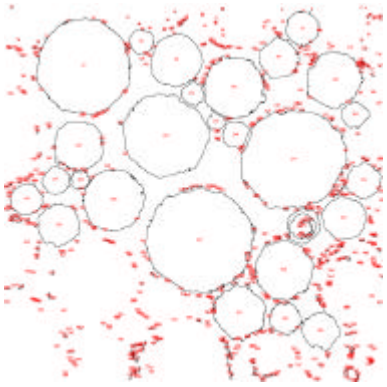

Figure 6. 4: Analysed image.

The procedure for image analysis is given as follows,

1. Convert the image into 8-bit data,
2. Define the scale, check Appendix-D
3. Pass only the threshold value in order to analyze the foam bubbles,
4. Get the average size and circularity of each and every foam bubble.

6.3 Image Analysis Results

Predicting pressure loss of foam flowing through a circular conduit of known distance is more accurate if average bubble size and texture information are included in calculations. Texture of the foam is defined as circularity in equation 6.1.

$$Circularity = \frac{4 \times p \times A}{Perimeter^2} \quad \text{..... (6. 1)}$$

where *A*, is the area of the bubble. When circularity approaches 1, the bubbles are more like a circle in shape, and when approaches to 0, more polyhedral like in shape.

Fig. 6.5 through Fig. 6.8 gives the Average Diameter and Circularity vs. Quality relation for two Surfactants and Foam Generators used in the experiments. Fig. 6.5 is the curve drawn for Average Diameter and Circularity vs. Quality for Birka Old. Quality level increases with increasing average diameter. This means that an increase in average bubble size is in close relation with the quality.

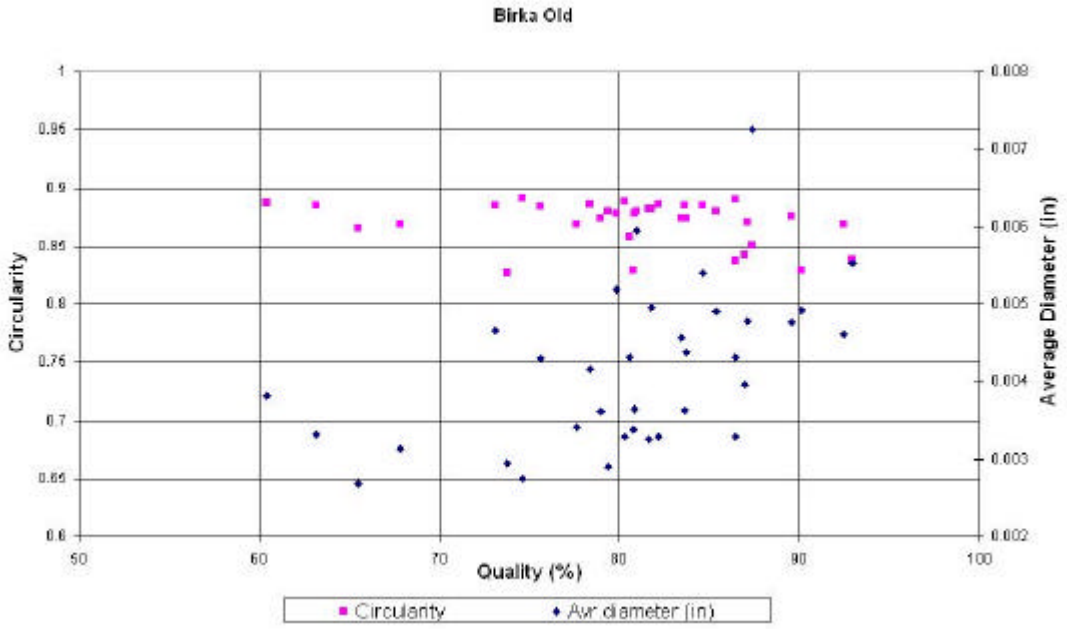

Figure 6. 5: Average Diameter and Circularity vs. Quality, Birka Old.

Fig. 6.6 is the same curve except with a different type of foam generator (FG) used, this time 17 Mesh. When the mesh size increases the number of apertures per unit length increases, and so the screen of the foam generator becomes finer. When the two curves are compared one would realize that finer FG, in this case 17 Mesh FG, produced finer foam bubbles, and relatively higher quality levels of foam. This would also be commented, as there is a relation in between foam bubble dimensions and its quality levels.

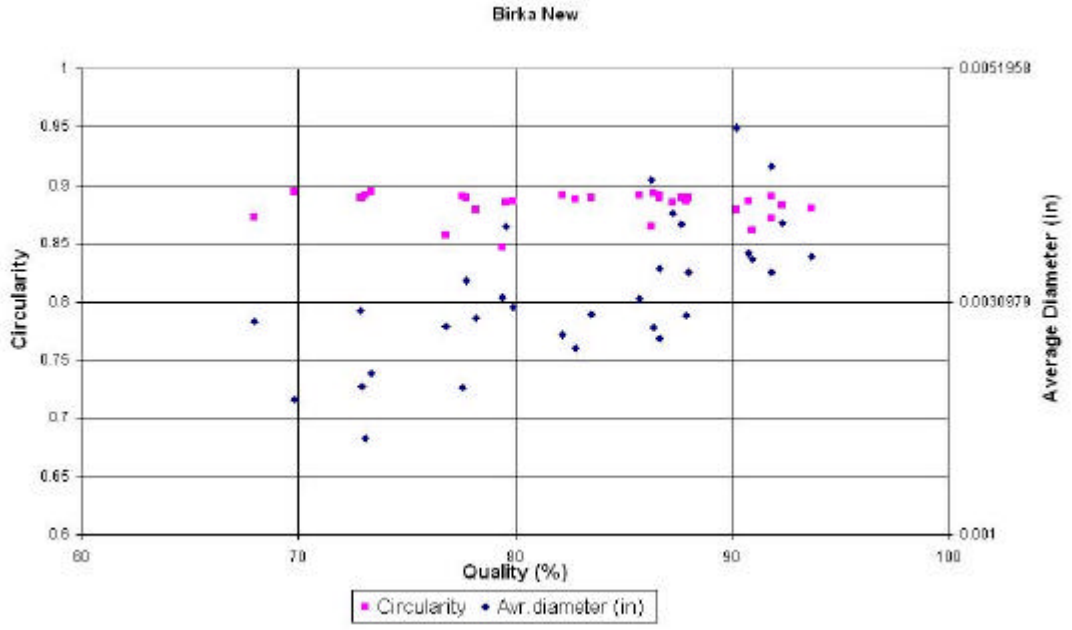

Figure 6. 6: Average Diameter and Circularity vs. Quality, Birka New.

When Fig. 6.7 and 6.8 are observed the same relation in the above two curves are valid. Fig. 6.7 is for Henkel Old, and when quality increases average diameter increased gradually. Also with increasing quality there is a slight decrease in circularity owing to non-circular bubble generation with increased air to liquid ratio.

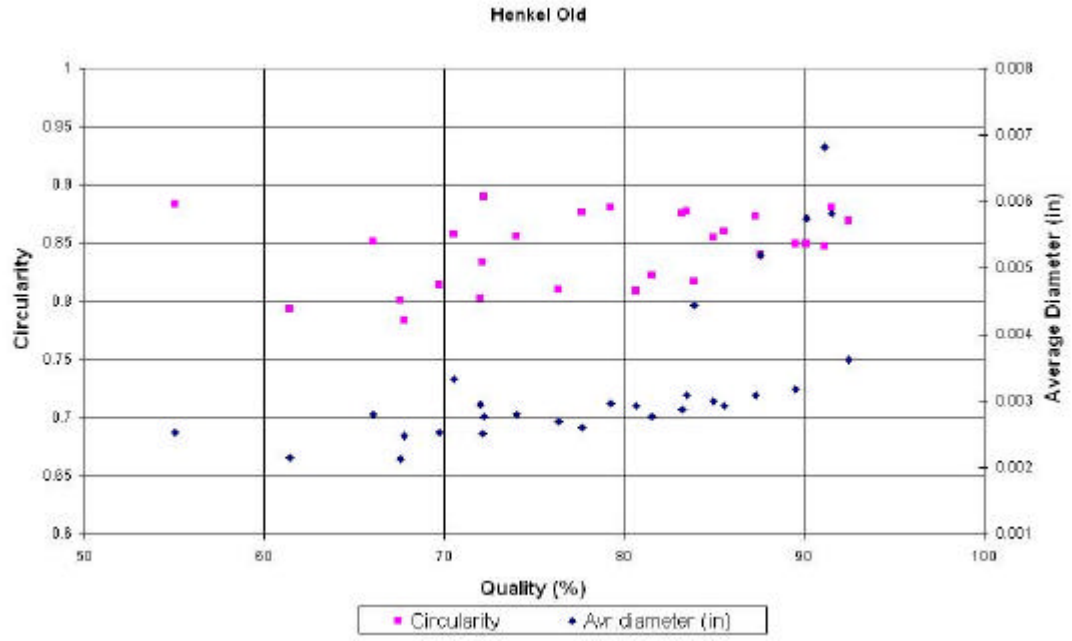

Figure 6. 7: Average Diameter and Circularity vs. Quality, Henkel Old.

FG in Fig. 6.8 generates finer foam bubbles, and there is also an increasing trend of average bubble diameter with increasing foam quality.

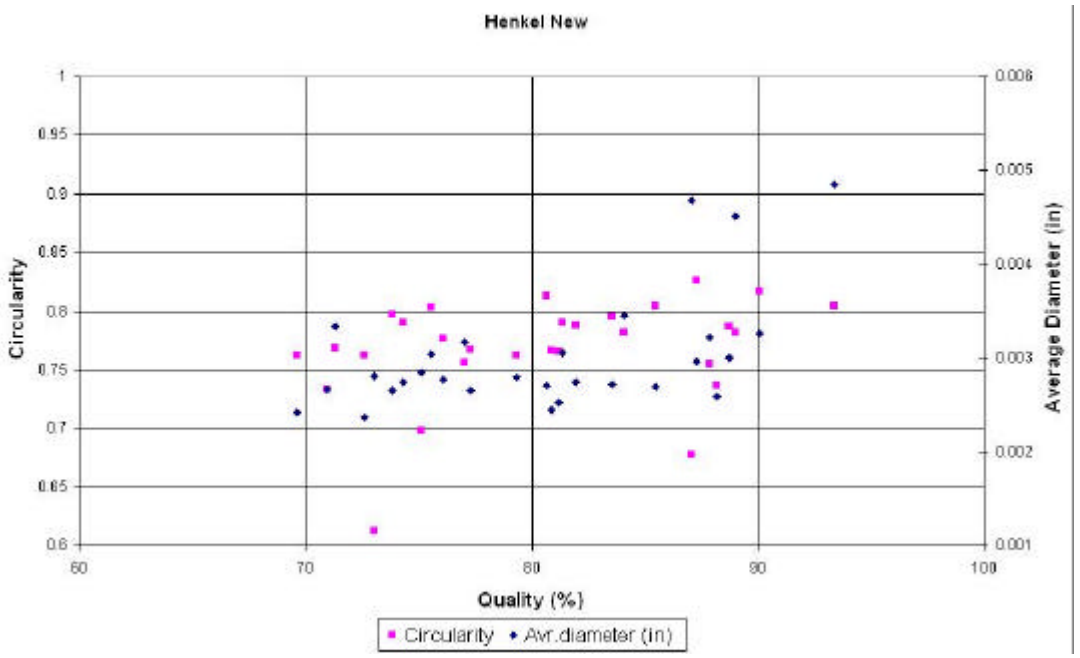

Figure 6. 8: Average Diameter and Circularity vs. Quality, Henkel New.

Fig. 6.9 and Fig.6.10 are the two graphs of K'_{GEVE} and N'_{GEVE} versus mean circularity and mean average diameter, respectively. It is observed that there is a definite relation in between mean circularity and mean average diameter. This is the testimony of the existing relation in between rheological constants and average bubble size, and texture of the foam bubbles.

Fig. 6.9 gives the relation in between K'_{GEVE} vs. Mean Circularity, and Mean Average Diameter, x-axis is the K'_{GEVE}, and the axis on the left of y is mean circularity, circularity is first in a trend of increase than in a decrease with increasing K'_{GEVE}.

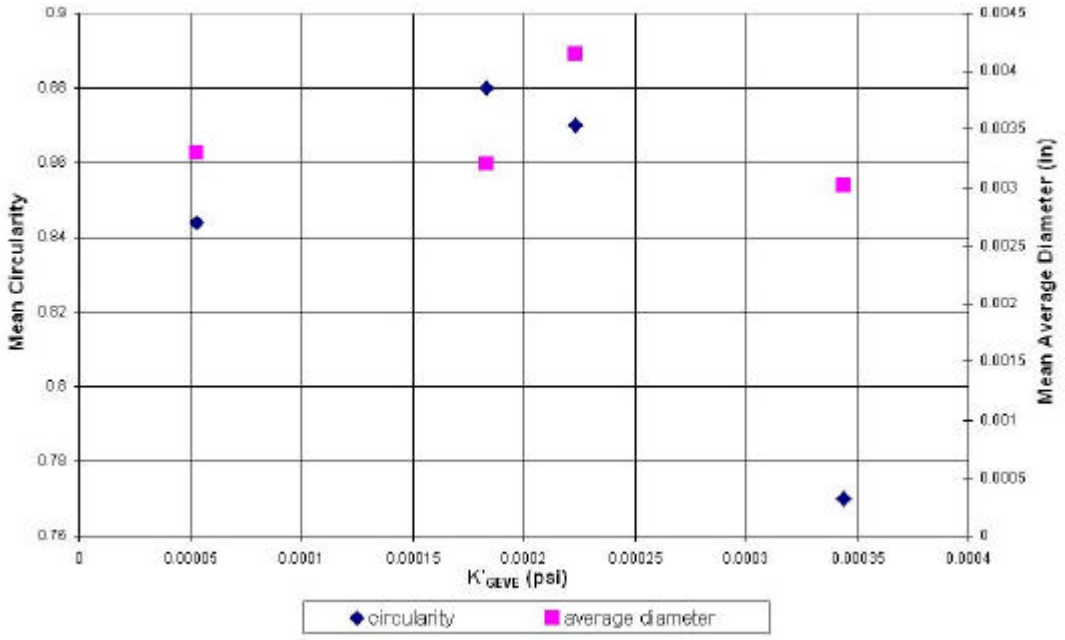

Figure 6. 9: K'_{GEVE} vs. Mean Circularity and Mean Average Diameter.

Fig. 6.10 is the N'_{GEVE} and mean circularity and mean average diameter. As given in equation 6.1 circularity is the parameter how much a shape resembles a perfect circle, the more the circularity is close to 1 the more the shape is circular. There is a decreasing trend of K'_{GEVE} when plotted against circularity, however the trend is increasing when circularity is drawn against N'_{GEVE}, this means that a foam with greater value of N'_{GEVE} is much more circular in shape than with foams of less value of N'_{GEVE}.

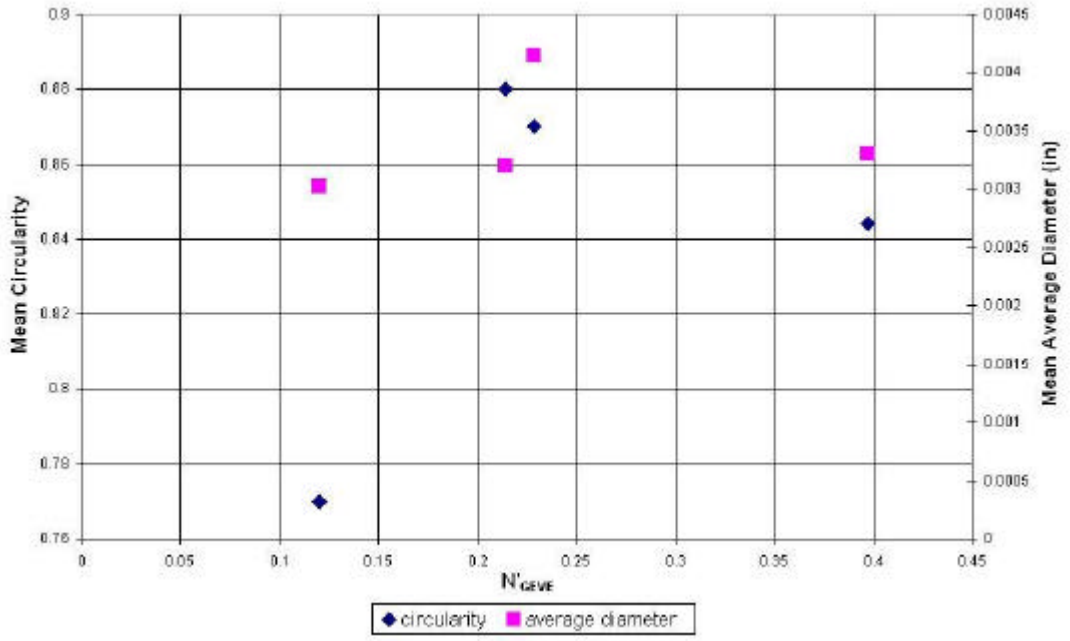

Figure 6. 10: N'_{GEVE} vs. Mean Circularity and Mean Average Diameter.

Using information provided in Fig. 6.9 and Fig. 6.10, K'_{GEVE} and N'_{GEVE} are determined by means of the following equations, equation 6.2, and 6.3,

$$N'_{GEVE} = 5.25 * 10^{7} * \mathrm{Cir}^{(1.585)} * \mathrm{d}_{ave}^{(3.314)} \quad \text{..... (6. 2)}$$

$$K'_{GEVE} = 2.57 * 10^{-4} * \mathrm{Cir}^{(-38.3905)} * \mathrm{d}_{ave}^{(0.856735)} \quad \text{..... (6. 3)}$$

Because the N'_{GEVE} term is dimensionless the given coefficient in the equation 6.2 does bear the necessary terms in order to have a dimensionless N'_{GEVE} value. The same modification is also adopted in the calculation of K'_{GEVE} so as to have the proper unit, $psi.sec^{N}$.

6.4 Results of the Analysis

The three different methodologies to better define the foam behavior were adopted in the course of this study. Different methodologies investigated the foam behavior

by taking into account only rheology affects, only image effects, and combination of both.

6.4.1 Rheological Prediction (Calculated)

In this study effects of compressibility, and the slip along the pipe wall are discarded, by adopting ***Generalized Volume Equalized Principle***. After having determined rheological parameters, N'_{GEVE} *and* K'_{GEVE} of a specific surfactant with its respective foam generator, a **calculated** rheological behavior could be determined by substituting the determined rheological parameters for a desired shear rate into the following equation, equation 4.36.

$$\left(\frac{t_w}{e}\right)_{Calculated} = K'_{GEVE}\left(\frac{\left(\frac{8v_{slipcorreaed}}{D}\right)}{e}\right)^{N'_{GEVE}} \quad \text{..... (6. 4)}$$

6.4.2 Image Prediction (Image)

In this correction methodology only image parameters are the required inputs, in order to have a good estimate of the shear stress. Calculation of K'_{GEVE} and N'_{GEVE} are already given in equation 6.2 and equation 6.3 as a function of average bubble diameter and circularity.

The following equation will use the K'_{GEVE} and N'_{GEVE} parameters as input and derive an only *image* corrected shear stress.

$$\left(\frac{t_w}{e}\right)_{Image} = K'_{GEVE}\left(\frac{\left(\frac{8v_{slipcorrected}}{D}\right)}{e}\right)^{N'_{GEVE}} \quad \text{..... (6. 5)}$$

6.4.3 Image + Rheology Prediction (Image Calculated)

A correction factor is determined from statistical analysis in order to include the Circularity, and Average Diameter to have a better estimate of shear rate. Statistical analysis was conducted by including as many data as possible, then running a matching equation to give a corrected form of Image Calculated prediction. The following correction factors were found,

Table 6 2: Image Correction Factors.

Surfactant & Foam Generator	Correction Factor (C)
Birka New	$4.18*10^{-1}*d_{ave}^{(-1.55E-12)}*Cir^{1.8E-1}$
Birka Old	$8.87*10^{-1}*d_{ave}^{(1.27E-2)}*Cir^{(-1.33)}$
Henkel New	$2.98*10^{-12}*d_{ave}^{(-4.18)}*Cir^{(-6.28)}$
Henkel Old	$0.12*d_{ave}^{(-0.55)}*Cir^{(4.57)}$

By using C (*Image Correction Coefficient*) as given in Table 6.2, Image Corrected shear stress values could be found. The coefficient after having been determined is multiplied by the calculated volume equalized shear stress. Although the correction coefficients are readily determined for this study the next correction step would not need the determination of correction coefficients, instead giving a relation to be of use for all applications.

$$\left(\frac{t_w}{e}\right)_{ImageCorrected} = C*\left(\frac{t_w}{e}\right)_{Calculated} \quad \text{..... (6. 6)}$$

6.5 Analysis Results

Fig. 6.11 gives the comparison of the predicted shear stresses, for Birka Old, x axis is the experimental volume equalized shear stress, and the y-axis is the predicted respective corresponding value. The solid line gives the perfect match of the experimental results and the calculated results. Dashed lines are ±20 % error. The graph below gives that the rheologically calculated, and image based calculated points are in a better fit when compared to only image predicted values.

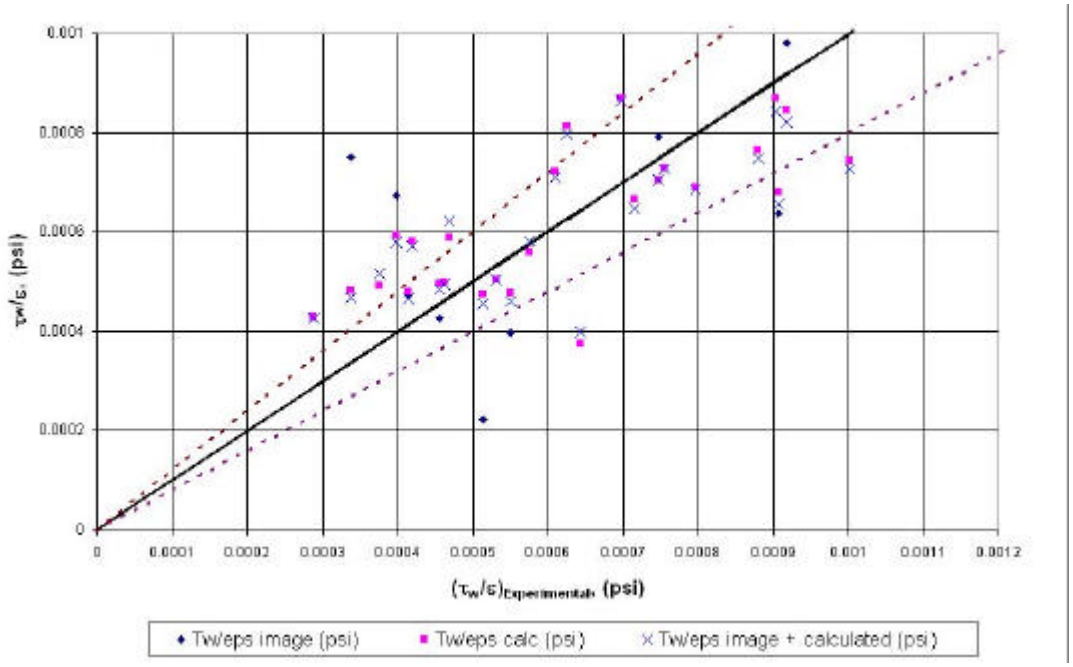

Figure 6. 11: Birka Old Prediction Comparison.

Fig. 6.12 is the comparison of the predicted values for Birka New. In this graph as well the orientation of rheology calculated, and image based calculated values are in a better fit than only image based prediction, pointing that a good estimate of rheology behavior is able to be determined by image calculated values.

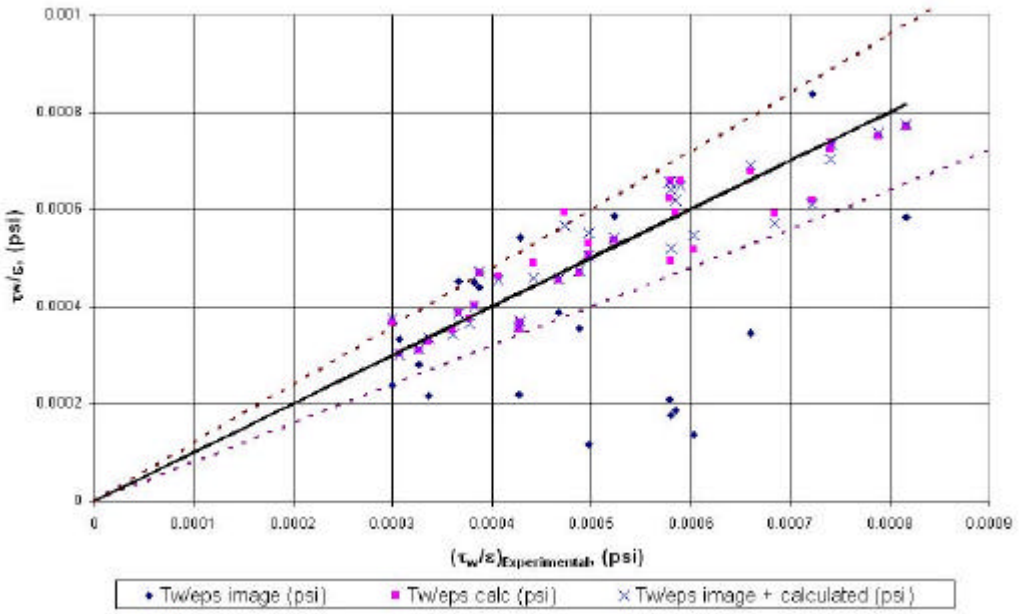

Figure 6. 12: Birka New Prediction Comparison.

Fig.6.13 is the prediction comparison graph for Henkel Old. In this graph as well the only image-based prediction appears to be weak when compared to other prediction methodologies.

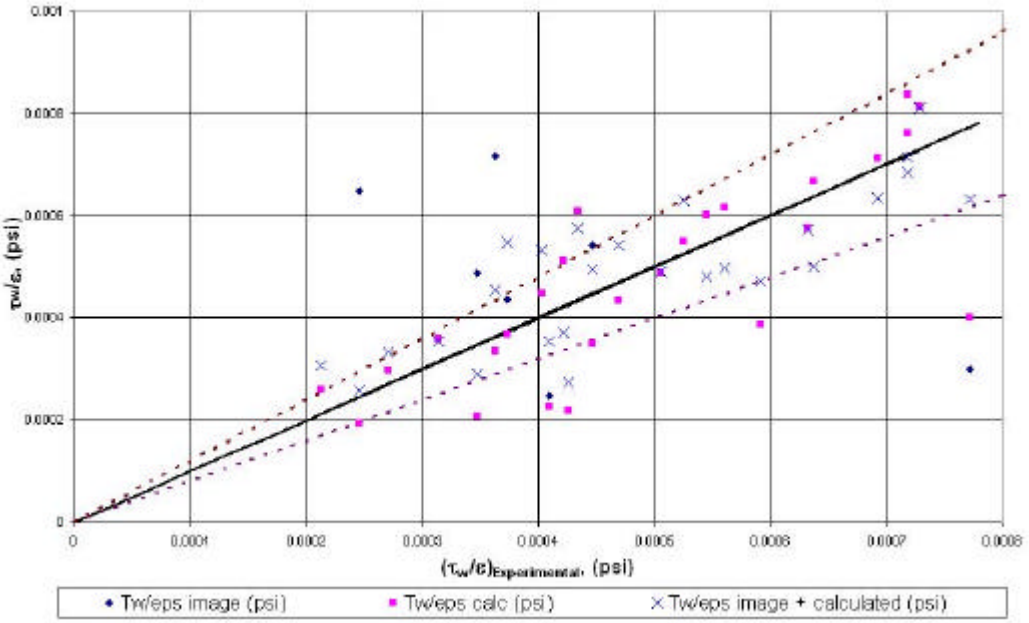

Figure 6. 13: Henkel Old Prediction Comparison.

Fig. 6.14 is the graph that includes all of the predicted shear stress values. Apparently most of the points do fall into the ±20 % error margin, pointing to the usefulness of the methodology adopted in the filed under engineering limitations.

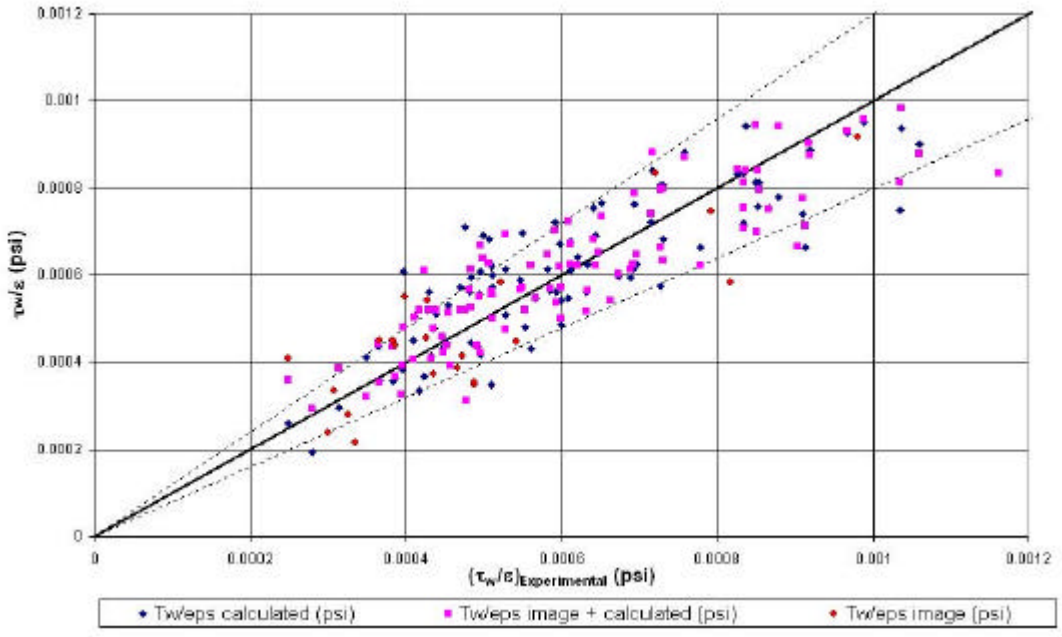

Figure 6. 14: Comparison all Surfactants.

Fig. 6.15 is the plot of errors for each experiment recorded in this study. It is observed that most of the errors are below 20%. Although there are error readings above 20%, these readings could be because of the experimental errors those, which could have possibly occurred in the course of the experiments.

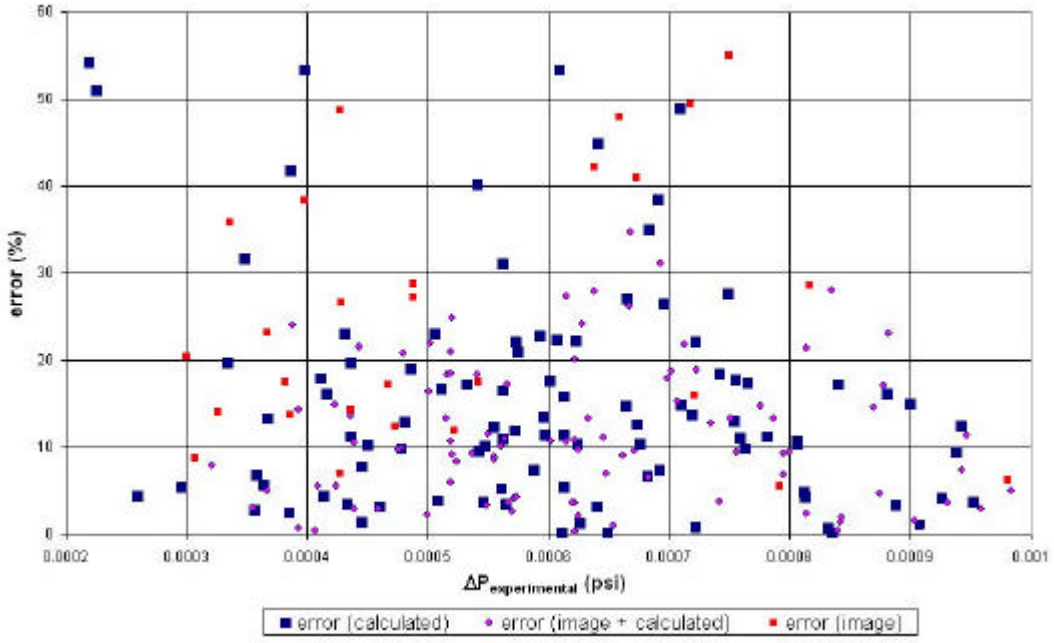

Figure 6. 15: Error Percentages of the predicted shear stresses.

From Fig. 6.14, and 6.15 it can be observed that the accurate results were obtained using the combination of image and rheological information together for estimating frictional pressure loss for flowing foam through circular conduits. From figure 6.15, it is observed that, for rheological prediction (calculated) method, the about 60% of the points are accumulated within 10-20 % error range; for image based prediction method, 50 % of the points are accumulated within 10-30 % error range, and for combined method, 65 % pf the points are accumulated within 5-20% error range. It is observed that, although the predictions using only the image information is the least accurate, it is still promising to be used in foam characterization methodology since the only required data is the average bubble size and circularity. The accuracy of the estimation of generalized foam parameters as a function of bubble size and circularity can be improved by using better quality images in dynamic conditions, as well as including chemical composition of the foam surfactants into consideration.

6.6 Application of the findings in the field:

The findings of this study are very useful for foam pressure drop calculations; the only necessary input is to get the image of the foam for a known quality level, this point of sampling could be any point along the foam flow line, and processing it for its average diameter and circularity. Once these are readily available, one of the two equations for pressure loss calculation is to be utilized, either equation 6.5 or 6.6.

Equation 6.2 would calculate the theoretical pressure loss gradient if the fluid was incompressible, and exhibited no slip along the wall of the conduit it flows. K'_{GEVE} and N'_{GEVE} values are used in calculation of equation 6.3, that is the GEVE wall shear rate calculation However for foam flow case the theoretically calculated pressure loss gradient has got to be corrected. Consider equation 6.5, and substitute all of the pertinent parameters, as necessary. Average foam bubble diameter, and circularity are acquired by only image processing of the foam image that has been captured from any point along the foam flow line.

CHAPTER VII

CONCLUSIONS

An attempt of foam characterization is conducted by including the bubble size and texture of the foam into consideration. The rheological characterization is achieved using the experimental data obtained. The two different industrial foam samples were experimented using two different foam generators, and flown through a constructed setup that consisted of four different pipe sizes. During each flow test, digital images are collected, and bubble sizes and texture information is obtained using digital image processing techniques. During the rheological analysis, generalized volume equalized principle is adopted and improved by correcting for the wall slip effects. The effect of bubble size and texture is included into rheological calculations. The results are compared with experimental data as well as estimations without considering bubble size and texture information. In summary the following three achievements are established by this study:

- Corrected rheological parameter determination
- Shear rate estimation as a function of image only
- Shear rate estimation as a function of image and rheology.

The estimated values of pressure losses are improved significantly when bubble size and texture is considered in the calculations as well as corrected rheology parameters. Average error was about 20 % without including the bubble size and texture, however, average error dropped to 15 % after bubble size and texture is taken into account. Although pressure losses estimated using the generalized

parameters calculated from the image information are the least accurate among the three methods, this methodology is still very promising in characterizing the foam rheology, since the only required information is average bubble size and the circularity of the foam.

As the foam quality increases, the average bubble size of the foam increases, and the circularity of the foam decreases. Therefore, analyzing the bubble size and texture could give approximate information about the physical properties of the foam.

CHAPTER VIII

RECOMMENDATIONS

The study can be further improved if more foaming surfactants are used. Also, the chemical properties of surfactants can also be included into consideration.

Including the effect of temperature would also improve the performance of the correction factor. Working in higher temperatures and pressures during the experiments would also enhance the accuracy.

Considering the stability of foam in the characterization methodology may enhance the outputs to have more accurate results.

Longer and larger pipe systems would characterize the field conditions in a more realistic way. A longer and larger setup would increase the quality of the experimental data collected.

If higher quality image acquisition techniques were adopted far better successful results could have been achieved at the end of this study, so image acquisition technique if improved would add invaluable contribution to this sort of studies.

REFERENCES:

[1] Lord D.L., *"Mathematical Analysis of Dynamic and Static Foam Behavior,"* SPE Paper 7927, 1979, SPE Symposium on Low Permeability Gas Reservoirs, Colorado

[2] Ozbayoglu M.E., Kuru E., Miska S., Takach N., *"A Comparative Study of Hydraulic Models for Foam Drilling,"* SPE/Petroleum Society of CIM 65489, SPE/PS-CIM International Conference on Horizontal Well Technology

[3] Herzhaft B., Toure A., Bruni F., Saintpere S., *"Aqueous Foams for Underbalanced Drilling: The Question of Solids,"* 2000 SPE Annual Technical Conference and Exhibition held in Dallas, Texas, 1–4 October 2000, SPE Paper 62898.

[4] Bonilla L.F, Subhash N. Shah, *"Experimental 'investigation on the Rheology of Foams,"* SPE Paper 59752, SPE/CERI Gas Technology Symposium, Canada, 2000

[5] Kuru, E., Miska, S., Pickell, M., Takach, N., and Volk, M., "*New Directions in Foam and Aerated Mud Research and Development*," SPE paper 53963, Latin American and Caribbean Petroleum Conference, Caracas, Venezuela, 21-23 April, 1999

[6] Okpobiri G.A., and Ikoku C.U., *"Volumetric Requirements of Foam and Mist Drilling Operations,"* SPEDE (February 1986), 71-88

[7] Beyer A.H., Millhone R.S., Foote R.W., *"Flow Behaviour of Foams as Well Circulating Fluid,"* SPE Paper 3986, 1972 SPE Annual Fall Meeting

[8] Russel B.A., *"How Surface Hole Drilling Performance was Improved by 65%,"* SPE/IADC 25766, 1993, 23-25 February, Amsterdam

[9] Mitchell B.J, *"Test Data Fill Theory Gap on Using Foam as a Drilling Fluid,"* Oil and Gas J., September 1971, 96-100

[10] Rankin M.D., Friesenhahn T.J., Price W.R., Pool Co, *"Lightened Fluid Hydraulics and Inclined Boreholes,"* SPE/IADC 18670, 1989, New Orleans

[11] *"Baroid Fluids Handbook,"* Baroid Drilling Fluids, Inc., Houston

[12] Kuhlman M.I., Lau H.C., Falls A.H., "Surfactant Criteria for Successful Carbon Dioxide Foam in Sandstone Reservoirs," SPE 60855, 2000

[13] *"Multiphase Flow in Pipes and Annulus,"* Ozbayoglu M.E., PhD, University of Tulsa, PhD Dissertation, 2000

[14] Raza S.H., Mardsen S.S, "The Streaming Potential and the Rheology of Foam," SPE 1748, 1966

[15] Amiel D., and Mardsen S.S, *"The Rheology of Foam,"* SPE 2544, 1969

[16] Mitchell, B.J., *"Test Data Fill Theory Gap on using Foam as a Drilling Fluid,"* Oil and Gas Journal, September 1971

[17] Beyer, A.H., Millhone, R.S., and Foote, R.W., "Flow Behaviour of Foam as a Well Circulating Fluid," SPE paper 3986, SPE Annual Fall Meeting, San Antonio, TX, 1972

[18] Blauer R.E., Mitchell B.J., and Kohlhall C.A., *"Determination of Laminar, Turbulent, and Transitional Foam Flow Losses in Pipes,"* SPE Paper 4885, 1974, 44th Annual California Regional Meeting of SPE

[19] Sanghani V., and Ikoku C.U., *"Rheology of Foam and Its Implications in Drilling and Cleanout Operations,"* paper ASME A0-203 presented at the 1983 Energy Sources Technology Conference and Exhibition, Houston, Jan 30-Feb 3

[20] Okpobiri G.A, Ikoku C.U., *"Volumetric Requirements for Foam and Mist Drilling Operations,"* SPE Paper 11723, SPE Drilling Engineering 1986

[21] Reidenbach V.G, Harris P.C., Lee Y.N., Lord D.L., *"Rheological Study of Foam Fracturing Fluids Using Nitrogen and Carbon Dioxide,"* SPE Production Engineering, January 1986, 31-41, SPEPE 12026

[22] Reidenbach V.G., Harris P.C., *"High Temperature Rheological Study of Foam Fracturing Fluid,"* Journal of Petroleum Technology, May 1987, SPE Paper 13177, 613-619

[23] Harris P.C., *"Effects of Texture on Rheology of Foam Fracturing Fluids,"* SPE Paper 14257, SPE Production Engineering, August 1989, 249-257

[24] Calvert J.R., Nezhati K., *"A Rheological Model for a Liquid-Gas Foam,"* Int J. Heat & Fluid Flow, 1986

[25] Cawiezel K.E., Niles, *"Rheological Properties of Foam Fracturing Fluids Under Downhole Conditions,"* SPE Paper 16191, SPE Hydrocarbon Economics and Evaluation Symposium, Dallas, 1987

[26] Khan S.A., Schnepper C.A., Armstrong R.C., *"Foam Rheology: III Measurement of Shear Flow Properties,"* Journal of Rheology, 32 (1), 69-92 (1988)

[27] Valko P., Economides M.J., "Volume Equalized Constitutive Equations for Foamed Polymer Solutions," J. Rheol., 36(6), August 1992

[28] Sporker H.F., Trepess P., Valko P., and Economides M.J., "System Design for the Measurement if Downhole Dynamic Rheology for Foam Fracturing Fluids," SPE Paper 22840, 1991

[29] Valko P., and Economides M.J., *"The Rheological Properties of Carbon Dioxide and Nitrogen Foams,"* SPE Paper 23778, SPE Int. Symposium on Formation Damage Control, Louisiana, 1992

[30] Winkler W., Valko P., Economides M.J., *"Laminar and Drag-Reduced Polymeric Foam Flow,"* J.Rheol. 38(1), January/February 1994, Page 111-127

[31] Enzendorfer C., Harris R.A., Valko P. and Economides M.J., *"Pipe Viscometry of Foams,"* J.Rheol. 39(2), March/April 1995, Page 345-358

[32] Gardiner B.S., Dlugogorski B.Z., Jameson G.J., *"Rheology of Fire Fighting Foams,"* Fire Safety Journal, July 1998, Page 61-75

[33] Saintpere S., Herzhaft B., Toure A., Jollet S., "*Rheological Properties of Aqueous Foams for Underbalanced Drilling*" SPE Paper 56633, SPE Annual Technical Conference and Exhibition held in Houston, Texas, 3–6 October 1999.

[34] Alvarez J.M., Rivas H.J., Rossen W.R., *"Unified Model for Steady-State Foam Behavior at High and Low Foam Qualities*", 1999 SPE Annual Technical Conference and Exhibition held in Houston, Texas, 3–6 October 1999, SPE Paper 56825.

[35] Rommetveit R., Sævareid O., Guarneri A., Georges C., Nakagawa E., Bijleveld A., *"Dynamic Underbalanced Drilling Effects are Predicted by Design Model*", 1999 Offshore Europe Conference held in Aberdeen, Scotland, 7–9 September 1999, SPE Paper 56920.

[36] Silva V. Jr., Shayegi S., Y. Nakagawa E., *"System for the Hydraulics Analysis of Underbalanced Drilling Projects in Offshore and Onshore Scenarios"*, 2000 SPE International Petroleum Conference and Exhibition in Mexico held in Villahermosa, Mexico, 1–3 February 2000, SPE Paper 58972.

[37] Fernando B. L., Shah S. N., *"Experimental Investigation on the Rheology of Foams"* 2000 SPE/CERI Gas Technology Symposium held in Calgary, Alberta Canada, 3-5 April 2000, SPE Paper 59752.

[38] Martins A.L., Lourenço A.M.F., *"Foam Properties Requirements for Proper Hole Cleaning While Drilling Horizontal Wells in Underbalanced Conditions,"* SPE Paper 64382, SPE Asia Pacific Oil and Gas Conference and Exhibition held in Brisbane, Australia, 16–18 October 2000.

[39] Rojas Y., Kakadjian S., Aponte A., Márquez R., and Sánchez G., *"Stability and Rheological Behaviour of Aqueous Foams for Underbalanced Drilling,"* SPE Paper 64999, 2001 SPE International Symposium on Oilfield Chemistry held in Houston, Texas, 13–16 February 2001.

[40] Sani A. M., Shah S. N., Baldwin L.," *Experimental Investigation of Xanthan Foam Rheology,"* SPE Paper 67263, Production and Operations Symposium held in Oklahoma City, Oklahoma, 24–27 March 2001.

[41] Martins A. L., SPE, Lourenço A. M. F., Silva C. H. M. Sá, V. Jr.," *Foam Rheology Characterization as a Tool for Predicting Pressures While Drilling Offshore Wells in UBD Conditions*," SPE/IADC 67691, SPE/IADC Drilling Conference held inAmsterdam, The Netherlands, 27 February–1 March 2001.

[42] Alvarez J.M., Rivas H.J., and Rossen W.R., *"Unified Model for Steady-State Foam Behavior at High and Low Foam Qualities,"* SPE Paper 56825, presented at the 1999 SPE Annual Technical Conference and Exhibition, Houston, 3–6 October.

[43] Sudhakar D., Khade, Subhash N. Shah, *"New Emprical Friction Loss Correlation for Foam Fluids in Coiled Tubing,"* SPE Paper 74810, SPE/ICoTA Coiled Tubing Conference and Exhibition Houston, Texas, April 2002

[44] Sudhakar D. Khade, Subhash N. Shah, *"New Rheological Correlations For Guar Foam Fluids,"* SPE Paper 80895, SPE Produciton and Operations Symposium, OK, USA, March 2003

[45] Guo B., Sun K., Ghalambor A., *"A Closed Form Hydraulics Equation for Predicting Bottom-Hole Pressure in UBD with Foam,"* IADC/SPE 81640, IADC/SPE Underbalanced Technology Conference and Exhibition, TX, USA, March 2003

[46] Burgoyne A. T. Jr., Milheim, Keith K., Chenevert, Martin E. and Young, KS. Jr. 1986. *Applied Drilling Engineering*. Richardson, TX: Society of Petroleum Engineers.

[47] Winkler W., *"Polymer Foam Rheology in Circular Pipes,"* MSc thesis, Institute of Drilling and Production, Mining University Leoben, Austria, (1992)

[48] Ozbayoglu M.E., *"Cuttings Transport with Foam in Horizontal and Highly-Inclined Wellbores,"* SPE/IADC Drilling Conference, Amsterdam, 19-21 February 2003, SPE/IADC 79856

[49] Jastrzebski Z., *"Entrance Effect and Wall Effect in Rheometer During the Flow of Concentrated Suspension,"* Ind. Eng. Chem. Res., 6, 445-454, 1966.

[50] Skelland, A.H.P.: *"Non-Newtonian Flow and Heat Transfer,"*, John Wiley and Sons, Inc., Chapter 2, pp.27-67, New York, 1966.

[51] Govier, G.W., and K. Aziz, *"The Flow of Complex Mixtures in Pipes,"* R.E. Krieger Publishing Company, Huntington, NY, (1977).

[52] "*Underbalanced Drilling Manual*," published by Gas Research Institute, 1997

[53] ImageJ, official web site, *"http://rsb.info.nih.gov/ij/docs/intro.html"*, visited on 09.June.2004

APPENDIX A

HALF LIFE EXPERIMENTS

Half-life tests for the foaming agents are conducted in order to determine the *critical foaming agent concentration* to be mixed with water. Surfactant is to be mixed with water by different volumetric concentrations and stirred by means of a blender, and then transferred into a graduated cylinder. Initial total foam volume is measured and recorded. Then, the volume of liquid phase collected at the bottom of the graduated cylinder is measured and recorded as a function of time. When half of the total liquid volume drained at the bottom of the graduated cylinder, the time of this period is recorded as the *half-life* of the foam.

A.1. Procedure:

The method is based on the measurement of the liquid phase drained volume as a function of time. Foams are to be prepared through stirring at 5200 Rpm of 100 ml of the liquid phase during 60 seconds in a blender. The prepared foam is immediately transferred to a 1000ml graduated cylinder and the drained volume of the liquid at the bottom of the graduated cylinder is recorded every 15 seconds, in the range of 15-300 seconds. Besides this, as half of the total liquid phase has been drained the time is to be registered as half-life for this surfactant.

Fig. A.1 is half-life versus surfactant volume percent graph, for the two samples tested. The x-axis is the surfactant concentration in percentage added to the fresh water, and y-axis is the half-life recorded in seconds. This graph gave the optimum critical concentration for the two surfactants tested. Birka drained faster than Henkel,

with a critical concentration of 1.50%. Henkel with a higher half-life required to be mixed with fresh water with less concentration, 1.00%

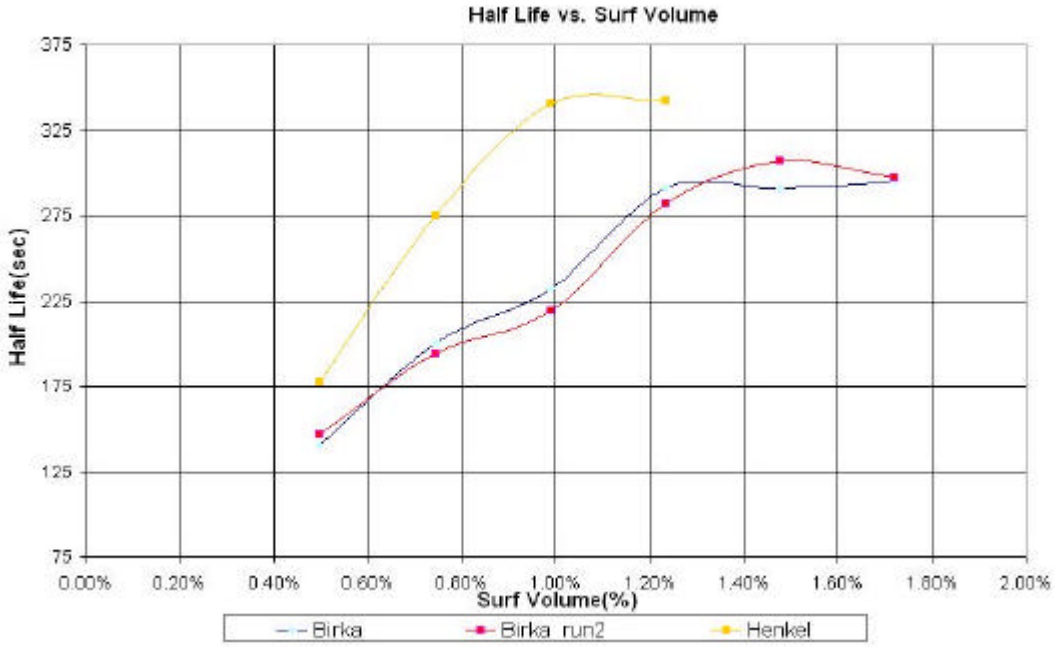

Figure A. 1: Half-Life vs. Surfactant Volume Graph.

Fig.A.2 is initial volume vs. surfactant volume percent graph for the samples. The y-axis in this graph is the Initial Foam Volume, ml. Initial foam volume that is read from the graduated cylinder right after the end of the mix process is plotted in y-axis. In accordance to half-life vs. surfactant volume percent graph, this graph also gave similar results , and surfactant critical concentration is determined to be the same. Table A.1 gives the critical foaming agent concentration by volume that is required to be mixed with water.

Table A. 1: Surfactants, and Their Percentages to be added to the liquid.

Surfactant Name/ Supplier	Foaming Agent, by Volume %
BIRKA	1.5
HENKEL	1.0

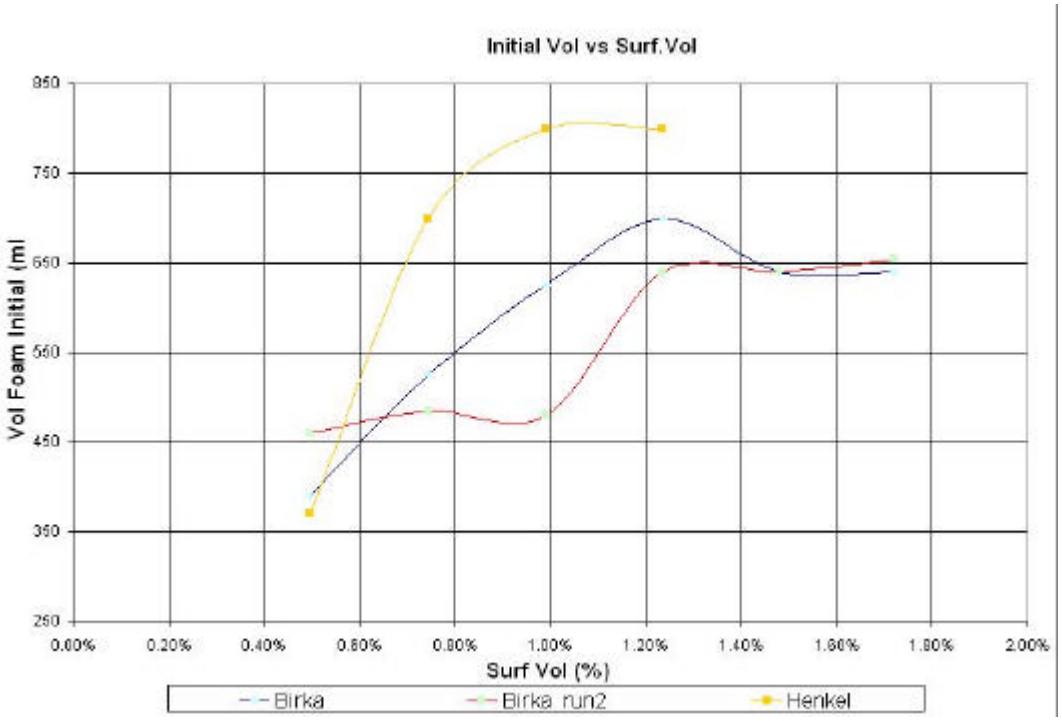

Figure A. 2: Initial Volume vs. Surfactant Volume Graph.

APPENDIX B

RABINOWITSCH-MOONEY DERIVATION FOR COMPRESSIBLE FLOW

Fig 4.2 represents a compressible fluid element in a circular pipe.

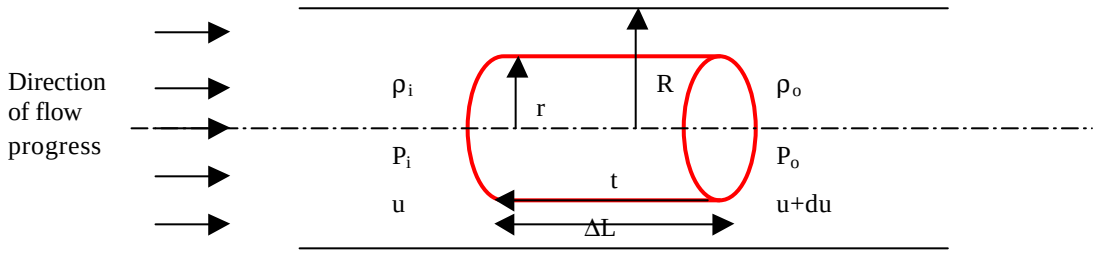

Figure 4.2: Free body diagram of a flowing medium inside a pipe.

When any *compressible* fluid flows horizontally in a circular pipe, under steady state conditions, the mass conservation (continuity) equation can be put into the form of;

$$\int_C \int_A (\vec{n}) r\, v dA = 0 \quad \text{..... (B. 1)}$$

For steady state, isothermal conditions, the time rate of linear momentum is

$$\sum \vec{F} = \iint_{CS} \vec{v}\, \bar{r}\, (\vec{v}.\vec{n})\, dA \quad \text{..... (B. 2)}$$

where the mean fluid density, $\bar{r}$, is

$$\bar{r} = \frac{r_i + r_o}{2} \quad \text{..... (B. 3)}$$

The forces acting on a fluid element, as shown in Fig. 5.2 is

$$\sum \vec{F} = P_i p r^2 - P_o p r^2 - t\, 2p r \Delta L \quad \text{..... (B. 4)}$$

Equalizing equation B.2 and equation B.4, and solving for shear stress, t, yields

$$t = \frac{\Delta P}{\Delta L}\frac{r}{2} - r\bar{r}v\frac{dv}{dL} \quad \text{..... (B. 5)}$$

The relation between the specific expansion ratio and the foam density and base fluid density is given by

$$e = \frac{r_1}{r_2} \quad \text{..... (4.6)}$$

where

ρ_1, ρ_2= Density at the base and foam after having been generated, respectively. Rearranging equation B-5 yields

$$t = \frac{\Delta P}{\Delta L}\frac{D}{4} - \frac{r_l}{e} rv\frac{dv}{\Delta L} \quad \text{..... (4.5)}$$

At the wall, the shear stress is

$$t_w = \frac{\Delta P}{\Delta L}\frac{R}{2} - R\bar{r}v\frac{dv}{dL} \quad \text{..... (B. 6)}$$

For a time-independent fluid, a steady-state laminar flow, the flow rate through a circular pipe of radius *R* can be defined as;

$$Q = 2p\int_0^R vrdr \quad \text{..... (B. 7)}$$

Using integration by parts, equation (B.7) yields,

$$Q = 2p\left[v\frac{r^2}{2} - \int\frac{r^2}{2}dv\right]_0^R \quad \text{..... (B. 8)}$$

Taking the ratio of equation 4.5, equation B.6 can be approximated as

$$\frac{t}{t_w} = \frac{r}{R} \quad \text{..... (B. 9)}$$

It is known that, the shear rate is a function of shear stress, i.e.,

$$f(t) = -\frac{dv}{dr} \quad \text{..... (B. 10)}$$

The minus sign in the equation (B.10) is because the velocity is maximum at $r = 0$, and velocity is minimum at $r = R$.

The following relation could be derived from the equation (B.10) as,

$$dr = \frac{R}{t_w} dt \quad \text{..... (B. 11)}$$

And from equation (B.11) we have,

$$dv = -f(t)dr \quad \text{..... (B. 12)}$$

Since the velocity of the fluid is zero at the wall of the pipe, the first term of equation B.8 drops, and the following equation is developed,

$$Q = -2p \int_0^R \frac{r^2}{2} dv \quad \text{..... (B. 13)}$$

Changing variables, as described in equations B.11 and equation B.12, equation B.13 can be put into the form

$$Q = p \int_0^{t_w} \left(\frac{t}{t_w} R \right)^2 f(t) \frac{R}{t_w} dt \quad \text{..... (B. 14)}$$

After making necessary simplifications,

$$Q = p \frac{R^3}{t_w^3} \int_0^{t_w} t^2 f(t) dt \quad \text{..... (B. 15)}$$

Getting the derivative of both sides in equation (B 15) with respect to wall shear stress yields,

$$\frac{\partial\left(\frac{Qt_w^3}{pR^3}\right)}{\partial t_w} = \frac{\partial}{\partial t_w}\int_0^{t_w} t^2 f(t)dt \quad \text{..... (B. 16)}$$

Expanding the above differential equation,

$$\frac{3t_w^2 Q}{pR^3} + t_w^3 \frac{\partial\left(\frac{Q}{pR^3}\right)}{\partial t_w} = \int_0^{t_w} \frac{\partial}{\partial t_w}(t^2 f(t)dt) + t^2 f(t)\Big|_0^{t_w} \quad \text{..... (B. 17)}$$

The first term on the right-hand side of the equation (B.17) will drop because of the Leibnitz –Rule, after dividing every term by t_w^2, equation would yield,

$$f(t_w) = \frac{3Q}{pR^3} + t_w \frac{\partial\left(\frac{Q}{pR^3}\right)}{\partial t_w} \quad \text{..... (B. 18)}$$

Flow rate is defined in terms of velocity and flow rate,

$$Q = pR^2 v = \frac{p}{4} D^2 v \quad \text{..... (B. 19)}$$

Substituting flow rate as in equation B.14 into equation B.19, the following is achieved,

$$f(t_w) = \frac{3\left(\frac{p}{4}D^2 v\right)}{\frac{pD^3}{8}} + \left(\frac{\Delta P}{\Delta L}\frac{D}{4} - \frac{r_l}{e} rv\frac{dv}{\Delta L}\right)\frac{\partial\left(\frac{\frac{p}{4}D^2 v}{\frac{pD^3}{8}}\right)}{\partial\left(\frac{\Delta P}{\Delta L}\frac{D}{4} - \frac{r_l}{e} rv\frac{dv}{\Delta L}\right)} \quad \text{..... (B. 20)}$$

Rabinowitsch-Mooney defined the following relation, [49],

$$N = \frac{\partial \ln t_w}{\partial \ln \frac{8v}{D}} \quad \text{(B. 21)}$$

applying the following differential rule,

$$\frac{\partial x}{x} = \ln x \quad \text{(B. 22)}$$

Equation (B.20) would become,

$$f(t_w) = 3.2\frac{v}{D} + \left(\frac{\Delta P}{\Delta L}\frac{D}{4} - \frac{r_l}{e} rv \frac{dv}{\Delta L}\right) \frac{\partial\left(2\frac{v}{D}\right)}{\partial\left(\frac{\Delta P}{\Delta L}\frac{D}{4} - \frac{r_l}{e} rv \frac{dv}{\Delta L}\right)} \quad \text{(B. 23)}$$

Multiplying and dividing every term in the equation above by 4, equation (B.23) becomes,

$$f(t_w) = \frac{4}{4}3.2\frac{v}{D} + \frac{4}{4}\frac{2\frac{v}{D}\partial \ln\left(2\frac{v}{D}\right)}{\frac{\partial\left(\frac{\Delta P}{\Delta L}\frac{D}{4} - \frac{r_l}{e} rv \frac{dv}{\Delta L}\right)}{\left(\frac{\Delta P}{\Delta L}\frac{D}{4} - \frac{r_l}{e} rv \frac{dv}{\Delta L}\right)}} \quad \text{(B. 24)}$$

Rabinowitsch-Mooney [50] gave the following equation;

$$f(t_w) = \frac{3}{4}\frac{8v}{D} + \frac{1}{4}\frac{8v}{D}\frac{\partial \ln\left(\frac{8v}{D}\right)}{\partial \ln\left(\frac{\Delta P}{\Delta L}\frac{D}{4} - \frac{r_l}{e} rv \frac{dv}{\Delta L}\right)} \quad \text{(B. 25)}$$

which is also,

$$= \frac{3}{4}\frac{8v}{D} + \frac{1}{4}\frac{8v}{D}\frac{1}{\frac{\partial \ln\left(\frac{\Delta P}{\Delta L}\frac{D}{4} - \frac{r_l}{e} rv \frac{dv}{\Delta L}\right)}{\partial \ln\left(\frac{8v}{D}\right)}} \Rightarrow = \frac{3}{4}\frac{8v}{D} + \frac{1}{4}\frac{8v}{D}\frac{1}{N} \quad \text{(B. 26)}$$

The following relation for shear rate definition is achieved,

$$f(t_w) = \frac{8v}{D}\left[\frac{3}{4} + \frac{1}{4N}\right] \quad \text{(B. 27)}$$

Yielding the following result,

$$f(t_w) = \frac{8v}{D}\left[\frac{3N+1}{4N}\right] \quad \text{(B. 28)}$$

APPENDIX C

SLIP CORRECTION

Although the rheological behavior of the tested foams are quality depended; making use of Generalized Volume Equalized Principle turns out the data points to be aligned collapsing them into a unique curve for a constant pipe diameter. Moreover, it was observed that slip existed on the vicinity of the pipes, from the following Fig., C.1. The rheograms for different pipes when plotted as a function of volume equalized shear rate and volume equalized shear stress are not aligned on a single curve, which shows the existence of slip at the pipe wall.

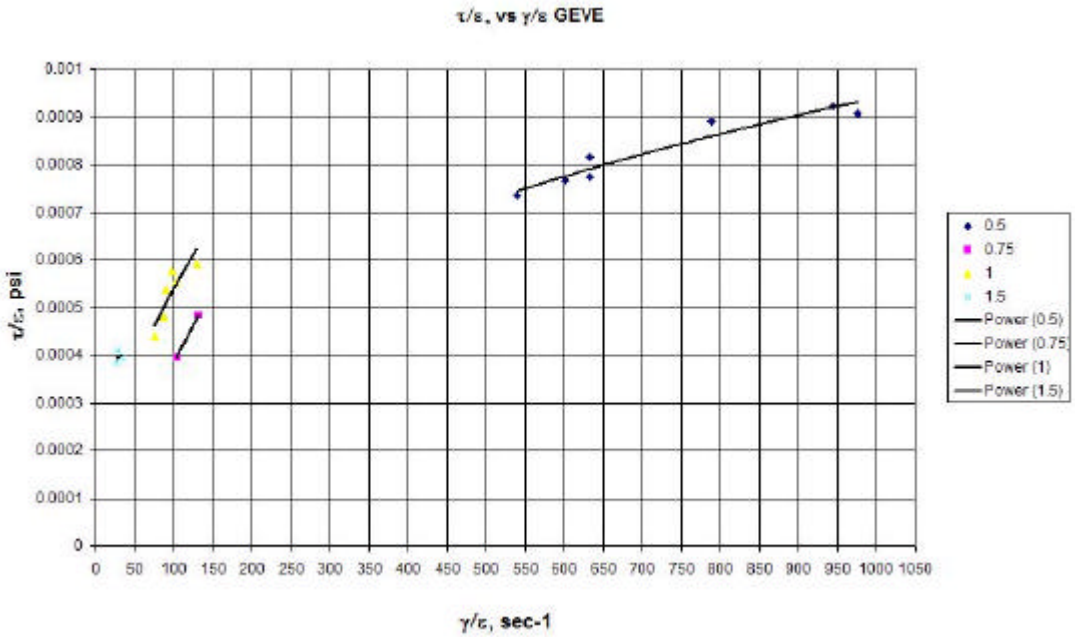

Figure C. 1: t/e **vs.** g/e **Curve.**

Section 4.2 gives the procedure for slip correction. Drawing g/e?vs. $1/D^2$, Fig. C.2 (for Birka New) would yield $16b_c t_w/e$ as the slope for each selected value of shear

stress, as in Equation 4.12. Dividing each term by $16t_w$ yields the slip coefficient, b_c, and it is presented as a function of volume equalized wall shear stress, τ_w/ε.

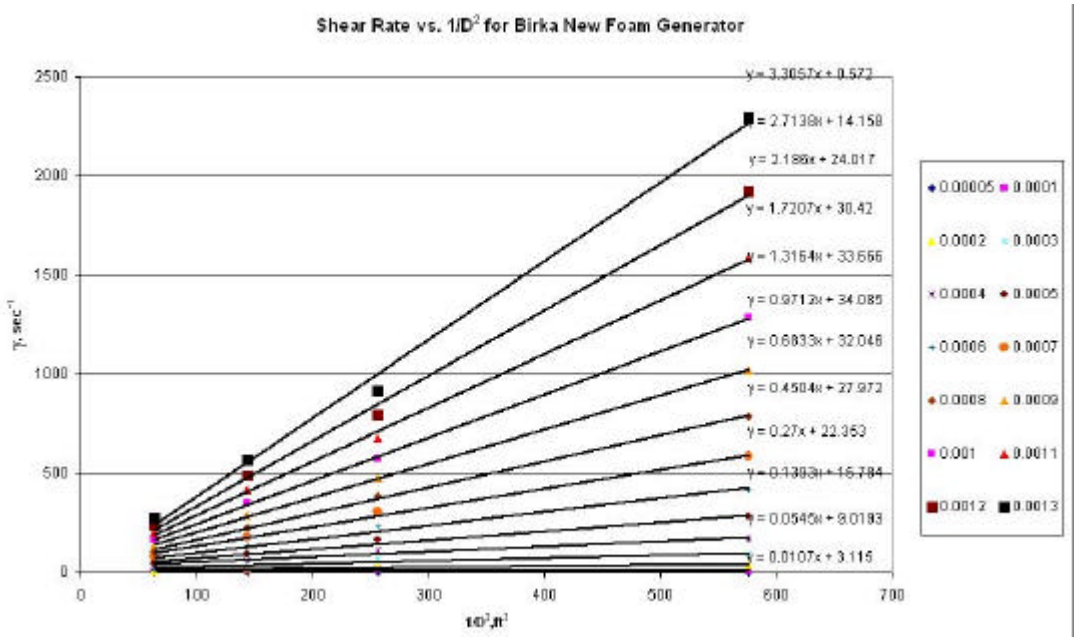

Figure C. 2: g/e **vs. 1/D^2 for Birka New.**

Fig. C.3 is *g/e*?vs. 1/D^2 for Birka Old, the same trend of slopes is also observed on this graph as well.

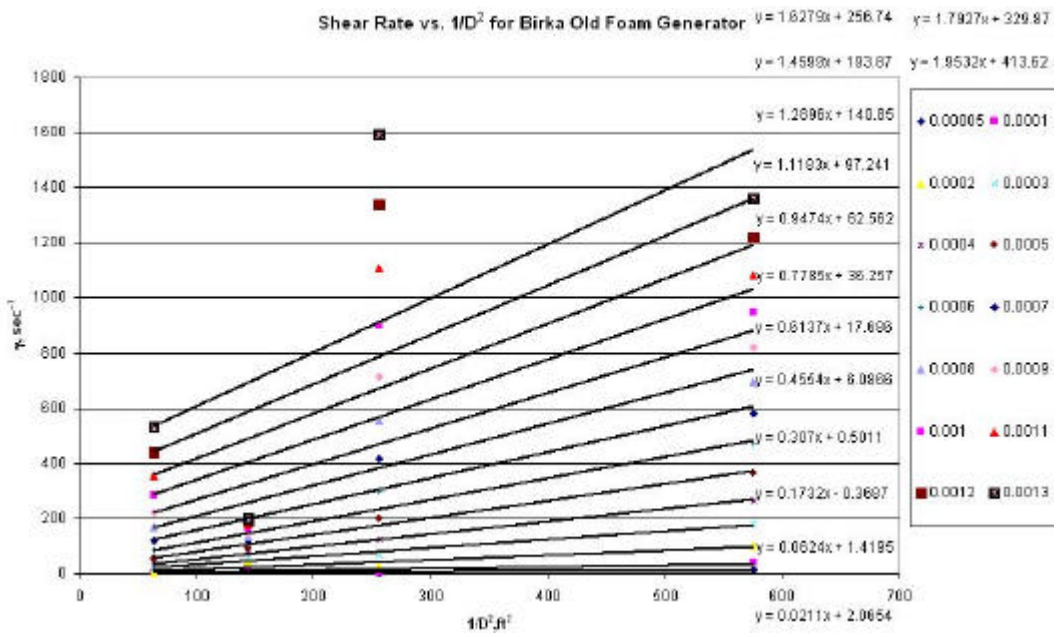

Figure C. 3: g/e **vs. 1/D^2 for Birka Old.**

Fig. C.4 is for Henkel New, the slope of g/e?vs. $1/D^2$ curves are going to be used in determination of β_c.

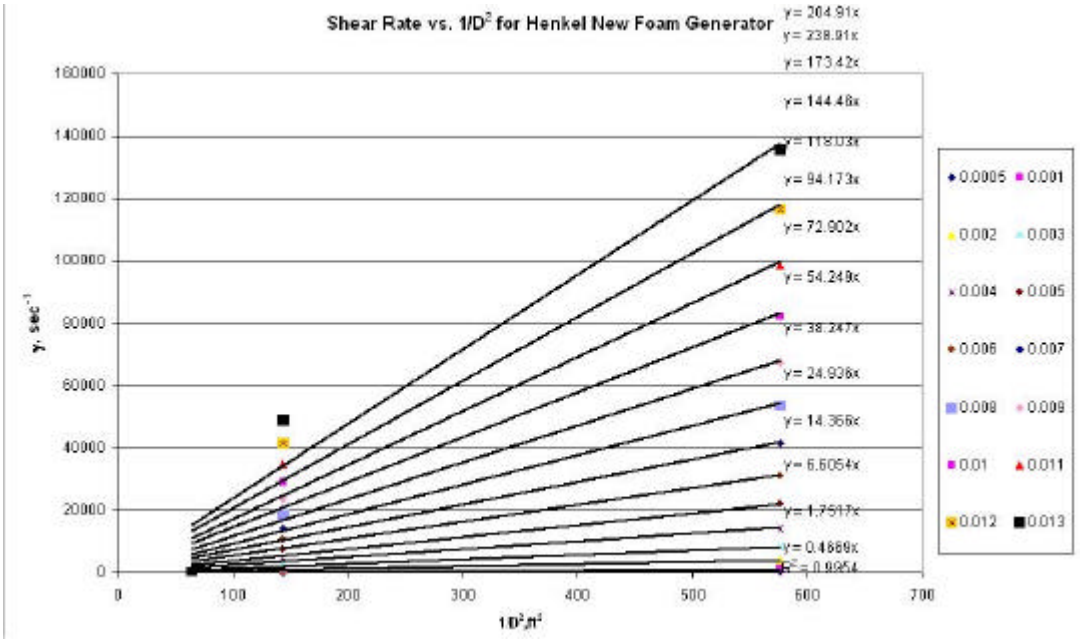

Figure C. 4: g/e **vs. 1/D² for Henkel New.**

Fig. C.5 is the g/e?vs. $1/D^2$ curve drawn for Henkel Old.

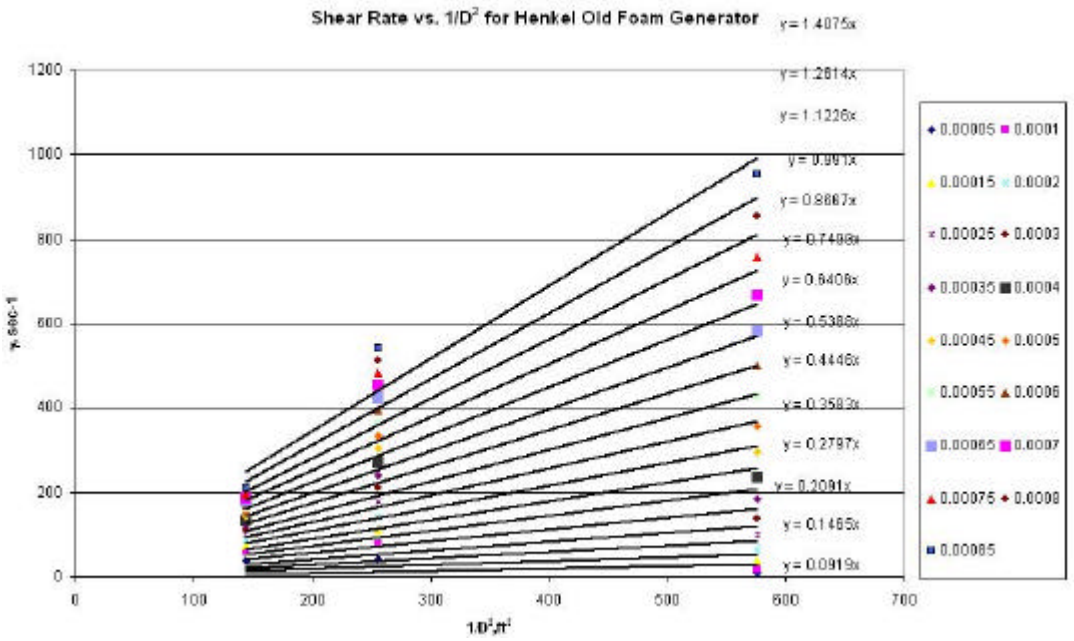

Figure C. 5: g/e **vs. 1/D² for Henkel Old.**

Fig. C.6 is the b_c vs. t_w/e graph for Birka New. From this graph b_c is determined as a function of t_w in order to be submitted into the equation 4.18.

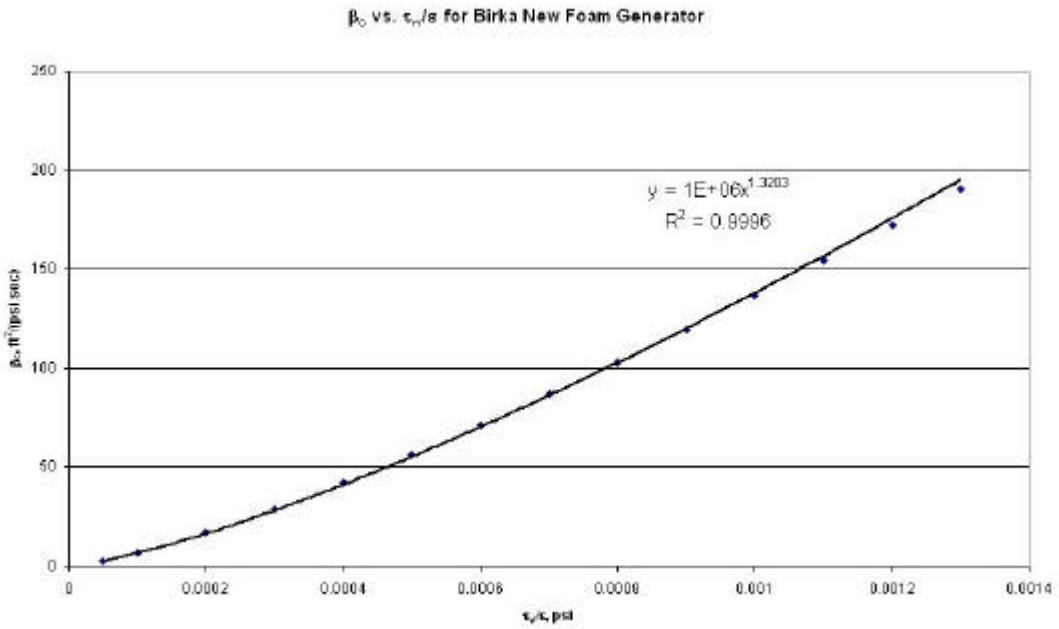

Figure C. 6: b_c **vs.** t_w/e **Birka New.**

Fig. C.6 gives the b_c vs. t_w/e graph for Birka New, notice that the relation in between b_c vs. t_w/e is going to be used in determination of slip around the pipe walls. There is a power type relation in between corrected slip coefficient and volume equalized wall shear stress.

Fig. C.7 is the same graph as above, for Birka Old, the relation in this case is also power type.

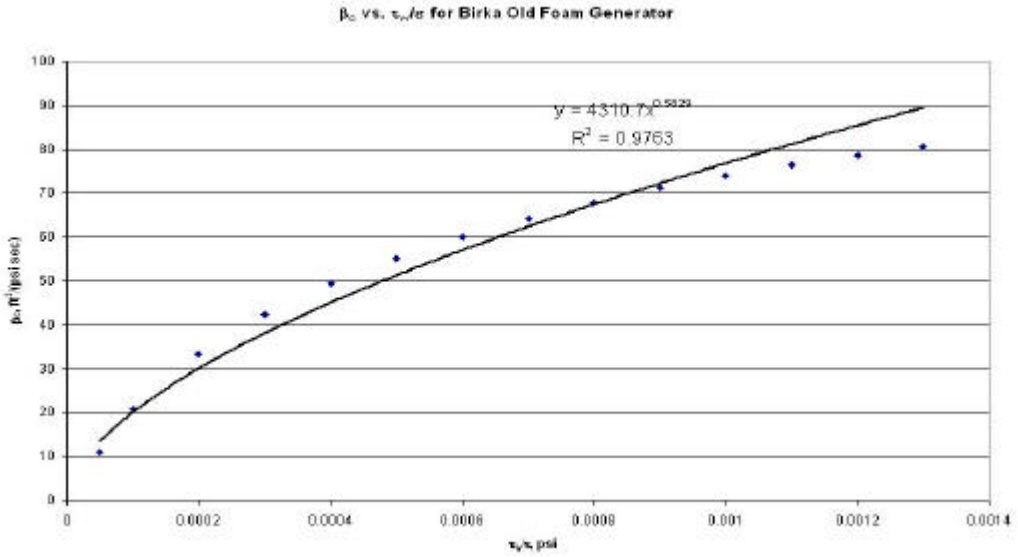

Figure C. 7: b_c **vs.** t_w/e **Birka Old.**

Fig. C.8 is b_c vs. t_w/e graph for Henkel New. A linear relation in this case is easily observed.

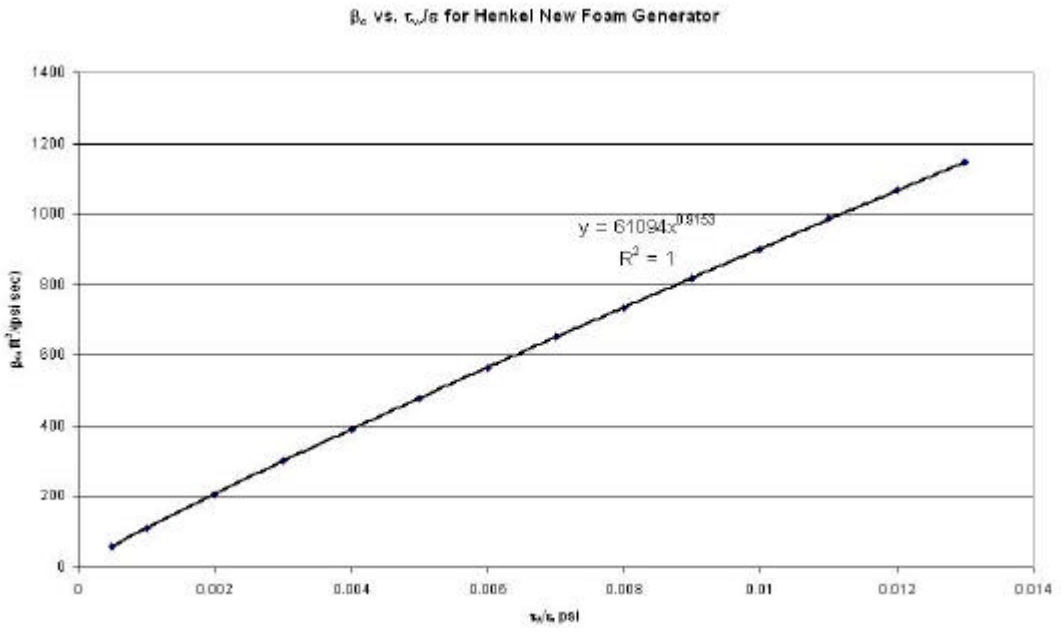

Figure C. 8: b_c **vs.** t_w/e **Henkel New.**

Fig. C.9 is b_c vs. t_w/e graph for Henkel Old.

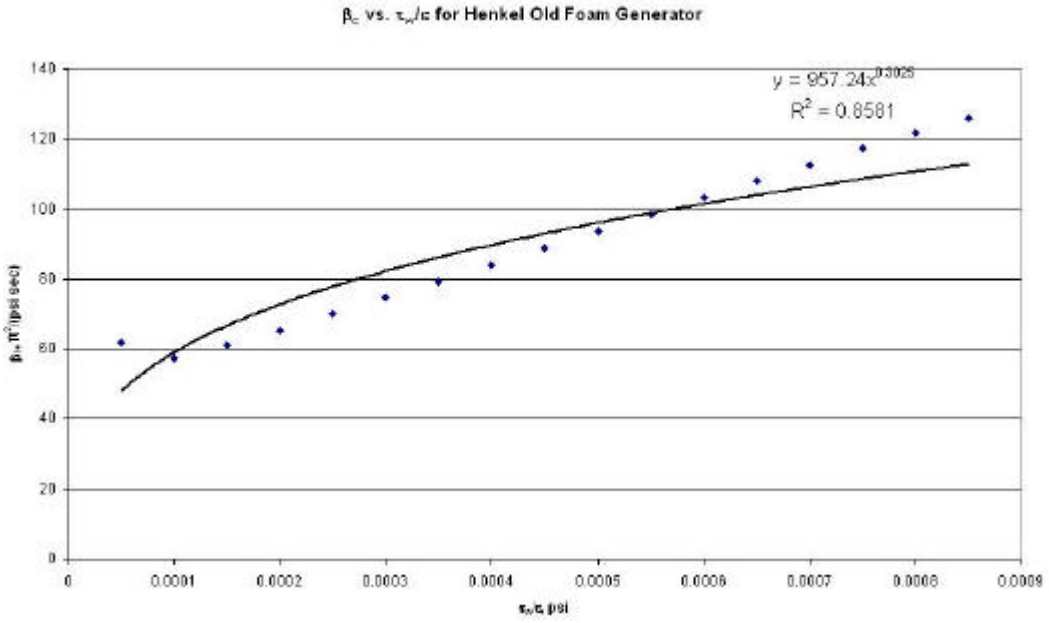

Figure C. 9: b_c **vs.** t_w/e **Henkel Old.**

Fig. C.10 shows Volume Equalized and the slip corrected form of the data for Birka New, it is observed that the data has been collapsed into one single curve, and effects of wall slip discarded, so that generalized terms required for rheology definition could better be determined. N'_{GEVE} and K'_{GEVE} for instance are 0.2068 and 1.3012 $Pa.s^{0.2011}$ respectively. It is clear that the curve below does follow a Power Law type behavior.

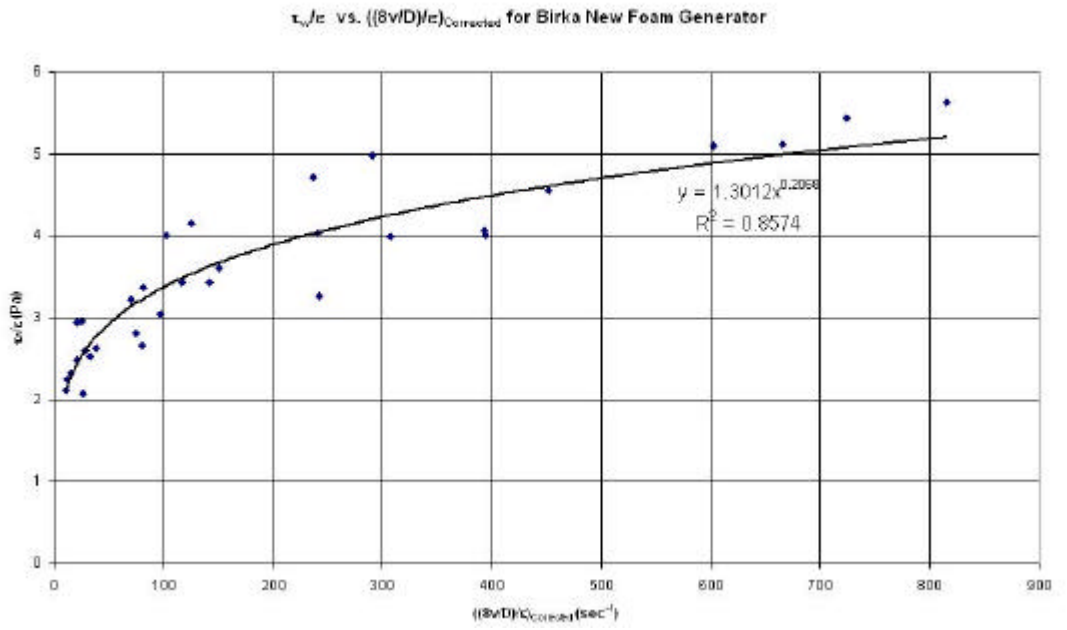

Figure C. 10: t_w/e **vs.** g/e, **for Birka New.**

Fig. C.11 is the rheology graph of Birka old, power law behavior is also observed in this curve as well.

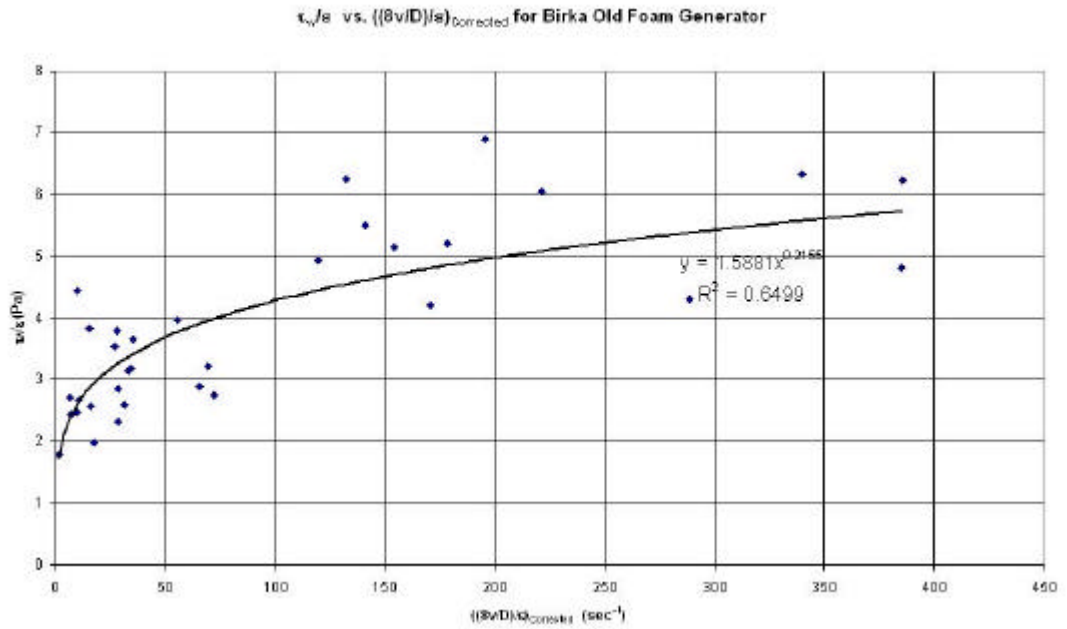

Figure C. 11: t_w/e **vs.** g/e, **for Birka Old.**

In the same manner when rheology curve is drawn for Henkel New, power law behavior is observed, as given in Fig. C.12.

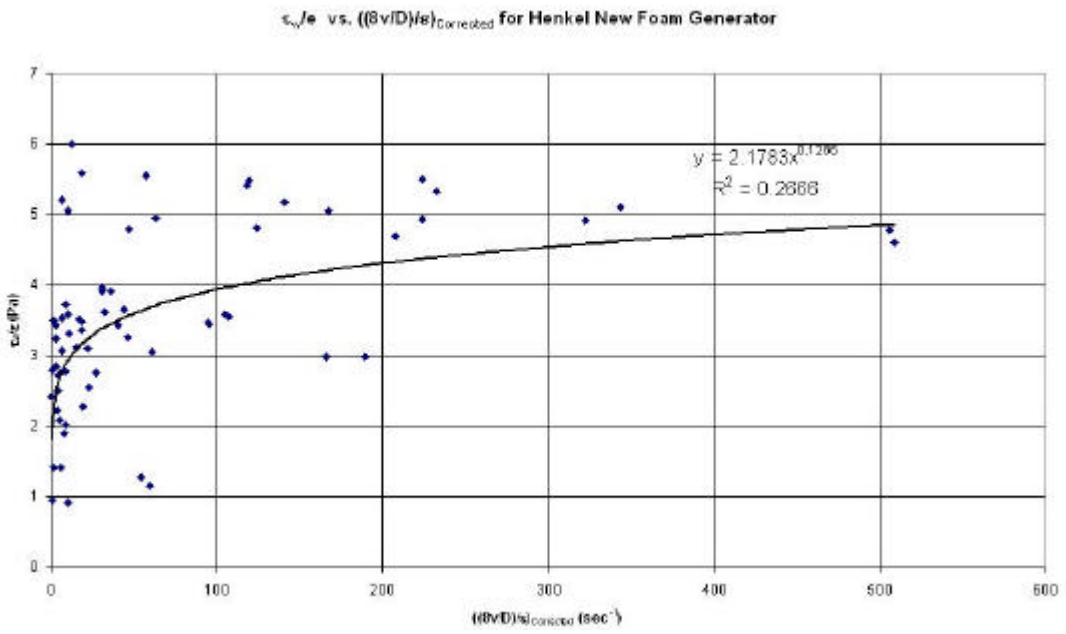

Figure C. 12: t_w/e **vs.** g/e, **for Henkel New.**

Fig. C.13 is the rheology curve for Henkel Old. Henkel Old has N'_{GEVE} and K'_{GEVE} values of 0.3779 and 0.3435 Pa.s$^{0.3779}$, respectively. When all generalized parameters are compared it is clear that they are close in value to each other. When finer foam generator used (e.g. 17 Mesh Foam Generator is finer than 8.38 Mesh Foam Generator, because of the more and smaller apertures in the screen) the generalized flow behavior indices for both surfactants are observed to decrease, because of the finer size of foams bubbles to exist in the foam body.

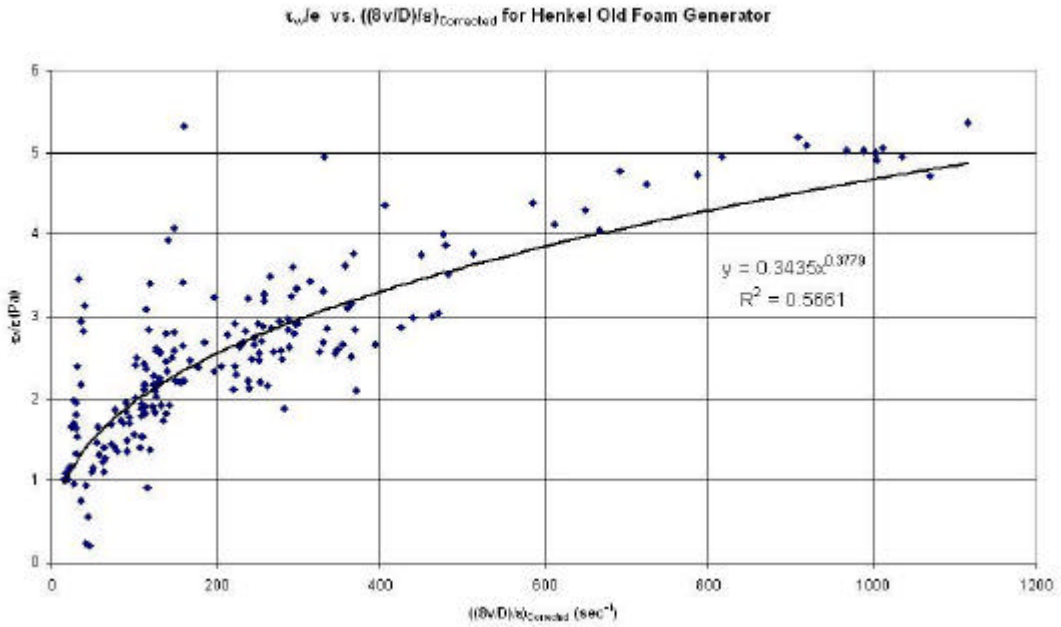

Figure C. 13: t_w/e **vs.** g/e, **for Henkel Old.**

APPENDIX D

FOAM IMAGES FOR DIFFERENT QUALITY VALUES

The bubble size and texture of the foam bubbles is determined by means of using *"ImageJ 1.30V"* image processing program. The images are taken from the visual cells those of which have been placed in the mid point of the pipes. Images are processed in 2D.

Foam images are captured by means of a microscope that magnifies the images up to 40 times. The lens of a digital camera is then placed to the lid of the microscope; the photo of each individual foam sample is recorded at 2400x1800 pixels. The following window in Fig. D.1 is the main operating frame of the *"ImageJ"*. The program can display, edit, analyze, process, save and print 8-bit, 16-bit and 32-bit images.

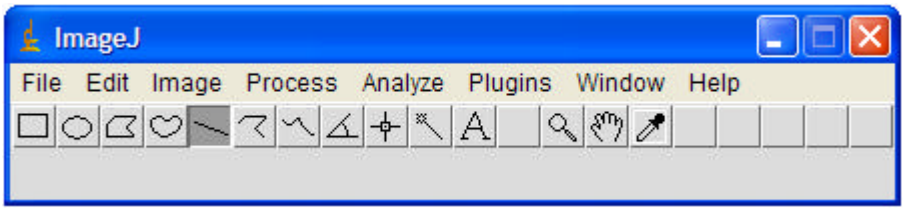

Figure D. 1: Main Operating Window of "ImageJ".

It can calculate area and pixel value statistics of user-defined selections. It can measure distances and angles. It can create density histograms and line profile plots. It supports standard image processing functions such as contrast manipulation, sharpening, smoothing, edge detection and median filtering [53].

Fig. D.2 is the reference photo that is used in dimension determination. The main distance between the mid points of the lines in this figure is $1/100^{th}$ of an inch.

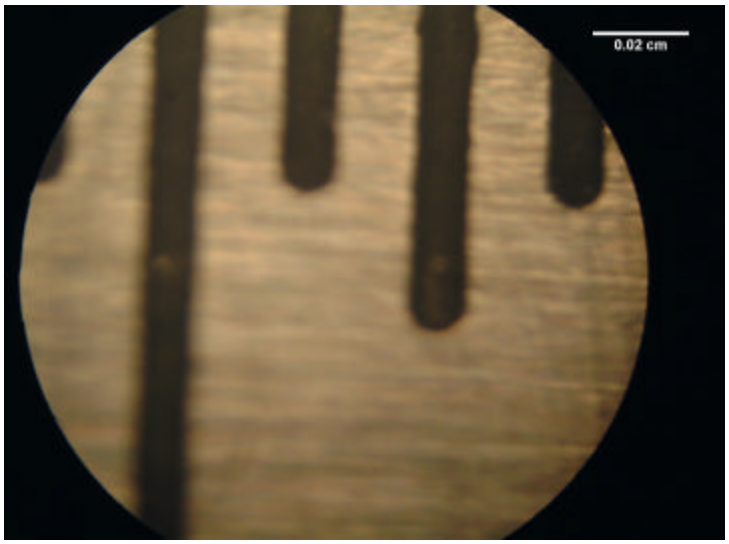

Figure D. 2: Image Scale Calibration.

D.1 Henkel New

Fig. D.3 shows the foam image sample for 69 % quality for the Henkel New foam generator, for 1.0 inch pipe. Bubbles are circular in shape, and almost there is no interaction in between bubbles.

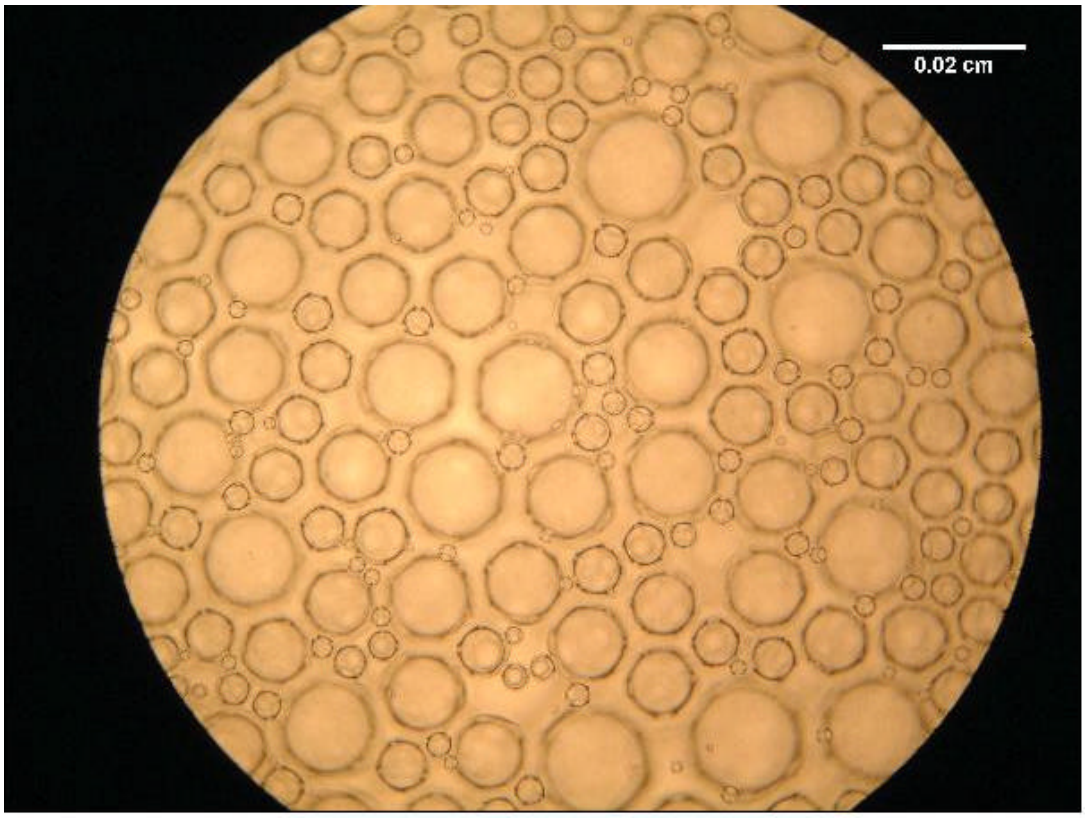

Figure D. 3: Foam Image, 69% Quality, Henkel New.

In Fig. D.4 larger bubbles are observed since the quality is at a level of 80%, in 1.50-inch pipe, larger than 69%. There is still no interaction of bubbles with each other at such a quality level.

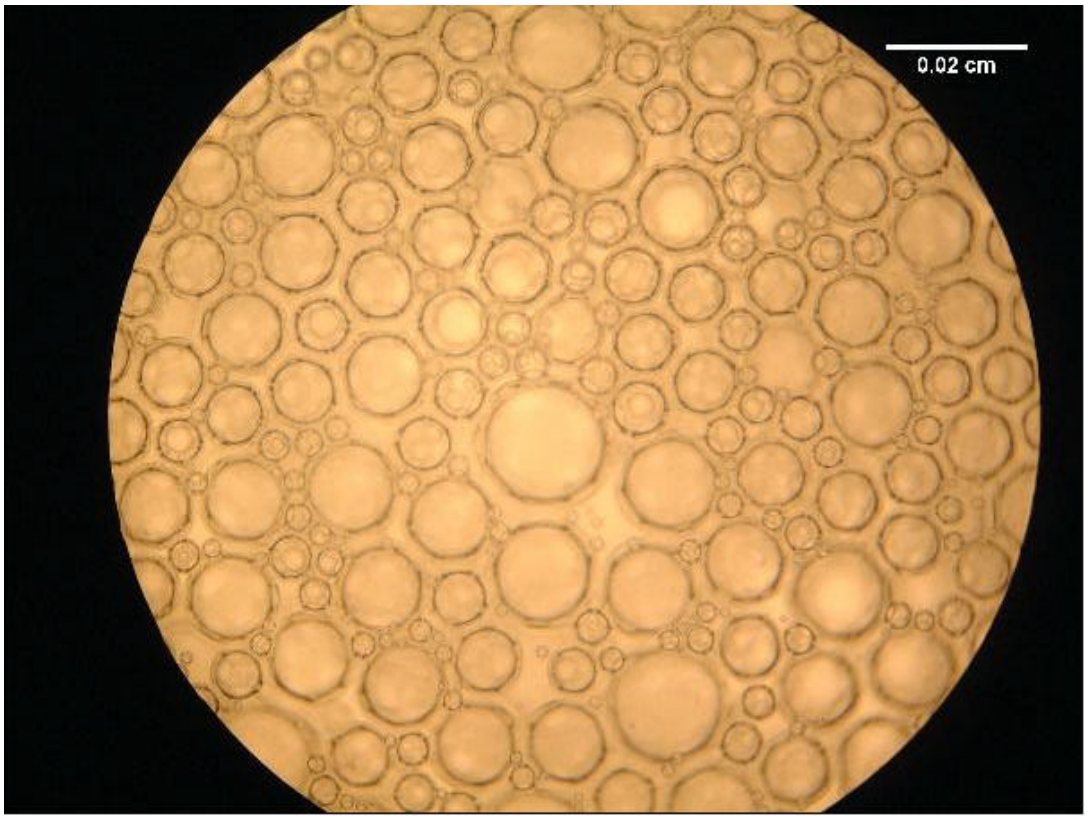

Figure D. 4: Foam Image, 80% Quality, Henkel New.

When Fig. D.5 is observed, larger bubbles are noticed with shapes other than circles. Bubble sizes are also greater in high quality foams due to higher gas content foam the foam itself. The 93% quality is photographed for 1.00-inch pipe.

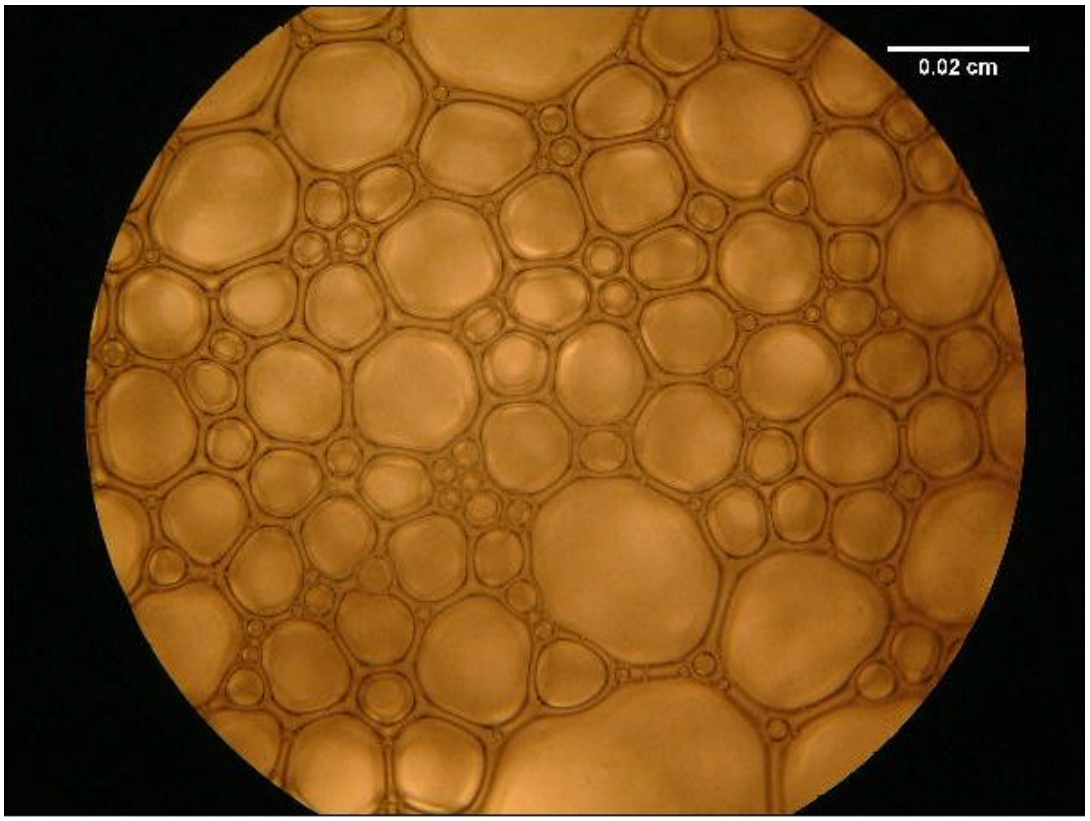

Figure D. 5: Foam Image, 93% Quality, Henkel New.

D.2 Henkel Old

Fig. D.6 is the image of the foam in 1.00-inch pipe for 70 % quality. Foam bubbles are easily observed to be greater than less quality level foams.

Fig. D.7 is the image of 80% quality level for 0.50-inch pipe. In this image it is observed that the bubble sizes are greater than a less quality level foam. There is still no interaction of bubbles with each other. It is important to note that the dissemination of small bubbles is higher for 70% quality foam.

Fig D.8 is the view of 87% quality, for 0.50-ich pipe. In this image bubble sizes of the bubbles are observed to be greater in size, and their circularity value is less than a perfect circle.

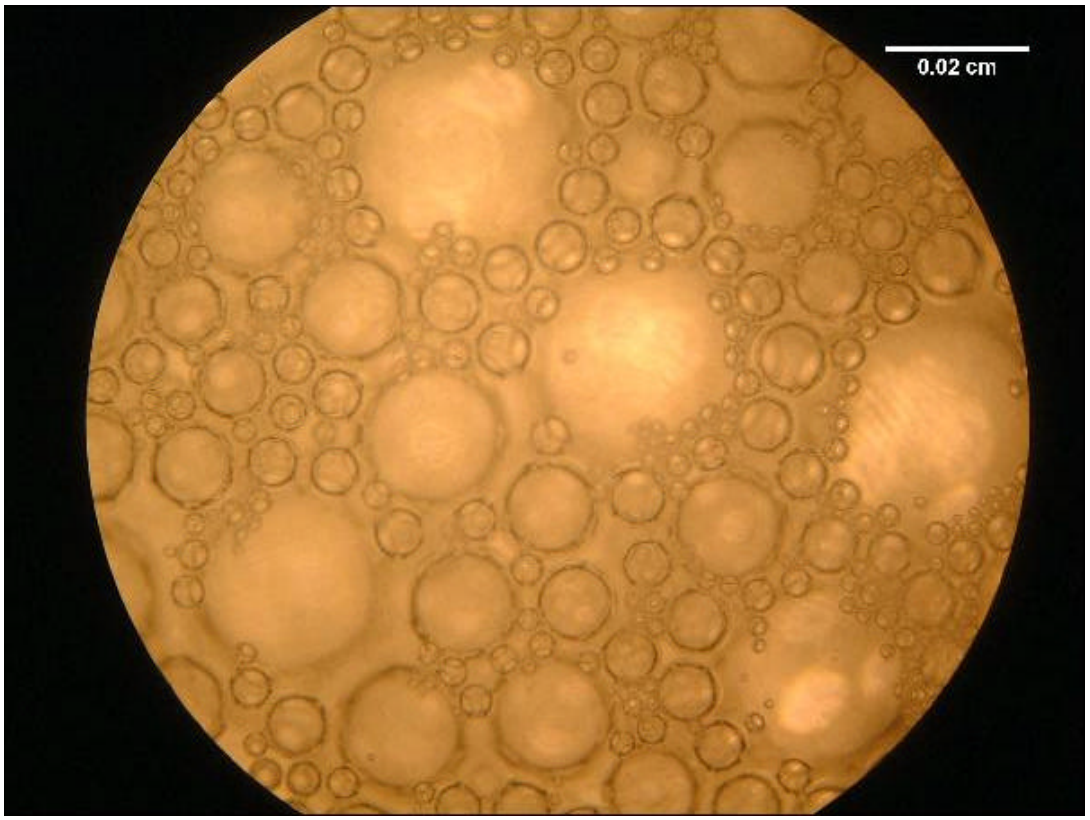

Figure D. 6: Foam Image, 70% Quality, Henkel Old.

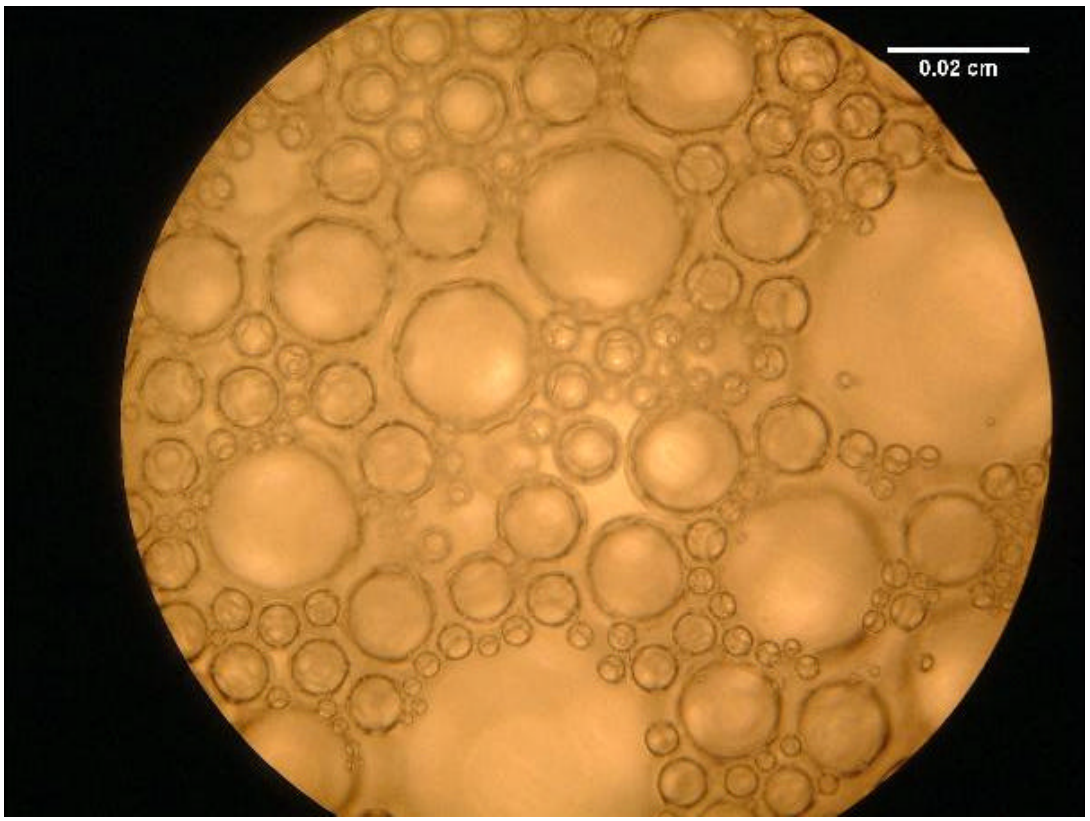

Figure D. 7: Foam Image, 80% Quality, Henkel Old.

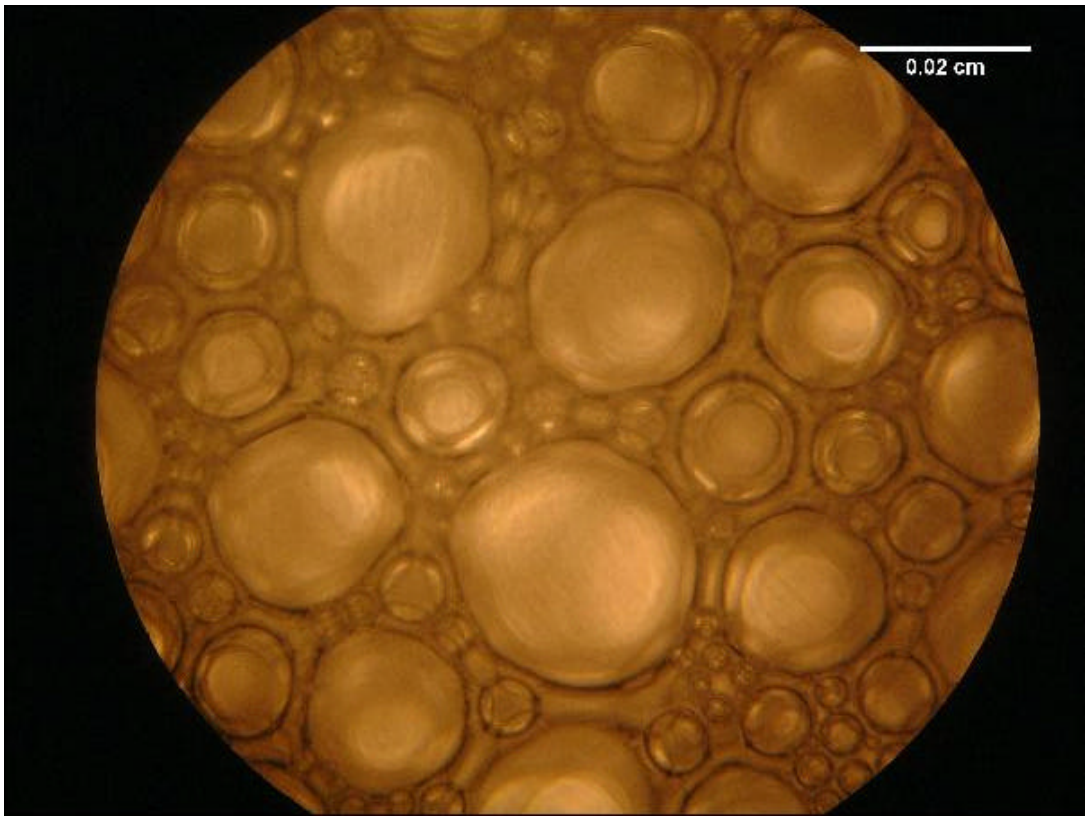

Figure D. 8: Foam Image, 89% Quality, Henkel Old.

D.3 Birka New

Fig. D.9 is the image of the Birka New foam generator, in 0.5-inch pipe. The quality of the image is 72%, it could be observed that bubble sizes are not that big as it is in higher quality levels, and there is no interaction of bubbles with each other.0.5

Fig. D.10 is for 82% quality level, the same surfactant and same foam generator, but for 1.5-inch pipe. Bubble sizes of the foam spheres are slightly greater than it is in 72% case. The intensity of the background light is weaker as quality value escalated.

Fig. D.11 is the image of 90% quality level, for 0.5-ich pipe. The intensity of background light is weaker than less quality levels. The bubble sizes are greater, and their circularity is different than a perfect circle.

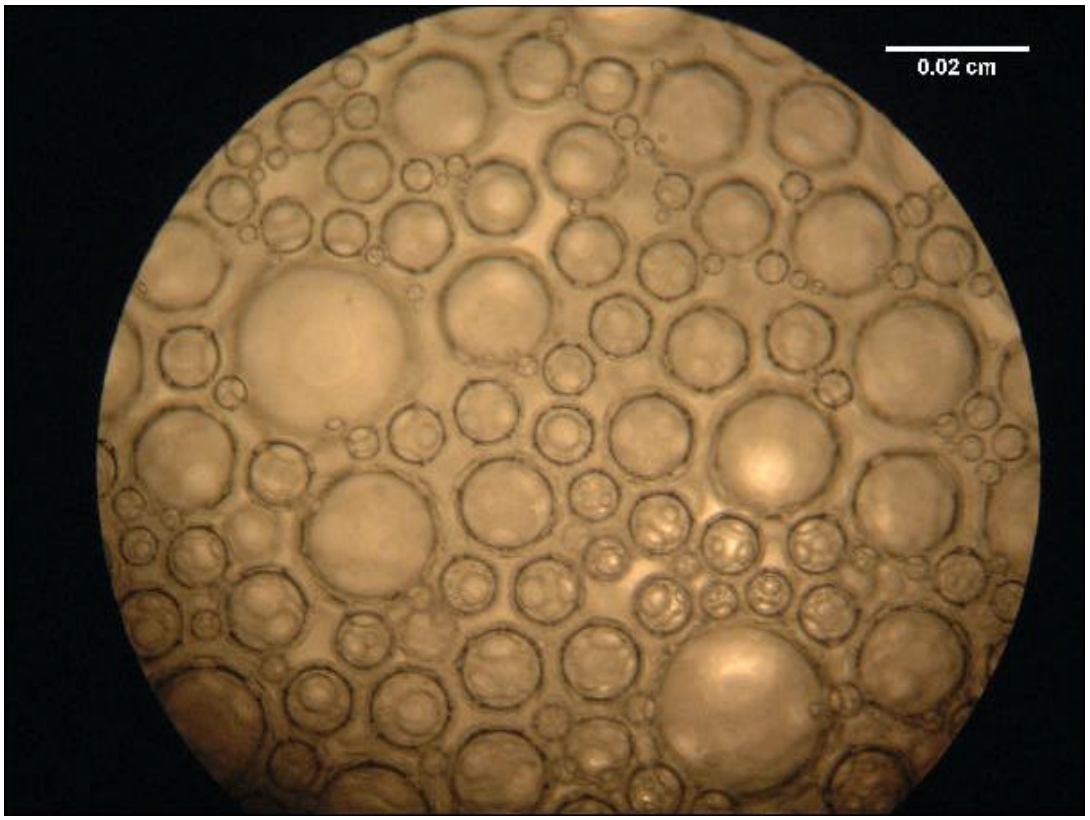

Figure D. 9: Foam Image, 72% Quality, Birka New.

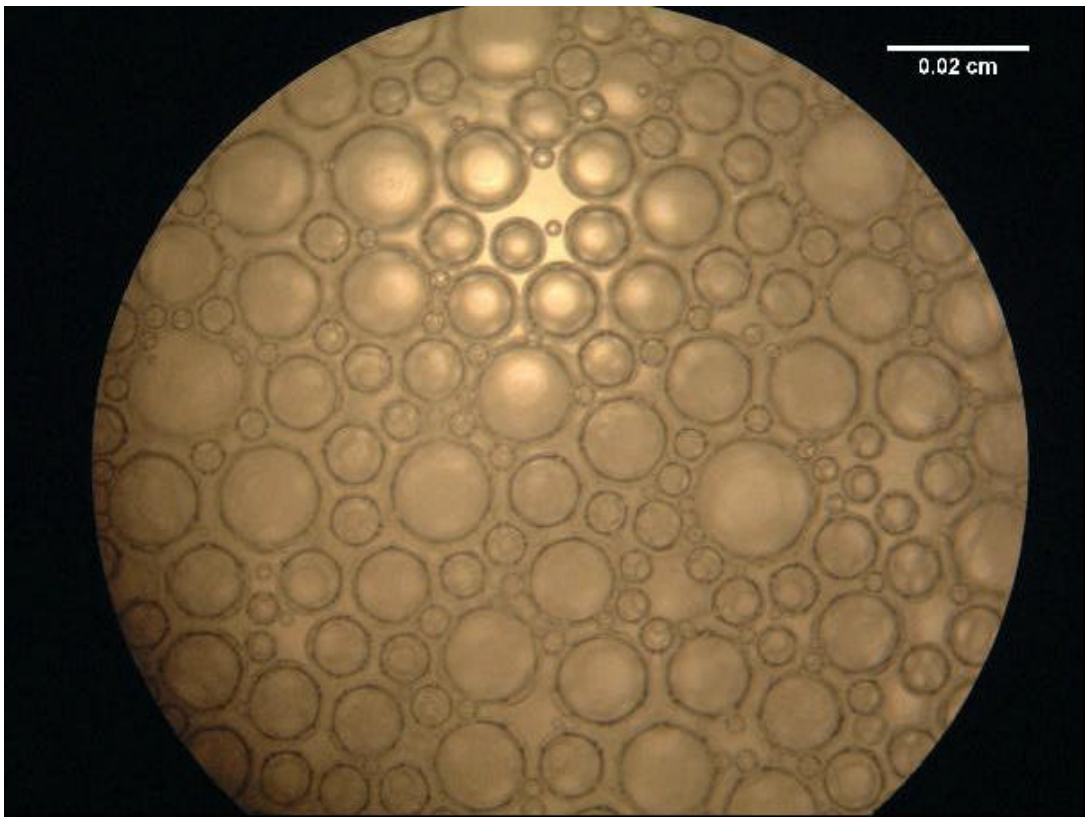

Figure D. 10: Foam Image, 82% Quality, Birka New.

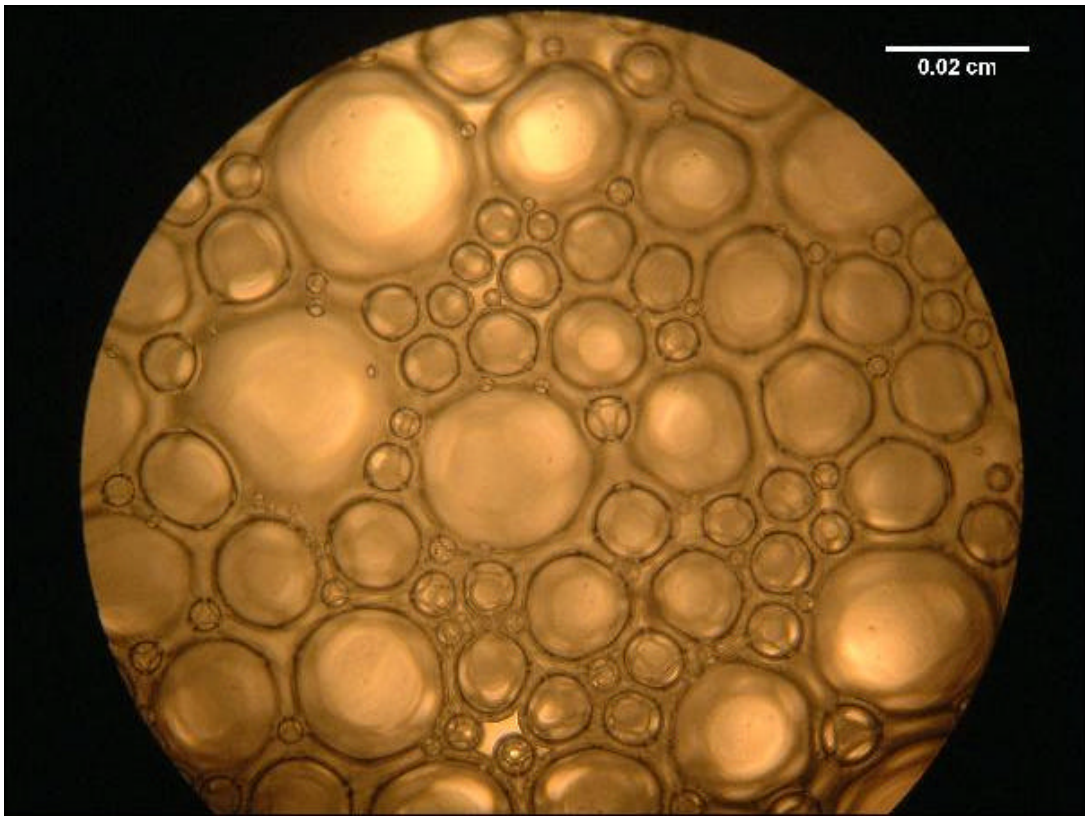

Figure D. 11: Foam Image, 90% Quality, Birka New.

D.4 Birka Old

Fig.D.12 is the image of the 67% quality foam flowing through 0.5-inch pipe. The circularity of the bubbles is observed to resemble a perfect circle, since there is not interaction of bubbles with each other.

Fig. D.13 is the image of 80% quality foam in 0.5-inch pipe. The bubble size is greater in size than it is in 67% quality level. In this image as well there is no interaction of bubbles with each other.

Fig.D.14 is the image of 90% foam quality level in 0.75-inch pipe. In this image the size of the foam bubbles are greater in size, and their circularity is not similar to a circularity of a perfect circle.

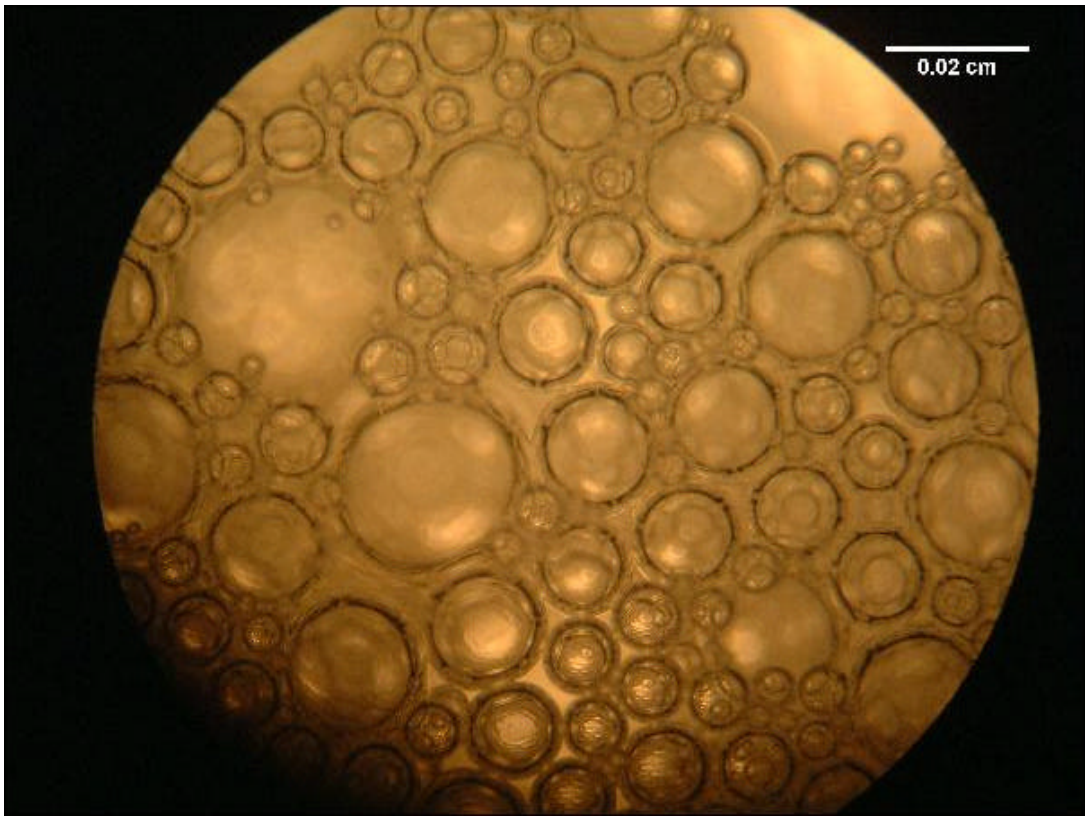

Figure D. 12: Foam Image, 67% Quality, Birka Old.

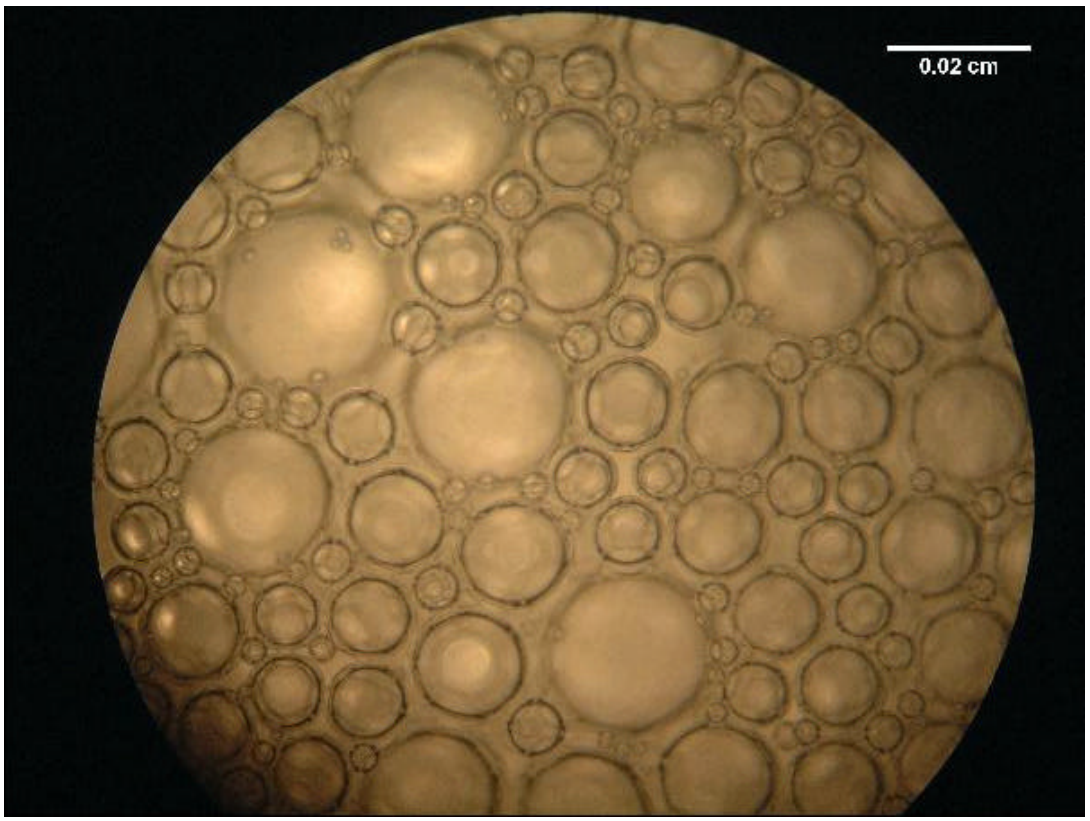

Figure D. 13: Foam Image, 80% Quality, Birka Old.

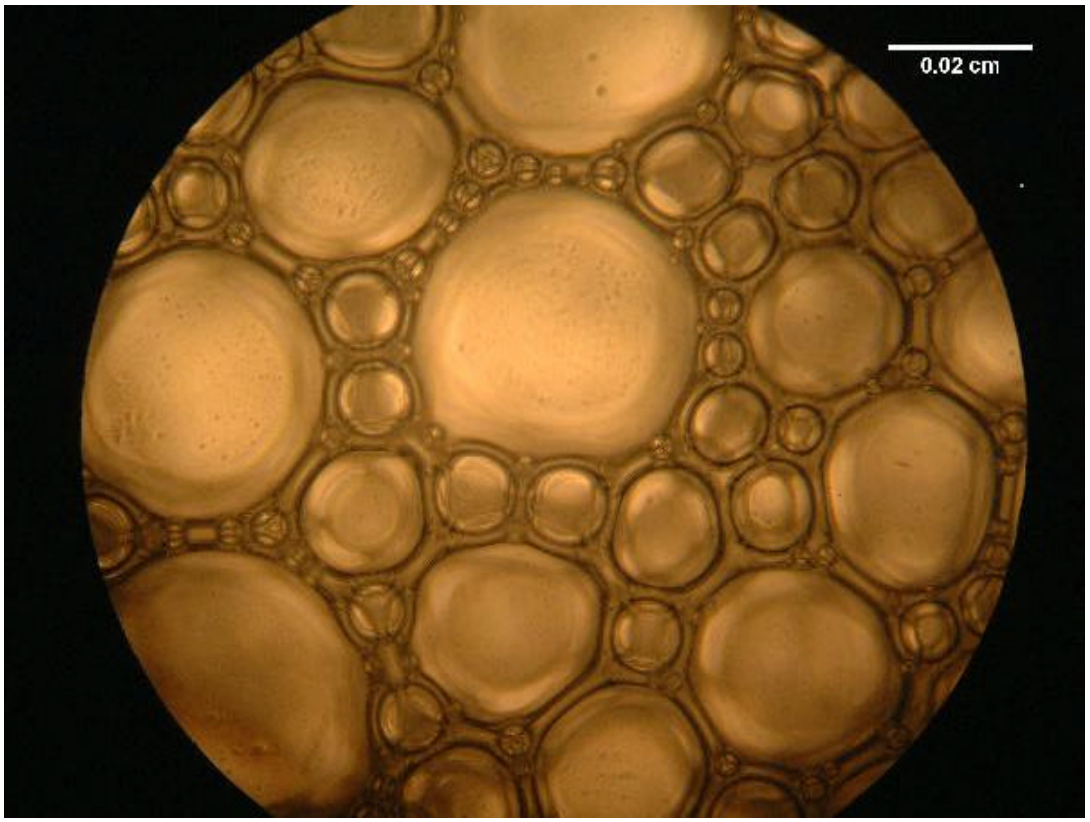

Figure D. 14: Foam Image, 90% Quality, Birka Old.

APPENDIX E

RHEOLOGICAL ANALYSIS EXAMPLE

An *example* calculation is given as follows to ease the understanding of the rheological analysis procedure. The following parameters are given for the example calculations; *Liquid flow rate*, 3.03 gpm, *diameter* of the pipe being experimented is 0.5-inch, *pressure* readings in *transducers* along the flow path from greater pressure to lower respectively are 9.12 psig and 6.19 psig, *gas pressure* at the junction point where liquid and gas constituents met is 14.55 psig, and *gas flow rate* is 6.51 gpm, the diameter of the gas flow line is 1.5 inch in.

The first step in processing is to calculate the velocity of the gas at the junction point of gas and liquid intersection, (please note that the diameter of the gas flow line pipe is 1.5-inch).

$$v_{@\,GasTransducer} = \frac{Q_{Gas}}{2.448 \times (f)^2} = \frac{7.51}{2.448 \times (1.5)^2} = 1.36\ ft/s$$

where, Q_{Gas} is the gas flow rate, gpm, f, diameter of the pipe under consideration; Velocity at the middle transducer along the pipe, from which image data is acquired is found from the following relation, a relation derived from the real gas law,

$$v_{@\,Mid-Trans} = \frac{(P_{Gas} + P_{atm}) \times (f_{GasPipe})^2 \times V_{@GasTransducer}}{(P_{@\,Mid-Trans} + P_{atm}) \times (f_{Pipe})^2}$$

$$= \frac{(14.55 + 12.96) \times (1.5)^2 \times 1.36}{(9.12 + 12.96) \times (0.5)^2} = 15.3\ ft/s$$

Where P_{atm} is the atmospheric pressure at the elevation that the laboratory is located, Section 6.5.

Gas flow rate at the mid-transducer is calculated as;

$$Q_{Gas@Mid\_Trans} = v_{@Mid\_Trans} \times 2.448 \times \left(f_{Pipe}\right)^2 = 15.3 \times 2.45 \times \left(0.5\right)^2 = 9.36 gpm$$

Quality as defined in equation 1.1, can be modified as if it is defined in terms of flow rate, rather than volumes, is calculated as;

$$\Gamma = \frac{Q_g}{Q_g + Q_l} \times 100 = \frac{9.36}{9.36 + 3.03} \times 100 = 75.55\%$$

Air is approximately composed of 21.0-mol% oxygen and 79.0-mol% nitrogen. Air's average molecular weight is 28.9 lbm/mol. Density of air under pressure inside the pipe whilst flow is calculated by the following equation, 10.732 is the Universal Gas Constant (psi.ft^3/(lbm.^{o}R)).

$$r_{air} = 28.9 \times \frac{\left(P_{@Mid-Trans} + 12.96\right)}{533} \times \frac{1}{10.732} = 28.9 \times \frac{\left(9.12 + 12.96\right)}{533} \times \frac{1}{10.732}$$

equals to

$$r_{air} = 1.79 * 10^{-3} g / cc$$

Air density is going to be used in calculation of foam density, as in the following equation; mix density is the density of the mixture of water and surfactant,

$$r_{Foam} = r_{air}\Gamma + r_{mix}(1 - \Gamma)$$

$$r_{Foam} = 1.79*10^{-3} \times 0.76 + 0.98 \times (1 - 0.76) = 2.4*10^{-1}\, g/cc$$

specific expansion ratio is calculated using equation 5.6,

$$e = \frac{r_{mix}}{r_{foam}} = \frac{0.98}{2.42*10^{-1}} = 4.07$$

is the specific expansion ratio, the correction parameter to Volume Equalize the foam shear stress-shear rate data.

Velocity of the foam is calculated from total flow rate,

$$v_{Foam} = \frac{Q_{Total}}{2.448 \times \left(f_{Pipe}\right)^2} = \frac{12.39}{2.448 \times (0.5)^2} = 20.25\, ft/s$$

The pressure readings from the pipe trajectory are used in calculation of the wall shear stress. The first pressure reading that is inherently greater in value than the pressure reading to follow is used in the equation. The wall shear stress for the acquired data is calculated from;

$$t_w = \frac{\Delta P}{\Delta L}\frac{D}{4} = \frac{(9.12 - 7.194)}{6.56168}\frac{0.5}{4}\frac{1}{12} = 3.06*10^{-3}\, psi$$

the shear stress value found above is volume equalized when divided by the specific expansion ratio,

$$\frac{t_w}{e} = \frac{3.06*10^{-3}}{4.06} = 7.53*10^{-4}\, psi$$

Rheological analysis of the acquired data is analyzed by calculation of the pertinent parameters.

Volume equalized shear rate is calculated by,

$$\frac{g}{e} = \frac{8v}{De} = \frac{8 \times 20.25 \times 12}{0.5} = 956.09 \sec^{-1}$$

Calculated volume equalized shear rate is then processed in order to discard the wall slip effect along the pipe wall, Appendix C gives the slip correction methodology.

Volume equalization discards the effect of quality dependency of rheograms, collapsing the data into one single curve as if it flows like an incompressible fluid.

APPENDIX F

EXPERIMENTAL DATA

The following table gives the ranges of the experimental data gathered in the course of the study.

Table F.1: Experimental Data.

		SURFACTANT			
PARAMETER		***BIRKA OLD***	***BIRKA NEW***	***HENKEL OLD***	***HENKEL NEW***
LIQUID FLOW RATE, GPM	MIN	0.700	0.700	0.750	0.100
	MAX	3.400	3.500	5.677	5.452
GAS FLOW RATE SCF/SEC	MIN	0.894	1.420	0.394	0.616
	MAX	3.494	3.386	6.537	2.322
QUALITY, %	MIN	60.413	67.994	55.008	69.639
	MAX	92.945	93.671	92.515	93.394
PRESSURE LOSS, PSI/2.5Mt.	MIN	0.338	0.260	0.022	0.077
	MAX	3.210	3.261	3.259	3.438
AVERAGE DIAMETER, IN	MIN	0.003	0.002	0.002	0.002
	MAX	0.007	0.005	0.007	0.005
CIRCULARITY	MIN	0.827	0.847	0.783	0.613
	MAX	0.891	0.895	0.890	0.826